

Cryptochrome Expression in the Zebrafish Retina: Potential Implications for  
Magnetoreception

by

Spencer David Balay

A thesis submitted in partial fulfillment of the requirements for the degree of

Master of Science

in

Physiology, Cell, and Developmental Biology

Department of Biological Sciences  
University of Alberta

© Spencer David Balay, 2018

## ABSTRACT

A variety of organisms have been shown to use the Earth's magnetic field to orient in local-spaces and to navigate long-distances. Although behavioural evidence of magnetoreception has been reported in a diverse range of taxa, the proximate mechanisms of this phenomenon have yet to be revealed. Some animals such as birds, appear to use a light-dependent radical-pair-based magnetic compass. Ancient, light-sensitive proteins called Cryptochrome (Cry) are currently the only known molecule found in vertebrates to create radical-pairs, and thus are putative receptors. Cry is associated with the visual system where it is co-localized with both short- and long-wavelength retinal cone photoreceptors in adult birds, and therefore well-suited for light-dependent magnetoreception. Unfortunately, due to the molecular inaccessibility of the avian model, Cry-cone interactions have seldom been manipulated, and the requirement of Cry for magnetoreception has yet to be tested in vertebrates. Additionally, Cry's location in photoreceptors of other animals that display magnetic behaviors is largely unknown.

This thesis utilized zebrafish (*Danio rerio*) to test if *cry* was associated with cones in developing and adult fish retina. Zebrafish have six paralogs of *cry* and while most participate in the circadian clock, the function of *cry2* and *cry4* are unknown. Here, I show that *cry4* is expressed in larval and adult zebrafish short-wavelength-sensitive (Ultraviolet-sensitive (UV)) cones. Using nitroreductase (NTR)-mediated cell ablation and reverse transcription quantitative-PCR (RT-qPCR), I found that *cry4* expression decreased when UV cones were ablated but was unaffected when neighboring blue cones were ablated in larval and adult retina. *cry2* did not appear to be expressed in UV cones and was unchanged after UV or blue

cone ablation in both developmental stages. Although zebrafish magnetic behavior has only been reported in adults, this work suggests larval fish may also have the molecular framework for magnetoreception. While zebrafish are non-migratory, they can be used to model other fish that migrate long-distances. Salmonids regenerate UV cones as they prepare to migrate back to their natal streams for spawning. Currently, the functional significance of this process has yet to be determined. These findings could provide one explanation for this as UV cones may enable magnetoreception via *cry*. In summary, I describe the localization of *cry4* in the zebrafish retina towards understanding whether fish have the molecular mechanisms for light-dependent magnetoreception.

## **PREFACE**

This thesis is an original work done by Spencer D. Balay.

Approval for this study was obtained from the Animal Care and Use Committee: Biosciences, under protocol AUP00000077.

Chapter 2 is modified from a manuscript submission to *Current Biology*, S. D. Balay and W. T. Allison, “Exploring potential for light-dependent magnetoreception in zebrafish: Cryptochrome expression in retinal photoreceptors.” This thesis abstract is modified from the manuscript abstract in S.D Balay and W.T. Allison, “Exploring potential for light-dependent magnetoreception in zebrafish: Cryptochrome expression in retinal photoreceptors.”

*Dedicated to the late Dr. Fred Oscar Schreiber.*

## **ACKNOWLEDGEMENTS**

I would like to thank my supervisor Dr. Ted Allison for his guidance, mentorship and friendship throughout the duration of my thesis and time at the University of Alberta. I am also extremely grateful for my Supervisory committee members: Dr. Colleen Cassady St. Clair, for always lending an ear and giving me my first start in research and Dr. Douglas Wylie, for welcoming me into his lab family and furthering my passion for visual neuroscience. Thank you to Dr. Kimberley Mathot and Dr. Heather Proctor for sitting on my examination committee. I am also indebted to Dr. Phil Oel, Dr. Michele Duval, Nicole Noel and Emily Dong for introducing me to the Allison lab and for initiating the start of my molecular training. I thank the current and former members of the Allison lab for making it a such a warm work environment.

I would also like to thank Troy Locke, Jeff Johnston and Dr. John Phillips for their technical and personal support throughout the duration of this thesis.

Thanks to the Department of Biological Sciences and the Faculty of Graduate Studies for the funding support I received during this thesis.

I would like to especially thank my family for always being supportive throughout my academic career. To June Schreiber, Dr. Gaylene Schreiber, Reg Wilkes, Kim Balay, Dave Balay, Kevin Balay and Terry Kosabeck- you all have helped me grow exponentially. A very special thank you to Sonya Widen, my life-partner, for constantly inspiring me to do and be my best. Your words of wisdom have helped me more than you will ever know. I couldn't have reached this mountain top without you.

## TABLE OF CONTENTS

<b>ABSTRACT</b> .....	<b>ii</b>
<b>PREFACE</b> .....	<b>iv</b>
<b>ACKNOWLEDGEMENTS</b> .....	<b>vi</b>
<b>TABLE OF CONTENTS</b> .....	<b>vii</b>
<b>LIST OF TABLES</b> .....	<b>ix</b>
<b>LIST OF FIGURES</b> .....	<b>ix</b>
<b>LIST OF ABBREVIATIONS</b> .....	<b>xi</b>
<b>1 INTRODUCTION</b> .....	<b>1</b>
<b>1.1 The Mystery of Magnetoreception</b> .....	<b>1</b>
<b>1.2 Magnetic Fields</b> .....	<b>2</b>
<b>1.3 Mechanisms of Magnetoreception</b> .....	<b>3</b>
1.3.1 Magnetite Based Magnetoreception .....	<b>3</b>
1.3.2 Light-dependent magnetoreception .....	<b>5</b>
1.3.3 Radical-pair generation .....	<b>8</b>
<b>1.4 Cryptochrome and Light-Dependent Magnetoreception</b> .....	<b>11</b>
<b>1.5 Zebrafish as a model for light-dependent magnetoreception</b> .....	<b>16</b>
1.5.1 Zebrafish Cryptochromes.....	<b>17</b>
1.5.2 Magnetoreception behavioral evidence and assays .....	<b>19</b>
1.5.3 Nitroreductase-mediated targeted ablation .....	<b>20</b>
<b>1.6 Purpose of study/ objectives</b> .....	<b>21</b>
<b>2 EXPLORING POTENTIAL FOR LIGHT-DEPENDENT MAGNETORECEPTION IN ZEBRAFISH: CRYPTOCHROME 4 IN A SELECT SUBTYPE OF RETINAL PHOTORECEPTORS</b> .....	<b>29</b>
<b>2.1 Introduction</b> .....	<b>29</b>
<b>2.2 Methods</b> .....	<b>30</b>
2.1 Animal Ethics.....	<b>30</b>
2.2 Zebrafish Maintenance .....	<b>30</b>
2.3 Nitroreductase-Mediated Ablation .....	<b>31</b>
2.4 Riboprobe production and Fluorescent <i>In-Situ</i> Hybridization .....	<b>31</b>
2.5 RNA Isolation.....	<b>32</b>
2.5.1 Whole Larvae .....	<b>32</b>

2.5.2 Adult Eye .....	33
2.6 RT-qPCR.....	33
2.6.1 cDNA synthesis .....	33
2.6.2 RT-qPCR Parameters .....	34
2.6.3 Endogenous Control Stability Assay.....	34
2.6.4 Primer Validation.....	34
2.7 Microscopy and Imaging and Figure Assembly.....	35
2.8 Statistics.....	35
<b>2.3 Results and Discussion.....</b>	<b>36</b>
2.3.1 Expression of <i>cry4</i> in larval zebrafish retina .....	36
2.3.2 <i>cry4</i> is specifically expressed in the UV cone subtype of larval zebrafish.....	37
2.3.2 <i>cry4</i> is expressed in adult zebrafish UV cones .....	39
2.3.3 Blue cone ablation does not measurably disrupt <i>cry4</i> abundance in adult retina	40
2.3.4 <i>cry4</i> and cone photoreceptors as potential magnetoreceptors in fish .....	41
<b>3 GENERAL DISCUSSION AND FUTURE DIRECTIONS.....</b>	<b>53</b>
<b>3.1 The role of UV cones and cone mosaics in magnetoreception.....</b>	<b>53</b>
3.1.1 UV vision may be suited for visually perceiving magnetic fields.....	55
3.1.2 Fine tuning of visually mediated magnetoreception may be accomplished by long-wavelength photoreceptors .....	57
<b>3.2 <i>cry2</i> and <i>cry4</i>'s function in zebrafish retina: magnetoreception, circadian photoreception or neither.....</b>	<b>59</b>
<b>3.3 Future Experiments to test LDRPM in Zebrafish .....</b>	<b>62</b>
3.3.1 Behavioral experiments to test for LDRPM.....	62
3.3.2 Genome editing of <i>cry</i> in zebrafish .....	65
3.3.3 Imaging magnetically dependent neuronal activity via Ca <sup>2+</sup> .....	67
<b>3.4 Final Conclusions.....</b>	<b>69</b>
<b>Literature Cited.....</b>	<b>72</b>
<b>APPENDIX A.....</b>	<b>91</b>
<b>A.1 Generation of <i>slc45a2</i> mutant zebrafish.....</b>	<b>91</b>
A.1.1 sgRNA creation .....	91
A.1.2 Injection process .....	91
A.1.3 Genotyping via sequencing and RFLP.....	92
A.1.4 Generation of <i>crystal</i> and <i>crystal</i> -based transgenics .....	93

## LIST OF TABLES

Table 1. Transgenic zebrafish lines used in experiments. ....	43
Table 2. Primers used for Cryptochrome riboprobe synthesis.....	43
Table 3. RT-qPCR primers used for Cryptochrome mRNA quantification.....	44
Table A1. Oligonucleotides used for sgRNA synthesis. ....	94
Table A2. Primers used for ua5015 and ua5020 genotyping. ....	94

## LIST OF FIGURES

Figure 1. The geomagnetic field. ....	24
Figure 2. Model of light-dependent magnetoreception. ....	26
Figure 3. Cryptochrome can create radical-pairs between FAD and Trp.....	27
Figure 4. How the magnetic field may alter animals' visual perception.....	28
Figure 5. Larval zebrafish UV cones express <i>cry4</i> during the day.....	45
Figure 6. Ablation of UV cones, but not blue cones, drastically decreases <i>cry4</i> in larval zebrafish. ....	47
Figure 7. UV cone ablation decreases <i>cry4</i> expression in adult zebrafish retina.....	48
Figure 8. Effective blue cone ablation does not disrupt <i>cry4</i> expression in adult zebrafish retina.....	49
Figure 9. <i>cry2</i> expression is not changed significantly after both UV cone and blue cone ablation in larval and adult zebrafish.....	50
Figure 10. No <i>cry4</i> probe control for double fluorescent <i>in situ</i> hybridization on adult retina. ....	51
Figure 11. $\beta$ - <i>actin</i> is a suitable endogenous control for RT-qPCR experiments.....	52

Figure 12. Molar absorption spectra of FAD in different Cry redox states.....	71
Figure A1. Larval nacre zebrafish injected with <i>slc45a2</i> CRISPR mix show mosaic pigment defects. ....	95
Figure A2. ua5015 ( <i>slc45a2</i> <sup>-/-</sup> ; <i>mitfa</i> <sup>-/-</sup> ) have no pigment in the RPE and can be observed through development.....	96
Figure A3. Pigmentless ua5020 mutants are generated from crossing ua5015 to casper....	98
Figure A4. <i>Tg<sub>ua5020</sub>(sws1:nfsb-mCherry; sws2:GFP)</i> transgenics allow easy visualization of fluorescent reporters in zebrafish retina. ....	99

## LIST OF ABBREVIATIONS

$\mu\text{l}$	microlitres
$\mu\text{M}$	micromolar
$\mu\text{s}$	microseconds
$\text{Ca}^{2+}$	calcium
CaMPARI	calcium modulated photoactivatable ratiometric integrators
Cas	CRISPR associated protein
CRISPR	clustered regularly interspaced short palindromic repeat
<i>cry</i> or <i>Cry</i>	cryptochrome
DMSO	dimethyl sulfoxide
dpf	days post fertilization
FAD	flavin adenine dinucleotide
FADH <sup>-</sup>	anionic fully reduced state of FAD
FADH <sup>•</sup>	neutral semiquinone radical of FAD
GCL	ganglion cell layer
GECIs	genetically encoded calcium integrators
HC	horizontal cells
hpf	hours post fertilization
INL	inner nuclear layer
LDRPM	light-dependent radical-pair magnetoreception
<i>lws1</i>	long-wavelength sensitive 1 (opsin)
<i>lws2</i>	long-wavelength sensitive 2 (opsin)
MBM	magnetite-based magnetoreception
MHz	megahertz
ms	millisecond
MS-222	tricaine methanesulfonate
MTZ	metronidazole

nl	nanolitre
nm	nanometers
nT	nanotesla
NTR	nitroreductase
ONL	outer nuclear layer
PCR	polymerase chain reaction
PTU	1-phenol-2-thiourea
RGC	retinal ganglion cell
<i>rh1</i>	rhodopsin
<i>rh2-1</i>	medium-wavelength sensitive 1 (opsin)
<i>rh2-2</i>	medium-wavelength sensitive 2 (opsin)
<i>rh2-3</i>	medium-wavelength sensitive 3 (opsin)
<i>rh2-4</i>	medium-wavelength sensitive 4 (opsin)
RP	radical-pair
RPE	retinal pigmented epithelium
RT-qPCR	reverse transcription quantitative polymerase chain reaction
${}^{\text{S}}\text{FAD}^*/\text{FAD}_{\text{ox}}$	neutral fully oxidized state of FAD
${}^{\text{S}}\text{FAD}^{\bullet-}$	singlet anionic semiquinone radical of FAD
<i>sws1</i>	short-wavelength-sensitive 1 (opsin)
<i>sws2</i>	short-wavelength-sensitive 2 (opsin)
${}^{\text{T}}\text{FAD}^{\bullet-}$	singlet anionic semiquinone radical of FAD
Tg	transgenic
Trp	tryptophan
UTR	untranslated region
UV	ultraviolet
ZT	zeitgeber

# 1 INTRODUCTION

## 1.1 The Mystery of Magnetoreception

Magnetoreception is argued to be one of the most complex and intriguing sensory pathways yet to be fully described. Consider it in relation to the understanding of much more palpable senses such as the visual perception of light, which is something humans experience everyday. We have a relatively firm grasp on the development and evolution of photosensitive organs, have identified countless receptors with specific functions, know detailed neural pathways in many animals, and can predict and treat related diseases. The stimuli (visible light) has certain properties we have long been aware of: it cannot pass through certain solid objects (like your arm), it acts like a particle and a wave and its tangible presence can be experienced with the flick of a switch or the strike of a match in a darkened room. Despite the centuries of progress made to understand vision, many things about this “well-described” sense remain unknown.

Now consider the perception of magnetic fields: a completely intangible experience to the conscious human sensory system. Nevertheless, this sense has been shown to exist in plants, many invertebrates and every major class of vertebrate. In this case, even the mere identification of magnetoreceptive organs cannot be made with certainty. Why is so little known about this apparently common occurrence? The stimuli here, can pass through any biological tissue, is present in almost every situation of our lives, and has been around for more than 4 billion years [1]. How animals detect this omnipresent entity has intrigued scientists for decades. Regardless, much progress has been made towards understanding the mysteries of magnetoreception and is briefly reviewed below.

## 1.2 Magnetic Fields

The magnetic field of the Earth can be most simply conceptualized akin to a bar magnet (Figure 1). It is dipole in nature such that it produces two magnetic poles closely positioned to the geographical poles of the Earth. This configuration permits several unique magnetic characteristics to exist, commonly described as declination, inclination and intensity. Declination is the angle that varies between geographic and magnetic poles, while inclination is the angle that the magnetic field makes with the Earth's horizontal; at the magnetic North pole, the magnetic field points directly down, (inclination= $+90^{\circ}$ ). This angle decreases as it approaches the Equator (inclination= $0^{\circ}$ ) and becomes negative (points up) as it reaches the South pole (inclination= $-90^{\circ}$ ). Similarly, intensity of the geomagnetic field exists in a gradient, where it is strongest at the poles ( $\sim 60,000$  nT) and weakest at the Equator ( $\sim 30,000$  nT) [2]. Despite some variation due to secular drift or anomalies created by magnetic storms and enriched deposits of iron in the crust of the Earth, the geomagnetic field acts as a reliable, constant spatial grid. This entity exists in a stable state regardless of weather, temperature or time of day, and has been shown to aid a variety of animals in orientation and navigation behaviors [3].

All major classes of vertebrates (fish, amphibians, reptiles, birds and mammals; [3-9]) and some invertebrate classes (molluscs, insects and crustaceans; [10-14]) have been shown to use magnetoreception for a suite of spatial behaviors. Magnetically derived compass (used to determine direction) and map (used to determine geographical position) information aids in animal homing, migration, predation and exploration of local environment [4,8,9,15-26]. Although a wealth of behavioral evidence for magnetoreception exists across a diverse range

of taxa, the underlying molecular, neural and physiological mechanisms of this phenomenon remain unknown. So far, two main magnetoreception hypotheses have predominately been suggested: magnetite-based magnetoreception (MBM; [27-29]) and light-dependent radical-pair magnetoreception (LDRPM; [30-36]). These two mechanisms appear to fulfill different roles in different animals and are not necessarily mutually exclusive; indeed, some animals such as birds, rodents, salamanders and fish display evidence of multiple modes of magnetoreception [37-40]. Generally, MBM is thought to mediate map sense, while LDRPM has been suggested to mediate compass sense. As such, the molecular underpinnings, neural pathways and behavioral outputs appear to be separate between MBM and LDRPM and are outlined in the following section.

### **1.3 Mechanisms of Magnetoreception**

#### **1.3.1 Magnetite Based Magnetoreception**

MBM involves inherently magnetic particles that are integrated into a sensory pathway; that is, they are physically coupled to ion channels in a sensory cell (for review see [27,29,41]). Mechanical force exerted on the particles by changing magnetic intensity or direction could be used to transduce a biologically relevant signal by opening or closing ion channels [42,43]. This type of magnetoreception would theoretically allow magnetic North to be distinguished from magnetic South relative to the position of the navigator (i.e. provides a map sense). This system exploits small intensity and potentially inclination changes in the magnetic field and does not require light to function [44]. This mechanism has been supported by the discovery of magnetite, an iron oxide derivative, in magnetotactic

bacteria [45]. Since its initial discovery, magnetite has been proposed to be found in a variety of animals such as bees, birds and fish [46-50]. Although a number of studies claim to have found magnetic material in magnetoreceptive animals, its presence in biological tissue remains controversial [51,52].

Notably, MBM is the most popular hypothesis for fish magnetoreception [41,49,53]. The olfactory system appears to be involved with MBM, as electrophysiological recordings from the trigeminal nerve of rainbow trout (*Oncorhynchus mykiss*) [49] and birds [54] show altered electrical output when the intensity of the magnetic field is changed. Magnetite has also been proposed to be found in trout olfactory lamellae and throughout the adult zebrafish [47,48,50]. The inactivation of trout's ophthalmic branch of the trigeminal nerve eliminates a physiological response to magnetic fields [55], supporting its role in magnetoreception. Some fish behavior also supports this mechanism: migratory Pacific salmon appear to have a map sense, where they swim along magnetic intensity and inclination field lines similar to their natal streams [21,23]. Additionally, zebrafish, medaka (*Oryzias latipes*), Chinook salmon (*Oncorhynchus tshawytscha*) and rainbow trout have been shown to be responsive to magnetic fields in the dark, which supports a light-independent based magnetoreceptor [40,55-60], similar to what is found in subterranean mole rats (*Spalax ehrenbergi*) and bats [6,61,62]. Other marine migrants, such as turtles, appear to have a magnetic map that is sensitive to the intensity and inclination of magnetic fields [63-65]. Interestingly, although magnetite is thought to mediate this behavior [63,66], application of radio-frequency fields (a diagnostic tool for LDRPM) has been shown to disrupt juvenile snapping turtle (*Chelydra serpentina*) alignment [67], which supports a light dependent radical-pair magnetoreception pathway (described in section 1.3.2). Additionally, salmon, zebrafish and medaka show

different behavioral responses to magnetic fields in conditions with light and without light [5,40,56-59]. These findings, among others, suggest that fish and other animals likely contain another mechanism of magnetoreception that is light-dependent.

### 1.3.2 Light-dependent magnetoreception

Light-dependent magnetoreception has been characterized in a variety of animals including birds, amphibians, rodents and insects [4,12,14,16,19,37,38,68-71]. The first step in this mechanism (described in section 1.3.3) involves the detection of light, rather than processing of magnetic information. In agreement with this, orientation ability of animals that exhibit light-dependent magnetic behaviors appear to be affected by intensity, wavelength and polarization of light. The most compelling evidence comes from the affect of wavelength on orientation ability seen in migratory birds and salamanders. Eastern red spotted newts (*Notophthalmus viridescens*) trained to orient under full spectrum light ( $\geq 450$  nm) show a  $90^\circ$  rotated orientation when tested under monochromatic light with wavelengths above 500 nm [4,16,37]. Many birds such as : European robins (*Erithacus rubecula*) garden warblers (*Sylvia borin*), chicken (*Gallus gallus*), Australian silvereyes (*Zosterops lateralis*) and carrier pigeons (*Columba livia domestica*) exhibit magnetoreceptive behaviors and appear to have a magnetic compass that operates best in short-wavelength light (370 nm to 570 nm; for review see[69]). When tested under wavelengths of 590 nm and above, compass orientation is abolished, and normally preferred headings are randomized. Even animals extremely divergent to birds, such as fruit flies (*Drosophila melanogaster*) [11] and the American cockroach (*Periplaneta americana*) [14], show a

magnetic behavior that is present under short-wavelength light but is disrupted under long-wavelength light.

In cockroaches, increasing the intensity of light permits this behavior to manifest in longer-wavelengths that normally do not allow the orientation behavior. This “behavioral rescue” is only observed up to a certain wavelength, where even extremely high intensities of light cannot force the behavior above 505 nm [14]. Additionally, intensity of light appears to alter orientation abilities in birds such as European robins [68,72-74]. The response to increased intensities of different wavelengths of monochromatic light causes a suite of behaviors including disorientation, polar orientation to magnetic North and rotated orientation in the East-West axis. Why these different responses were exhibited is currently unknown, but these findings suggest that photoreceptors, specifically those tuned to precise wavelengths, are likely important for magnetoreception. It is also proposed that polarized light may interact with the magnetic compass in zebra finches (*Taeniopygia guttata*). When finches were trained to polarized light cues that are parallel to magnetic field direction (or vice versa) magnetic orientation abilities were intact. When either the magnetic field or direction of polarized light are changed to be perpendicular in respect to each other, orientation abilities were randomized [75]. Although how (and if) polarized light and magnetic fields interact is currently under debate [76], light-dependent magnetoreception appears to be well-established in a variety of organisms.

Due to these findings and others, it is thought that light-dependent magnetoreception would most favourably be mediated in light-sensing organs such as the pineal (as seen in some vertebrates) or the retina. The pineal appears to play a role in salamander orientation

[77,78] and has been implicated as magnetosensitive in birds [79], but its magnetoreceptive role in other vertebrates who display this structure (fish and reptiles) is unknown. In birds, although the pineal can respond to magnetic fields, it is not necessary for magnetoreception [80,81], pointing towards the involvement of the retina. Indeed, neuronal areas such as the nucleus of the basal optic root (nBOR) of pigeon accessory optic system show electrophysiological changes to magnetic fields, suggesting retinal input aids in magnetoreception [82]. Also, the optic tectum has been described to show electrophysiological responses to magnetic fields [79], but these results remain controversial [83]. From a neurological perspective, the most compelling evidence of visually mediated magnetoreception involves experiments manipulating Cluster N in the Visual Wulst of birds [84]. Cluster N receives projections from retinal ganglion cells (RGCs) via the thalamofugal pathway and is highly active during magnetic compass orientation [85-87]. Lesion of Cluster N disrupts magnetic orientation abilities, but other navigational means (of sun and star compasses) remain fully functional, suggesting magnetic information is specifically processed in Cluster N and transduced via pathways that originate in the retina [84]. The hemispherical shape of the eye also may serve an important magnetoreceptive purpose, specifically the ordered array of cone/rod photoreceptors along the back of the retina [36,88-90]. This layout allows potential magnetoreceptors to receive magnetic information across various angles and orientations in respect to the animal. Additionally, the semi-fixed position of photoreceptors has historically been thought to be required for radical-pairs to function as directional magnetoreceptors [33,36,88-91]. The details of how these photoreceptors may be sensitive to magnetic fields, is outlined below.

### 1.3.3 Radical-pair generation

The central theory behind LDRPM involves the creation of magnetically sensitive radical-pairs<sup>1</sup> after a photochemical reaction. This biophysical model was first proposed by Schulten in 1978 [30,35], and since then has become one of the leading hypotheses of magnetoreception (for review see [33]). In LDRPM, light-induced electron transfer is responsible for creating radical-pairs. These radicals are magnetic in nature, due to a magnetic moment created by the quantum spin state of each unpaired electron. Spin state is dependent on the effect of the internal magnetic field, caused by the rotation of nearby nuclei (hyperfine interactions). After light absorption causes an electron to transfer from a donor to an acceptor, the spin of the radical-pair begins in a singlet-state, with each unpaired electron spinning in opposite orientations (or antiparallel; Figure 2C). Over time, hyperfine interactions cause the spins of the unpaired electrons to oscillate such that their orientations change with respect to each other. Eventually, the spin of the two unpaired electrons in each radical end up parallel (triplet-state) to each other [36].

After initial radical-pair formation (singlet-state), electrons usually back transfer to the more favourable ground-state and abolish the radical-pair (i.e. forbid the formation of the triplet-state). The radical-pairs that do proceed to the triplet-state, forbid the electron back transfer, and increase the life time of the active radical-pair. An external magnetic field (such as the geomagnetic field) can alter the interconversion rate of single-to-triplet radicals

---

<sup>1</sup> A radical is a molecule with an odd number of electrons. Radical-pairs are two radicals that are created simultaneously after some energy-level splitting stimulus.

by influencing how the electrons oscillate in relation to each other (Zeeman interactions)<sup>2</sup>. The ratio of the products created from each radical-pair reaction (i.e. chemical signals produced from either singlet or triplet-state) could be compared and cause the molecule to act differently depending on which state predominated in a certain scenario (Figure 2). If the triplet-state is favoured, where the ground-state promoting electron back transfer is prohibited, the molecule could theoretically spend more time in a signalling form. In LDRPM, the bias towards triplet-state is ultimately influenced by the presence of the geomagnetic field thus creating a biological magnetic sensor [32,33,36].

The direction of the geomagnetic field can also influence this process: the external magnetic field differentially affects interconversion rates based on its direction with respect to the radicals (i.e. not every radical will be influenced the same way). This anisotropy is what allows the magnetic field/ radical-pair interaction to actually provide directional information from magnetic fields (i.e. provide a compass sense), rather than just simply detect the presence or absence of magnetic fields, which would occur if all radicals reacted in the same fashion to external magnetic fields [33,36,88,89,92]. Indeed, a variety of studies have shown that geomagnetically relevant magnetic fields alter singlet-triplet interconversion rates of radical-pairs in vitro [93-96] and specifically the direction of the magnetic field can change the yield of radical-pair products, providing evidence that a chemical compass is biologically feasible [97].

Besides theoretical and recent experimental data, other diagnostic experiments have been developed to test if radical-pairs are involved in magnetoreception. Potentially the

---

<sup>2</sup> So long as the radical-pair intermediates persist long enough for the Earth's magnetic field to interact with them (longer than 1 $\mu$ s; [33,92]).

most compelling experiment is done by exposing orienting animals to low level radio frequency fields [36,98,99]. It is known that an isolated electron in a radical-pair (void of hyperfine interactions) spins at a well-characterized frequency (the Larmor frequency, around 1.4 MHz depending on location) in an ambient magnetic field. Application of frequencies that encompass the energy-level splitting required to switch radical-pairs from singlet to triplet states (1.4 MHz) can alter the interconversion process, and ultimately disrupt the effect of the external magnetic field (for review see [33]). In vitro, it has been shown that 1-100MHz frequencies disrupt radical-pair interconversion [100]. More convincingly, European robins that were exposed to broadband (0.1-10MHz) or discrete (1.3MHz) frequencies were disoriented when being tested for magnetic compass [98,101]. Additionally, low levels of anthropogenic electromagnetic noise (non-uniform radio frequencies), and weak broadband frequencies have been shown to disrupt orientation in birds, illustrating the range of this sensitivity [102,103]. Orientation of other animals such as garden warblers, zebra finches and cockroaches [104-106] also all appear to be disrupted by low-level radio frequencies, supporting a LDRPM mechanism. Interestingly, it has been shown that if juvenile turtles are acclimated in radio frequencies parallel to the magnetic field, they are able to exhibit a spontaneous magnetic alignment that is abolished when the radio frequency field is turned off [67]. This suggests some plasticity in the way radio frequency fields can influence magnetoreception. There is much to learn about how radio frequencies interact with radical-pairs (for review see [107]), but regardless, the idea that radical-pairs are likely to function as a chemical compass has gained considerable ground in the last two decades.

For almost 20 years after the initial conception of LDRPM, the theoretical molecule capable of radical-pair formation remained unidentified in animals that displayed light-dependent magnetic behaviors. In 2000, Ritz et al., [36] suggested that Cryptochrome (Cry), a recently characterized protein at the time [108], may fulfill the requirements as a light-dependent magnetoreceptor, as it can form light-induced radical pairs, and is found in a variety of organisms including vertebrates.

#### **1.4 Cryptochrome and Light-Dependent Magnetoreception**

Cry was first identified in plants as a “cryptic” blue light/UV-absorbing photoreceptor that controls development and growth [108]. Evolutionarily, Crys are homologous to photolyase, an ancient enzyme that catalyzes repair of UV-induced DNA damage in prokaryotes and eukaryotes [109]. Most Crys have lost DNA repair activity but all have retained two N-terminal domains from their photolyase ancestors; a photolyase domain and a flavin adenine dinucleotide (FAD) binding domain which both bind chromophore cofactors that are responsible for short-wavelength light absorption [110-112]. In photolyases and *Arabidopsis thaliana* Cry, phototransduction is mediated by electron transfer between a triad of Tryptophan (Trp) residues and the FAD cofactor [113,114]. In various animal Crys, the position of these tryptophan’s is highly conserved[112] and therefore, the magnetically sensitive radical pairs are proposed to be created between them and FAD (Figure 3). Recent evidence suggests the favoured electron transfer pathway may not be required for magnetically dependent Cry biochemical changes or magnetoreceptive behavior, but this notion requires further investigation [13,115].

Crys also have a well-characterized role in tuning biological rhythms as part of the circadian clock through both photic and aphotic mechanisms [110,116]. Crys photoreceptor function depends on which functional group they belong to [112,117-119]. The functional groups of Cry are commonly described as either: Type I Crys, which are directly light-sensitive and seem to act as circadian photoreceptors in invertebrates, Type II Crys which have no described light-dependent function and regulate transcription of clock genes in the vertebrate circadian clock, and Cry-DASH which appears to have retained the ability of photo repair but are mostly considered as intermediates between Photolyases and Cry. CryDASH is found in a unique subset of organisms such as plants, cyanobacteria, insects and zebrafish, and little is known about their potential role in magnetoreception (for review see [110]).

Crys' magnetoreceptive function is largely built off biochemical models describing the creation of magnetically sensitive radical pairs via redox reactions from *Arabidopsis* and *Escherichia coli* [95,120]. Stereotypically, after light is absorbed by the FAD co-factor, electron transfer reduces fully oxidized FAD to form the radical semiquinone form ( ${}^S\text{FAD}^* \rightarrow {}^S\text{FAD}^{\bullet-}$ ) and oxidizes the first surface exposed TrpH, to form the radical-pair  ${}^S[\text{FAD}^{\bullet-} \text{TrpH}^{\bullet+}]$ , which is conserved in singlet form. From the singlet-state, several things may occur: 1) singlet-triplet interconversion via hyperfine and Zeeman interactions with the internal and external magnetic field  ${}^S[\text{FAD}^{\bullet-} \text{TrpH}^{\bullet+}] \leftrightarrow {}^T[\text{FAD}^{\bullet-} \text{TrpH}^{\bullet+}]$ , 2) the radical-pair can reverse transfer it's electron, regenerating the ground-state of the protein  ${}^S[\text{FAD}^{\bullet-} \text{TrpH}^{\bullet+}] \rightarrow \text{FAD} + \text{TrpH}$ , or 3) the deprotonation of the radicals can give rise to a second radical-pair, whose spin is proposed to not be amendable by magnetic fields  ${}^S[\text{FAD}^{\bullet-} \text{TrpH}^{\bullet+}]$  or  ${}^T[\text{FAD}^{\bullet-} \text{TrpH}^{\bullet+}] \rightarrow [\text{FADH}^{\bullet} \text{Trp}^{\bullet}]$  which then is slowly ( $\sim 10$  ms) brought back to the ground-state [33,95]. It has been hypothesized that short-wavelength light permits the formation of the initial,

magnetically sensitive radical-pair to form (RP1 in Figure 3), while long-wavelength light may influence the formation of the second radical pair (RP2, Figure 3). This wavelength-dependent process could provide one reason why short and long-wavelength light appear to affect animals' magnetic compass antagonistically [121,122]. The different spectral properties of FAD intermediates and how they may relate to magnetoreception are discussed in Chapter 3 (Figure 12).

Aside from biophysical models and calculations, it has been recently shown that Cry4 has a high affinity for FAD and is thus suitable for light-dependent magnetoreception [123]. Most vertebrate Type II Crys (such as Cry1 and Cry2) have low binding affinity for FAD and are probably not functional for radical-pair generation [123]. Cry4 is also only found in animals that exhibit magnetoreceptive behaviors such as birds, amphibians, reptiles and fish [112,117,119]. Cry4 from zebrafish and chicken have been shown to undergo blue light dependent conformational changes and has been isolated with large amounts of FAD, making it biologically suited for magnetoreception and light-dependent radical-pair generation [123-126]. Also, Cry4 appears to be more closely related to photosensitive Type I Crys of invertebrates [112,119], and from phylogenetic studies in fish, is predicted to have evolved earlier than vertebrate and invertebrate Type 1/2 Crys, suggesting its form is the ancestral state [117]. For these reasons, Cry4 appears to be best biochemically suited to be a candidate molecular magnetoreceptor.

For functional support of Cry-based magnetoreception, when Type I Cry is expressed ectopically in larval fruit fly motoneurons, application of a magnetic field increases action potential firing, showing that Cry can influence neural activity [115]. In addition to

theoretical and electrophysiological data, behavioral experiments in both *Drosophila* and cockroaches have shown that Cry is necessary for magnetoreceptive behaviors: flies without Cry were unable to respond to a trained magnetic stimulus that wild-type flies could detect [12]. Insertion of Type II Crys (such as the human ortholog Cry2), and butterfly Cry2 in Cry-deficient flies was able to rescue light-dependent magnetoreception, showing that various Cry types are sufficient for magnetoreception in the right biological system [13,71]. In *Drosophila*, other behaviors such as geotaxis, seizure susceptibility and circadian clock entrainment appear to also be modulated by Cry and magnetic fields [127-131].

Over the last two decades a wealth of theoretical, physiological, behavioral, and molecular data has suggested that Cry participates in LDRPM of various animals. Despite this, how magnetic signals are processed and interpreted remain unknown. LDRPM's requirement of light, and the magneto-relevant architecture of the eye make the visual system likely involved. In support of this, Crys in every functional group have been shown to be associated with the visual system of many different taxa. In sponges who lack opsins, Cry is found in the pigmented eye ring and is thought to mediate phototaxis in free swimming larval stages [132,133]. Cry is also found in the compound eyes of invertebrates such as fruit flies and cockroaches, and is suggested to have roles in circadian regulation, sun-compass tuning, and magnetoreception [12,14,134,135]. In zebrafish, multiple Crys are found in all layers of the larval and adult retina, but their function and cellular location remain unknown, and understudied [118,119,125,126]. In birds such as the garden warbler, Cry1b is in the RGC's, and inner segments of photoreceptors and is thought to play a circadian or magnetoreceptive role [85,136,137]. Cry1a on the other hand, is localized to the outer segments of European Robin and chicken UV cones and appears to be well-suited for light-

dependent magnetoreception [138,139] but see [123]. Recently, Cry4 has been described to localize with single long-wavelength and double cones of the night-migratory European robin and the non-migrating chicken, but currently its role in magnetoreception remains unknown [124]. Even in some mammalian species, Cry is associated with the visual system: Cry1 localizes to the short-wavelength photoreceptors, which are homologous to bird and fish UV cones, of fox, bear, dog and orangutan [140]. In humans, Cry2 is localized in the RGCs and appears to participate in light-independent circadian regulation [141].

Crys' localization to cone photoreceptors is particularly interesting for magnetoreception because it fulfills several requirements of LDRPM [36,69,89]. Anchoring to the outer segments of UV or double cones allows some degree of fixation of one Cry protein to relation to another, allowing the radical-pair outputs to be compared across the retina. Also, if Cry is paired to a visually transducing receptor (opsin), it might exploit the electrochemical pathway cones use to send signals to neuronal areas that process visual information, allowing the magnetic field to alter the visual perception of an animal [36,90,142]. Indeed, one of the leading ideas of the how magnetic fields may be perceived is best described as a lined-spatial pattern which overlays an animals' visual field (Figure 4). The light and dark lines result from individual photoreceptor-Cry cells being activated or inactivated, due to orientation with respect to the magnetic field (and ultimately the ratio of the products generated by singlet or triplet radical-pairs). In birds, it is specifically thought that the changing inclination is what alters their visual perception. If inclination is reversed  $180^{\circ}$  ( $90^{\circ}$  to  $-90^{\circ}$ ), while the horizontal magnetic field is unchanged ( $mN=mN$ ) migratory birds reversed their orientation  $\sim 180^{\circ}$ , illustrating that they are sensing the inclination (poleward vs equatorward) rather than the polarity (North pole vs South pole) [143].

Inclination compasses have been suggested for other long-distance migrants such as turtles, and short distance migrants such as newts, suggesting even small inclination changes could alter magnetic field detection [37,144]. Regardless, magnetic fields could be manifested in many undescribed ways. Currently, this is the leading model for how light-dependent magnetic information is processed.

Although studied extensively, the molecular mechanisms of magnetoreception continue to remain a mystery. The vertebrate light-dependent magnetoreception field has historically lacked mechanistic experiments, where the necessity and sufficiency of proximate mechanisms, such as receptors and neuronal areas are manipulated in a reliable and repeatable way, as seen in the invertebrate literature. This calls for the use of a vertebrate model that permits precise testing of molecular machinery but still possesses magnetically-dependent behavioral outputs.

### **1.5 Zebrafish as a model for light-dependent magnetoreception**

Zebrafish are an ideal model for studying molecular mechanisms of visually-mediated behaviors: these teleost fish undergo external fertilization and are transparent at early stages, which allows for easy monitoring of the developing visual system. By 51 hours post fertilization (hpf) opsin expression is detectable, and by 5 days post fertilization (dpf) zebrafish exhibit behavioral responses to light [145,146]. Additionally, zebrafish retina continues to grow throughout the life of the fish and can robustly regenerate retinal neurons after chemical, physical and light-induced damage [147-150], a characteristic that is found in most teleosts [151,152] but is limited in other models such as mouse and birds [153].

The zebrafish eye is extremely anatomically, genetically and physiologically conserved with other vertebrates. Zebrafish are tetrachromats that have four cone subtypes: UV (*sws1*), blue (*sws2*), green (*rh2-1, rh2-2, rh2-3, rh2-4*) and red (*lws1, lws2*) cones that are defined by their wavelength sensitive opsin. Additionally, rods (*rh1*) are low-light photoreceptors that mediate dim and night vision, that are present in the zebrafish retina [154-156]. In adulthood, cone photoreceptors are laid out in the retina as a precise mosaic with alternating rows of UV and blue cones, parallel to rows of red and green double cones with rods packed in between the cones. The mosaic is arranged so that the red cones flank the blue cones, and the green cones flank the UV cones [157-161]. In the larval zebrafish, the row photoreceptor mosaic is not as apparent, although they do contain stereotypical amounts of each photoreceptor type relative to each other. As the fish grows, more photoreceptors are added at the periphery of the retina and organized into the mosaic [161]. Although many animals contain mosaics, their function is largely unknown. A potential role in magnetoreception is discussed in Chapter 3.

Within the well-characterized visual system of zebrafish, many Cryptochromes have been recently described [118,119,125]. Despite their presence, the specific functions and cellular locations of Cry are not fully understood.

### 1.5.1 Zebrafish Cryptochromes

Members of the teleost lineage have the largest number of Crys present in modern day genomes [112,117,119]. Zebrafish Cry has undergone three whole genome duplications including the teleost specific genome duplication about 350MYA (for review see [162]). As such, zebrafish possess seven distinct Crys named: *cry1aa, cry1ab, cry1ba, cry1bb, cry2, cry4*

and *cry-DASH*. The *cry1*-paralogs have been exclusively shown to participate in core circadian regulation, which requires a nuclear localization sequence (NLS) and the ability to bind other core circadian proteins such as BMAL1 [118,119,125]. Cry1aa appears to remain light-sensitive but acts extremely similar to non-light sensitive Cry1/2 involved in mammalian circadian regulation [118,125]. The function of *cry2* and *cry4* remain yet to be identified. *cry2* has evolved an NLS and is found in the nucleus and cytoplasm but cannot bind BMAL1 and inhibit transcription related with circadian regulation. Additionally, *cry4* does not have an NLS and even when forced into the nucleus is unable to bind to BMAL1, suggesting it does not participate in core circadian regulation [118,125]. Zebrafish Cry4 has also been isolated with relevant amounts of FAD and has been shown to undergo light-dependent conformational changes, suggesting it could participate in light-dependent magnetoreception [126].

The various *crys* show different expression patterns in zebrafish; in larval fish, all *crys* are found broadly in the retina and the brain [118,119]. *cry4* is specifically expressed in the optic tectum and the intestine. In adult retina, *cry* expression seems to oscillate, in various cell types: *cry1* paralogs are highly expressed in most retinal layers during light time points, and lowly expressed at night. Notably, *cry2* has been suggested to be found in the outer nuclear layer (ONL), specifically in the short-wavelength cones right before light is turned on (Zeitgeber Time<sup>3</sup>, ZT=23). *cry4*'s expression seems to be limited to cone photoreceptors in the ONL at around noon (ZT=4) and is broad in the ONL throughout the day, with

---

<sup>3</sup> A Zeitgeber is an environmental cue used in the synchronization of animal's clocks. In this case, light is the Zeitgeber. ZT refers to the time after the environment cue (light) has been introduced to the animal. In these studies, and our own, Zebrafish were raised on 14:10 light-dark cycles, so ZT<14 refers time points with light, while ZT>15 refers to times without light. Here, the ZT is a 24-hour clock (i.e. is in between ZT=0 and ZT=24).

expression decreasing markedly after the lights are turned off [119,125]. Due to *cry4*'s potential location in cones, expression during times where light information is available, the inability to participate in circadian regulation, and localization with bound FAD, it appears to be best suited for LDRPM. In summary, zebrafish appear to have a visual system that could participate in light-dependent magnetoreception. Is there evidence that these teleosts are sensitive to magnetic fields?

### 1.5.2 Magnetoreception behavioral evidence and assays

Magnetoreception in zebrafish has been demonstrated in a variety of ways. One of the first studies demonstrated that groups of zebrafish were able to be trained to avoid a strong magnetic field associated with an electrical shock [163]. Since then, bimodal orientation<sup>4</sup> has been demonstrated in adult zebrafish numerous times [40,58,164]. Recently, a unimodal<sup>4</sup> (polar) response was shown in adult zebrafish in the dark [40]. Indeed, zebrafish appear to be sensitive to magnetic fields in light and dark, but the behavioral outputs seem to be different, suggesting the potential for multiple magnetoreception mechanisms. In agreement with this, when zebrafish are placed in an extremely strong magnetic field (MRI strength) in the light, swimming orientations are severely disrupted to the point where they appear to be flopping out of water, in their tanks [57]. When tested in the dark, this response is not seen, and instead zebrafish merely increase their swimming speeds and velocities. This locomotory response was attributed to the vestibular system being overstimulated, but the affect of light cannot be fully explained by this type of processing. In a somewhat related

---

<sup>4</sup> Bimodal orientation refers to preference along an axis, such as North-South. Unimodal or polar orientation refers to preference to a certain vector such as North or South only.

study, larval zebrafish reared in strong magnetic fields appear to have a high proportion of fused otoliths (usually two distinct inner ear placodes) [56]. In the same study, strong magnetic fields caused larval fish to orient unimodally parallel in the direction of the magnetic field. Other behaviors, such as rheotaxis (orientation relative to water flow) has been shown to be affected by magnetic fields [165]. Specifically, ablation of the lateral line, a fish specific, mechanosensory organ used to detect vibrations, altered but did not abolish the magnetic field affect on shoaling zebrafish rheotaxis. These recent studies suggest that zebrafish may use magnetic fields for a variety of purposes in daily life, whether it is orienting when shoaling, or navigating from floodplains to streams in their natural habitat [166,167]. It is likely that the detection of magnetic fields is mediated by multiple systems, each transducing slightly different magnetic information to the animal. Manipulation of the lateral line and involvement of vestibular system has been shown in zebrafish magnetoreception, but other areas such as the eye have yet to be tested.

Despite an increasing number of studies showing that zebrafish have light-specific magnetoreceptive behaviors, and have the molecular components for LDRPM, few mechanistic experiments that test the requirement of photoreceptors or Cry exist in fish. Zebrafish are amenable to various molecular manipulations, including targeted cell ablation, which is described below.

### 1.5.3 Nitroreductase-mediated targeted ablation

To ablate specific cell types, transgenic expression of bacterial enzymes can be taken advantage of. Nitroreductase (NTR) is an enzyme isolated from *E. coli* that can convert normally harmless prodrugs such as metronidazole (MTZ) into DNA crosslinking agents,

which ultimately causes cell-death via apoptosis [168]. Transgenically, NTR (*nfsb* gene) can be expressed under a cell-specific promoter (such as *sws1* to ablate UV cones) with no effect on non-NTR expressing cells [169-171]. In support of this, ablation of zebrafish photoreceptor subtypes expressing NTR does not create a toxic bystander effect in other retinal cells [169,170,172-174]. For magnetoreception this is particularly practical since the location of the magnetoreceptor is unknown. Whole organism gene knockout of Cry would be useful to determine if Cry is involved but does not point to what sensory system Cry is specifically interacting with. Additionally, fluorescent proteins fused to NTR have been created, which allow the visualization of cells before and after ablation [172,174]. If expressed in a regenerating population, such as the zebrafish cones, regeneration of the cells can be observed via fluorescent microscopy. For these reasons, cell specific ablation is a powerful tool that is well-developed in zebrafish. There are many other tools designed to manipulate zebrafish genetics; those potentially interesting to magnetoreception are discussed in Chapter 3.

With a growing amount of behavioral evidence, the presence of currently untested molecular candidates, and the ability to selectively manipulate potential genetic and cellular mechanisms, zebrafish are ideally suited to study vertebrate light-dependent magnetoreception.

## **1.6 Purpose of study/ objectives**

The overall aim of this thesis was to generate evidence for a light-dependent, Cryptochrome-based magnetoreception complex in fish. Using zebrafish, I set out to test

whether *cry* interacted with cone photoreceptors, as seen in migratory birds. Since Cry activation and magnetoreception seem to largely require short-wavelength light, I focused on the short-wavelength photoreceptors found in zebrafish (UV and blue). Due to Cry1a's association with UV cones in birds, and the potential role that UV cones play in fish navigation, I hypothesized *crys* with unknown roles (either *cry2* or *cry4*) would be expressed in UV cones. To do this, I measured non-circadian *cry2* or *cry4* mRNA in larval and adult zebrafish retina using qualitative and quantitative gene expression assays such as *in situ* hybridization and RT-qPCR.

The visual system is highly similar between zebrafish and other vertebrates, including birds, but zebrafish are truly advantageous because they can be used to implement precise molecular manipulation of retinal photoreceptors. To experimentally test the Cry-cone association, I utilized targeted cell ablation to selectively ablate UV and blue cones from larval and adult zebrafish retina to test how *cry* mRNA expression patterns and levels changed after cone removal. I predicted that ablation of UV cones would decrease *cry* mRNA, while blue cone ablation would not disrupt *cry* expression. Ablation of neighboring blue cones served as an important control, to ensure the mere disruption of the cone mosaic (i.e. any cone being removed) didn't cause indirect expression changes of *cry*. I tested Cry-cone interactions throughout development, to see if any ontogenetic changes were present. Zebrafish magnetoreceptive behavior has been characterized in adults, and various larval fish appear to have well-established magnetic compasses but the way in which fish detect magnetic fields is still largely unknown.

Ultimately, the evidence generated here serves to build the molecular basis of fish LDRPM and will hopefully catalyze further mechanistic investigation into whether UV cones and/or Cry mediate magnetoreception in fish.

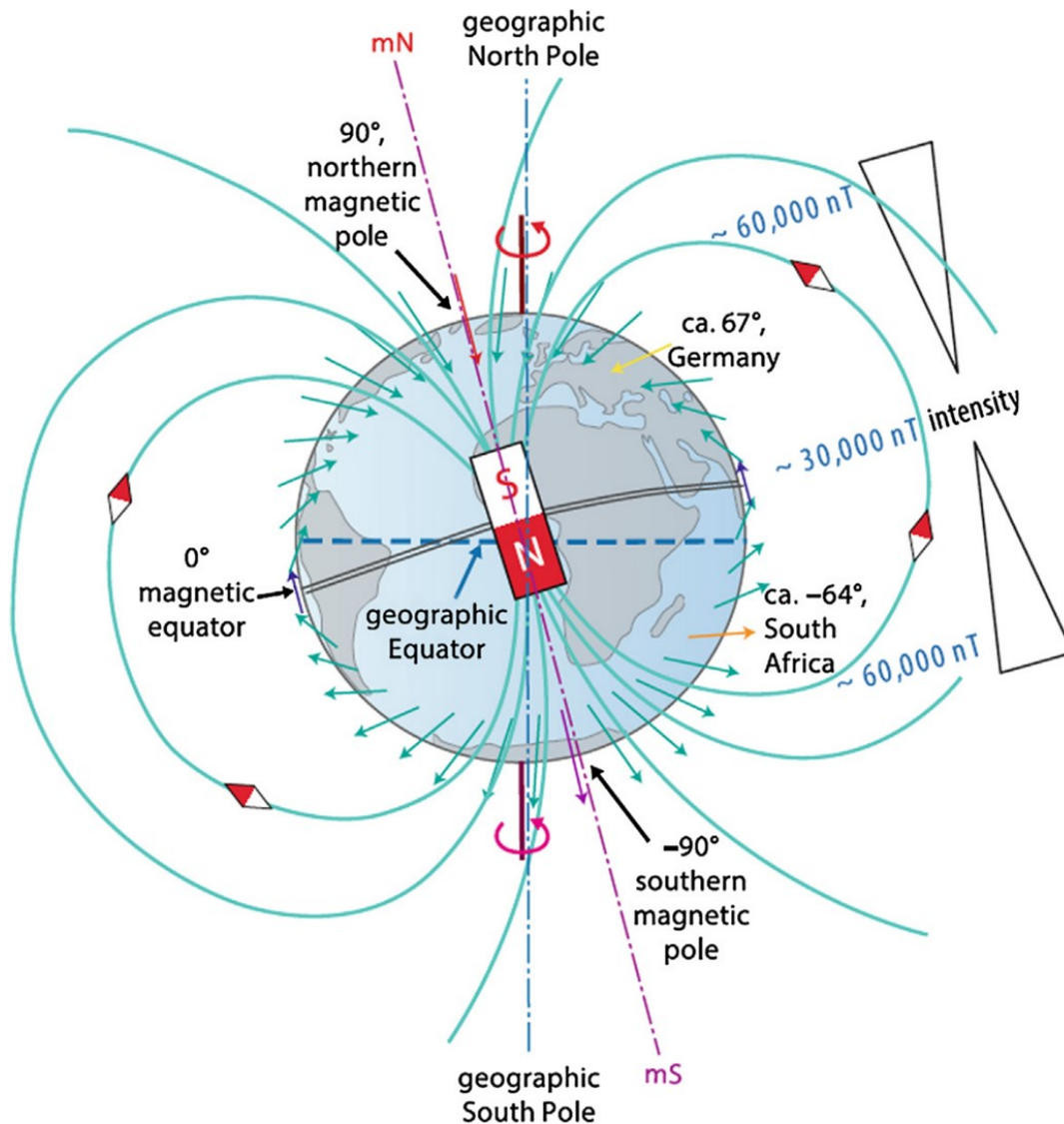


**Figure 1. The geomagnetic field.** The Earth's magnetic field is similar to a bar magnet, and somewhat confusingly does not align with our geographic poles. Despite this, we name the magnetic pole close to the geographical North pole, Magnetic North (mN) and same with the South pole. The angle between magnetic and geographical poles varies and can be measured as declination. Intensity is greatest at the poles and weakest at the Equator. Inclination is shown as green arrows that intersect with the Earth at different angles, with the greatest angles at the North (red arrow) and South (pink arrow) poles. mN= magnetic North, mS= magnetic South. Reused with permission from [2].

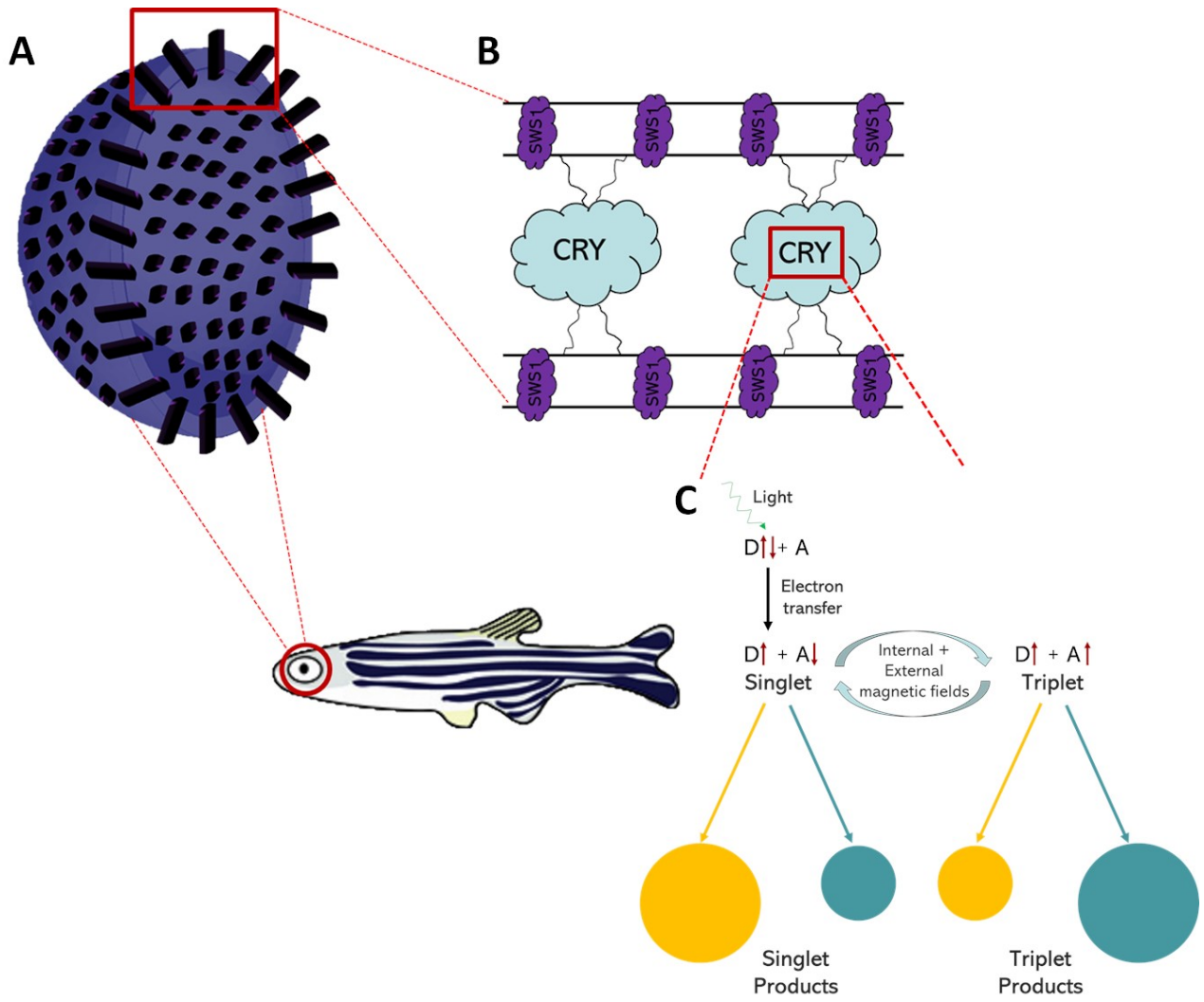


**Figure 2. Model of light-dependent magnetoreception.** **A)** Cone photoreceptors along the back of the hemispherical retina serves as an ideal scaffold for magnetoreception. **B)** Cry (aqua) may be located in cone outer segments between UV opsin proteins (*sws1*; magenta) as seen birds. This relationship allows Cry to be semi-fixed in cellular space and could permit communication between Cry and opsin, allowing visual transduction to be altered by magnetic fields. **C)** After light initiates an electron transfer from a Donor (D) to an Acceptor (A), both internal and external magnetic fields can alter singlet-triplet interconversion rates between radical-pairs. In the singlet-state, electrons spin antiparallel in relation to each other (illustrated by the same orientation of each red arrow). In triplet-state, electrons spin in parallel, increasing the time spent in signaling form. The time spent in each state could result in a different signal, such as a neurotransmitter or electrical output, resulting in a magnetic sensor. Adapted from [2,36].

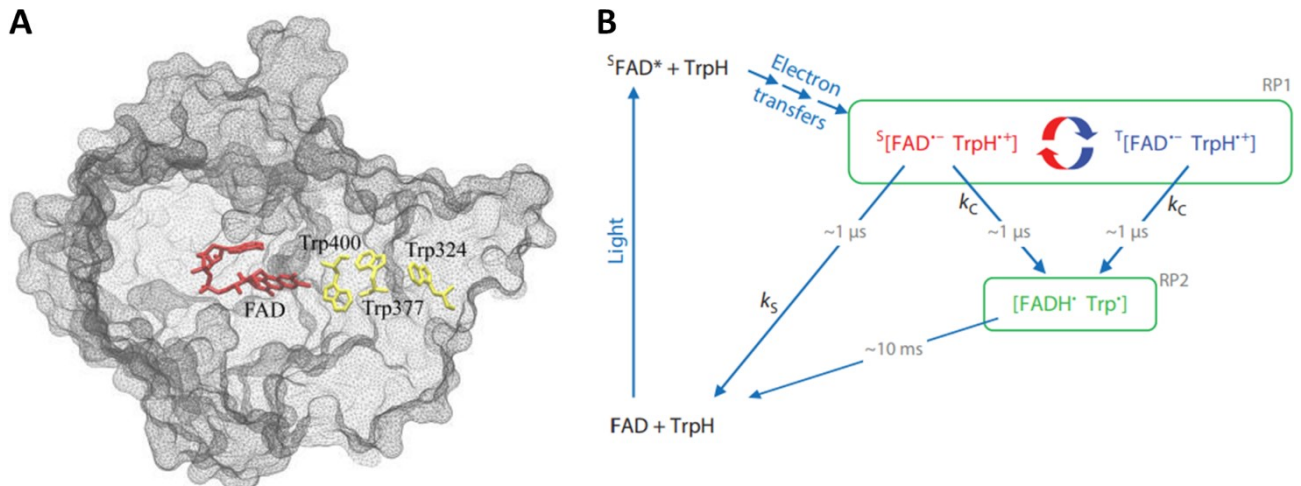


**Figure 3. Cryptochrome can create radical-pairs between FAD and Trp. A)** Protein model of *Arabidopsis* Cry highlighting the three conserved Trp residues in yellow, that mediate electron transfer between them and FAD co factor. **B)** Reaction scheme outlining the creation of the magnetically sensitive radical-pair (RP1) and the protonation of FAD, Trp or both to create the non-magnetically sensitive radical-pair (RP2). Light excites FAD to the fully oxidized form  $^5\text{FAD}^*$  which is conserved in the singlet-state. Electron transfer creates either singlet or triplet-state radical-pairs of FAD and Trp depending on the external or internal magnetic field (red/blue arrows).  $k_C$  is the equilibrium constant and time it takes for the radical-pairs to deprotonate ( $1\mu\text{s}$ ).  $k_S$  is the time it takes for the singlet RP1 to back transfer to ground-state. Reused with permission from [33,114].

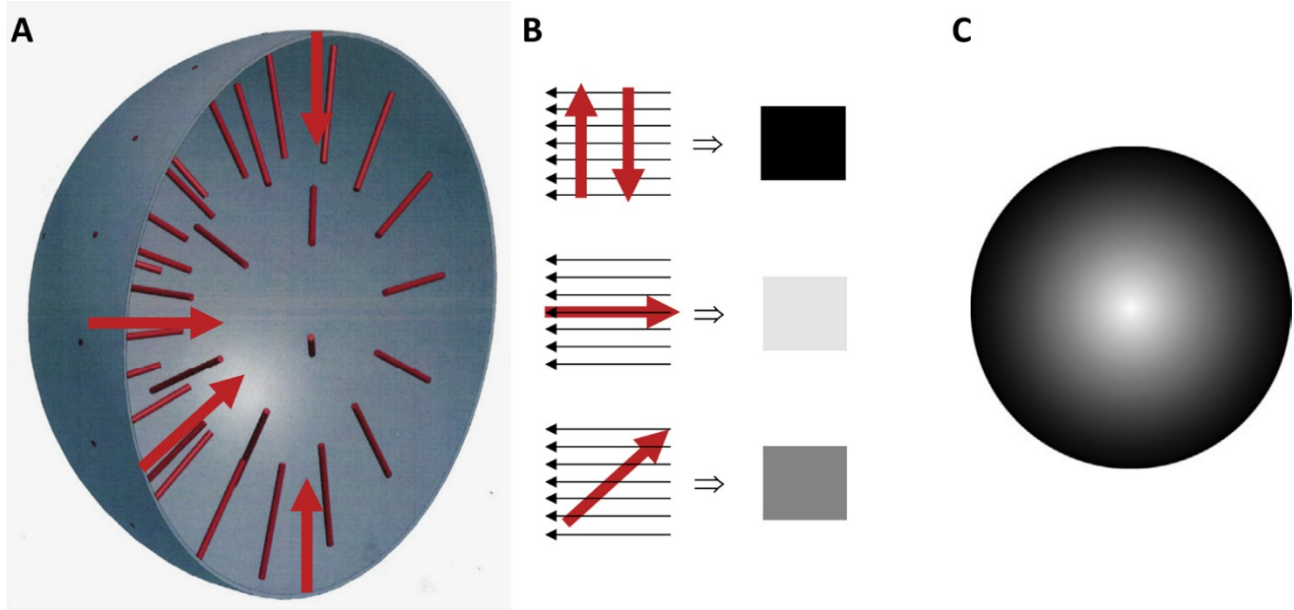


**Figure 4. How the magnetic field may alter animals' visual perception. A)** Magnetoreceptors are shown as red rods and are represented throughout all spatial orientations of the eye. **B)** Depending on the orientation of the magnetoreceptor relative to the magnetic field (black arrows), the resulting output (denoted as black, white or grey squares) may be different. **C)** If this interacted with the visual transduction process, it may cause a change in visual perception across the animal's visual field. Reused with permission from [2] based on [36].

## 2 EXPLORING POTENTIAL FOR LIGHT-DEPENDENT MAGNETORECEPTION IN ZEBRAFISH: CRYPTOCHROME 4 IN A SELECT SUBTYPE OF RETINAL PHOTORECEPTORS

### 2.1 Introduction

Many organisms use magnetic fields to orient in local spaces or to navigate long-distances. Although magnetoreception has been studied extensively, the underlying mechanisms remain debatable and unknown [175]. Cryptochrome (Cry) is the primary molecular candidate that creates light-dependent radical-pairs sensitive to magnetic fields [32,36,176]. Cry is associated with the bird visual system where it is co-localized with both short- and long-wavelength cone photoreceptors [124,138], and thus is well-positioned for light-dependant activity. Notably, *crys*' location in other animal's photoreceptors is unknown. Here, we used zebrafish to determine if fish *cry* might have a light-dependent magnetoreceptive role. Zebrafish have six *cry* paralogs; whereas most of these participate in circadian clock regulation, the function of *cry2* and *cry4* remain unknown [118,119]. We demonstrate that *cry4* is expressed in zebrafish retina, principally in the short-wavelength ultraviolet (UV) cone photoreceptors. Using nitroreductase-mediated cell ablation and RT-qPCR, we found that *cry4* expression decreased when UV cones were ablated, but not when blue cones were ablated. *cry2* expression was unchanged after either UV or blue cone ablation. Although zebrafish magnetic behavior has only been reported in adults [40,58,163,164], this work suggests larval fish may also have the molecular framework for light-dependent magnetoreception. Sockeye salmon fry, larval coral reef fish and larval

medaka have been shown to be responsive to magnetic fields [5,40,177], but the mechanisms remain mysterious. These findings provide one potential explanation, inasmuch that UV cones appear poised for light-dependant magnetoreception via photoreceptor subtype-specific expression of *cry*.

## 2.2 Methods

### 2.1 Animal Ethics

The Animal Care and Use Committee: BioSciences (an Institutional Animal Care and Use Committee at the University of Alberta, operating under the Canadian Council on Animal Care) approved this study under protocol AUP00000077.

### 2.2 Zebrafish Maintenance

Zebrafish (*Danio rerio*) were raised according to standard procedures [178]. Larvae were treated with PTU (1-phenol-2-thiourea) beginning at around 9 hours post fertilization (hpf) to block formation of melanin pigment [179]. Beginning at 5 days post fertilization (dpf), larval fish were fed powdered fish food. Larvae were maintained in E3 embryo media at 23-25°C on a 14L:10D cycle until fixation at 8 dpf.

Adult fish were maintained at 28°C under standard fluorescent lights on a 14L:10D cycle and were fed twice daily with brine shrimp and trout chow [178].

### 2.3 Nitroreductase-Mediated Ablation

*Tg(sws1:nfsb-mCherry)* or *Tg(sws2:nfsb-mCherry)* larvae were treated with either 10mM metronidazole (Sigma-Aldrich, Cat. No. M3761-25G; Oakville, O, MTZ) with 0.1% DMSO in E3 media or 0.1% DMSO in E3 media as a vehicle control for 24 hours beginning at 6dpf. Larvae were washed three times with E3 media and euthanized at 8dpf at either Zeitgeber Time (ZT)=4 or ZT=20. Tissues were fixed in 4% paraformaldehyde in 0.1M phosphate buffer + 5% sucrose, pH 7.4 (PFA), overnight at 4°C.

*Tg(sws1 or sws2:nfsb-mCherry)* adult zebrafish (approximately 1 year old) were treated with MTZ as described above except that system water replaced E3 media. Fundus imaging confirmed ablation of cones prior to euthanasia as per published methods [150]. After 6 days, adults were euthanized at either ZT=4 or ZT=20 with an overdose of MS-222. Fish were cervically dislocated before eyes were removed. Full eye was removed from fish in the day (ZT=4) or at night under minimal red light (ZT=20) and placed directly into either 1mL of RNALater (Invitrogen, AM7020) or 4% PFA on ice. Retinas were removed after eye dissection.

A complete description of fish lines used in this study can be found in Table 1.

### 2.4 Riboprobe production and Fluorescent *In-Situ* Hybridization

Riboprobe template primers with a T7 transcriptase binding site (TAATACGACTCACTATAGGG) were used to make template for riboprobe synthesis against *cry* paralogs (Table 2). Template was confirmed with the presence of a single band after gel

electrophoresis. Riboprobes to opsins were synthesized from plasmids as previously described [161]. DIG labelled *cry* and FLR labelled *sws1* riboprobes were made as previously described [180]. Reverse transcription was mediated by T7 polymerase overnight at 37°C. Riboprobe concentration and quality was determined by Nanodrop spectrophotometer (GE Healthcare 28 9244-02) and RNA gel electrophoresis.

Double fluorescent *in situ* hybridization for *sws1*, *cry2* and *cry4* was performed as previously described [161,180]. Tissue was hybridized with 1µg/ml of riboprobe at 58°C overnight. After SSCTw-stringency washes, and incubation of secondary antibody (1:100; α-DIG-POD, Roche 11207733910 or α-FLR-POD, Roche 11426346910 diluted) overnight at 4°C, the tissue was incubated in 1:100 tyramide conjugated to AlexaFluor 488, 555 or 647 TSA SuperBoost™ (Thermo Fisher Scientific, B40912, B40913, B40916). After development of each fluorescent signal (15-18 hours at 4°C for larval *sws1*, *cry2*, *cry4*, 10-15 minutes at 25°C for adult tissues) the antibody was deactivated by incubation in 3% H<sub>2</sub>O<sub>2</sub> in PBSTw for 30 minutes at room temperature, and the next antibody was added. After PBSTw washes, larval eyes were dissected as described above and flat mounted in 70% glycerol for imaging. Cuts were made on each side of adult retina, flattened, and mounted in 70% glycerol for imaging.

## 2.5 RNA Isolation

### 2.5.1 Whole Larvae

RNA was isolated from pooled samples of n=5 whole larval zebrafish (8 dpf) or single adult eyes raised on a 14L:10D cycle collected at either ZT=4 or ZT=20. Samples were stored in

RNAlater (Ambion AM7021) at 4<sup>0</sup> C until extraction. Total RNA was extracted from pools of larval zebrafish using the RNAeasy Mini Kit (Qiagen 74104) according to the manufacturer's instructions. Samples were homogenized in 600 µl of Buffer RLT containing 1% of β-mercaptoethanol with a rotor stator homogenizer (VMR 47747-370), and put through an on column DNase digestion using Qiagen DNase I. After Buffer RPE washes, RNA was eluted in 32 µl of Nuclease-free H<sub>2</sub>O (Ambion 4387936).

### 2.5.2 Adult Eye

RNA from single adult whole eyes was isolated using RNeasy Lipid/Tissue Mini Kit (Qiagen 74804) according to the manufacturer's instructions. Samples were homogenized in 700 µl of Qiazol with a rotor stator homogenizer. After phenol:chloroform extraction, DNase digestion and Buffer RPE washes, RNA was eluted in 32 µl of Nuclease-free H<sub>2</sub>O (Ambion 4387936). RNA quantity was determined by a Nanodrop spectrophotometer (GE Healthcare 28 9244-02) and Agilent 2100 Bioanalyzer (Agilent RNA 6000 NanoChip). All samples had similar rRNA (18s and 28s) profiles and RNA integrity numbers (RIN values) of 8.0 or greater.

## 2.6 RT-qPCR

### 2.6.1 cDNA synthesis

RNA input was standardized to 500ng per cDNA reaction. cDNA was generated using qScript cDNA Supermix (Quanta Biosciences 95048-025) as per manufacturer's instructions. Each reaction consisted of 10 µl, with x µl of RNA (500ng total RNA each reaction), 2 µl of qScript

Mastermix, and  $x$   $\mu$ l of Nuclease-free H<sub>2</sub>O. cDNA was diluted 1:10 for following RT-qPCR experiments.

### 2.6.2 RT-qPCR Parameters

Reverse transcription quantitative-PCR (RT-qPCR) experiments follow MIQE guidelines [181]. RT-qPCR was completed using a 7500 Real-Time PCR system (ABI, Applied Biosystems) with 2X QPCR Mastermix (\*Dynamite\*) (MBSU, University of Alberta). Transcript abundance for *cry2*, *cry4*, *sws1* and *sws2* was assessed relative to  $\beta$ -*actin*, an endogenous housekeeping gene optimized for zebrafish [182,183] (and see *Endogenous Control Stability Assay*). Technical replicates were performed in triplicate. Biological sample sizes are stated for each experiment in respective figure legends.

### 2.6.3 Endogenous Control Stability Assay

To ensure  $\beta$ -*actin* was a suitable endogenous control, an endogenous stability assay was performed (Figure 11). Average Ct values were compared between n=3 DMSO and n=3 MTZ treated pools of larvae after blue and UV cone ablation. Ct values ranged from 17.90 to 19.80 (Average =  $19.01 \pm 0.39$ ). Each biological replicate was tested in triplicate.

### 2.6.4 Primer Validation

RT-qPCR primers were designed using Primer Express 3.0 software and verified with a standard serial dilution to determine efficiency [181]. Primers were designed at the end of the 3' exon in each gene or the 3' UTR and were expected to amplify all splice variants. Primer

sequences and efficiencies are available in Table 3, where a slope of  $<0.1$  indicates the efficiency of the target amplification is approximately equal to the reference amplification, and thus the primers are suitable for the experiment [184]. To assess primer specificity disassociation curves were analyzed, and only primers producing a single peak indicating a specified product, were used.

## 2.7 Microscopy and Imaging and Figure Assembly

Fluorescent images were taken on an LSM 700 inverted confocal microscope mounted on a Zeiss Axio Observer.Z1, and captured using ZEN 2010 software (version 6.0, Carl Zeiss AG, Oberkochen). 63X oil (NA =1.4) or 40X water (NA 1.4) objectives were used to image flat mounted larval or adult zebrafish retina. Figures were assembled in PowerPoint (version 1710, Microsoft Office 365 ProPlus). Images were manipulated for contrast & brightness in Zen 2010. Cartoon zebrafish were obtained under a free culture Creative Commons license (CC BY-SA 4.0) from Mind the Graph (Version March 03, 2016, Mind the Graph LLC, [www.mindthegraph.com](http://www.mindthegraph.com)).

## 2.8 Statistics

For RT-qPCR experiments  $n>3$ , Mann-Whitney U Tests were calculated and performed in GraphPad Prism (Version 7.02 for Windows, GraphPad Software, La Jolla California USA, [www.graphpad.com](http://www.graphpad.com)). For RT-qPCR experiments  $n=3$ , unpaired t-tests with Welch's correction were performed in GraphPad Prism. Data is presented as mean  $\pm$  standard error

of the mean (SEM). Significance is denoted in figure legends ( $p$  at least  $<0.05$ ). Each pool ( $n=5$ ) of larval 8dpf zebrafish and each single adult eye is considered as an independent biological replicate.

## 2.3 Results and Discussion

### 2.3.1 Expression of *cry4* in larval zebrafish retina

Cry has been suggested to function in light-dependent magnetoreception in flies, cockroaches, butterflies and a variety of birds [13,14,71,143] but its role in fish magnetoreception has largely been overlooked. Many fish undertake long distance migrations, exhibit magnetic behaviour [5,9,21,24-26,40,58,60,163-165,185] and contain various *crys* [117-119,125], but little is known about the cellular location and function of these putative magnetoreceptors. To test if *cry2* or *cry4* mRNA was expressed in zebrafish UV cones (which express *sws1* opsin), double fluorescent *in situ* hybridization was performed on larval zebrafish aged 8 days post fertilization (dpf) that were fixed at midday (at zeitgeber time (ZT) = 4). *cry2* expression was apparent in the focal plane where cone photoreceptors reside, but did not strongly overlap with *sws1* opsin expression, suggesting it is not highly expressed in UV cones (Figure 5A-A'''), but perhaps is in other photoreceptor subtypes. *cry4* showed stronger expression throughout the retina and overlapped consistently with *sws1* expression (Figure 5B-B'''). *cry4* was expressed within the vast majority of labelled UV cones, and was not detected within neighbouring photoreceptors, suggesting it is UV cone specific. Expression of *cry2* and *cry4* has previously been described in larval zebrafish retina as being broadly distributed throughout all retinal layers at 5dpf, at least during time points in which they are highly expressed (ZT=23, ZT=15 respectively)

[119]. Specifically, *cry2* and *cry4* have been shown to be expressed strongly in the larval outer nuclear layer (ONL) where photoreceptors reside [119], in a cyclic circadian manner [118]. The results presented here support a cellular localization for *cry4* in larval zebrafish UV cones during the day.

### 2.3.2 *cry4* is specifically expressed in the UV cone subtype of larval zebrafish

The implied expression of *cry* within a specific photoreceptor subtype was very intriguing, as *cry* is the best candidate proximate mechanism of light-dependant magnetoreception. To validate that *cry4* was expressed within UV cones, a combination of pharmacological and transgenic technologies was used to specifically ablate the short-wavelength cones. *Tg(sws1:nfsb-mCherry)* and *Tg(sws2:nfsb-mCherry)* are well-characterized transgenic lines that have nitroreductase (NTR) expressed within UV or blue cones, respectively [174]. NTR expression alone appears to be inert to the cells. After addition of a prodrug (Metronidazole- MTZ), NTR converts MTZ into a cell-autonomous cytotoxin that causes DNA cross linking and induces the cells to undergo apoptosis [170,172]. Previous work supports that this technique is cell-specific and has no discernable bystander effects on adjacent photoreceptors [170,173,186].

As seen in untreated larvae (Figure 5B), we found that control fish with UV cones (NTR-transgenic larvae treated only with vehicle control DMSO) expressed *cry4* within UV cones (Figure 6A'-A'''). Following ablation of UV cones by treating NTR-transgenic larvae with prodrug MTZ, *cry4* abundance was dramatically decreased throughout the larval retina (Figure 6B'-B''') and was apparent only within the few surviving UV cones. RT-qPCR

confirmed this, as *cry4* mRNA levels decreased approximately 60% after UV cone ablation (Figure 6C; Mann-Whitney U,  $p=0.007$ ). On the other hand, *cry4* did not significantly change in abundance when the neighbouring blue cones were ablated (Figure 6E  $p>0.9999$ ). *cry4* expression was also unchanged when non-transgenic control larvae (AB/Wik strain) were treated with MTZ, confirming that the addition of the prodrug MTZ does not itself measurably influence *cry4* expression (Figure 6E,  $p=0.7182$ ). Further, a paralogous gene *cry2*, was not found to have its transcript abundance altered by ablation of UV cones ( $p=0.1081$ ) or blue cones ( $p>0.9999$ ) (Figure 9), suggesting a specialized expression pattern for *cry4*.

The localization of *cry4* to UV cones in larval zebrafish was thoroughly validated, because two independent methods confirmed that *cry4* abundance substantially decreased when UV cones were ablated; this did not occur when blue cones were ablated, and a paralogous gene, *cry2*, was unaltered in its abundance when UV cones or blue cones were ablated.

These findings suggest larval zebrafish retina contains the molecular basis of a light-dependent magnetoreception complex. Furthermore, *cry4* appears to be well-positioned, i.e. localized within a subtype of retinal cone photoreceptors, to mediate light-dependant mechanism(s). Although currently there is sparse evidence for larval zebrafish being magnetoreceptive [40,56], larval coral reef fish have a well-established magnetic compass that is primarily used when celestial compasses (sun/star) are unavailable [24,177]. *cry4*'s localization in zebrafish UV cones at ZT=4 (midday in our rearing conditions, 1200 MDT) coincides with a time when the sun is stereotypically directly overhead a tropical animal and

may not provide useful directional information. Indeed, at these time points, larval coral reef fish have near-random orientation when tested for sun compass orientation behavior [187]. Although this time varies seasonally and geographically (i.e. the sun is not always directly overhead at ZT=4 or 1200 MDT), and polarized light may influence magnetic orientations at solar noon [75], this could be a general time point where light-dependent magnetoreception would be useful. It would be interesting to see *cry4*'s expression in the retina of larval reef fish who have well-defined magnetic compasses.

### 2.3.2 *cry4* is expressed in adult zebrafish UV cones

Next we tested if *cry4* remains associated with UV cone photoreceptors throughout ontogeny into adulthood, where zebrafish magnetoreceptive behaviour has been demonstrated [40,58,163,164]. In adult zebrafish, *cry4* was found to be abundantly expressed in UV cones (Figure 7A-A''). As above, a paradigm ablating UV cones in adult fish at midday (ZT=4) demonstrated a concerted decrease in *cry4* abundance (Figure 7B-B''). Quantitatively, *cry4* mRNA was decreased approximately 40% at ZT=4 following UV cone ablation (Figure 7C, ZT=4,  $p=0.041$ ; Figure 7B).

In the adult zebrafish retina, *cry4* has previously been shown to be expressed in the ONL and the inner nuclear layer (INL) at ZT=4. In the ONL at ZT=4, it was suggested that *cry4* might be localized to cone photoreceptors [119]; that interpretation lends further support that UV cones are the specific photoreceptors in which *cry4* is expressed in. *cry4*'s abundance is also known to vary over circadian time [119,125]; thus, we considered if *cry4* might have different abundances at night following cone ablation. At night (ZT=20; 0400 MDT), UV cone

ablation did not measurably change *cry4* expression (Figure 7E;  $p=0.09$ ). This was expected, as *cry4* expression appears to be almost non-existent in the zebrafish retina at this time point [119]. The remaining *cry4* transcript that was detected is likely in other retinal cell types (not UV cones). The significant decrease of *cry4* between ZT=4 and ZT=20 (Figure 7E;  $p=0.031$ ) reinforces that *cry4* abundance appears to be cyclic in the retina [118,119,125]. In other animals, such as zebra finch, European robin and chicken, *cry4*'s expression in the retina appears to be constant throughout circadian time [124,188], irrespective of the presence of light. The effect of light on turnover rates of Cry4 protein is currently unknown, but when birds are exposed to 30 minutes of complete darkness, activated Cry1a that is usually localized in bird UV cones is not detectable in the retina [189].

### 2.3.3 Blue cone ablation does not measurably disrupt *cry4* abundance in adult retina

Ablation of blue cones in adult zebrafish at either ZT=4 or ZT=20 (Figure 8A-A') did not change *cry4* mRNA levels (Figure 8B; ZT=4  $p=0.771$ ; ZT=20  $p=0.856$ ) suggesting that *cry4* is not expressed in adult blue cones. A significant decrease of *cry4* from ZT=4 to ZT=20 was observable irrespective of blue cone ablation (Figure 8B; DMSO  $p=0.048$ ; MTZ  $p=0.011$ ) as described elsewhere (Figure 8, [119]). This data supports that *cry4* expression in the short-wavelength cones is primarily restricted to the UV cones in both larval and adult zebrafish. The apparent absence of *cry4* in blue cones, and its abundance in UV cones, could suggest a cellular connection with magnetoreceptive purpose; it has been theorized that to separate visual information from magnetic information, two side-by-side receptors that receive the same light input would be beneficial [33,124]. The most immediate retinal cells that compare information between adjacent photoreceptors are the horizontal cells in the

INL. Outputs from UV and blue cones are processed by a specific type of horizontal cell (H3 cells) [190-192]. The separation of magnetic signals could be accomplished by the output of *cry4*-containing UV cones being compared to the output of neighbouring, similarly short-wavelength-sensitive, non-*cry4* containing blue cones by H3 cells [139]. Additionally, zebrafish UV and blue cones were recently described to be connected at the synaptic level via telodendria [186]. The spectral sensitivities of UV and blue cones overlaps significantly at about 375 nm-400 nm in zebrafish [156,193,194] and the interesting synaptic connections they make at the cone pedicle suggests they are sharing information at the receptor level before sending signals downstream for further processing. This type of “immediate” signal integration could point to the retina’s early efforts to disentangle magnetic and visual information.

#### 2.3.4 *cry4* and cone photoreceptors as potential magnetoreceptors in fish

In summary, our results demonstrate that UV cones in larval and adult zebrafish express a putative molecular magnetoreceptor, *cry4*. This was observed in midday time points (ZT=4) and was disrupted by UV cone ablation but unaltered after blue cone ablation. Additionally, paralogous *cry2* was unchanged after UV and blue cone ablation in larval and adult zebrafish. Although it is still unknown if *cry4* or any Cry functions as a magnetoreceptor in vertebrates, it appears the relationship between Cry and cone photoreceptors is present in a diverse range of taxa. In European robins and chicken, Cry1a is localized in the UV cones and is active when exposed to short-wavelengths that permit magnetic orientation behavior [68,189,195]. Cry1 is also found in S1 short-wavelength cones (‘blue cones’ homologous to UV cones of birds and fish) in a variety of mammalian species [140]. *cry4*’s retinal location in

other fish has yet to be described, but in birds, Cry4 has recently been shown to clearly be localized in the long-wavelength single cones and double cones of European robin and chicken [124]. Why the cellular location of Cry4 may be different between fish and birds is currently unknown; the very divergent life histories of zebrafish and migratory birds cannot be ignored. The differences in the spectrum of available light in air versus water [196-198] could also point to why different photoreceptors may contain *cry4*. Additionally, photoreceptor subtypes vary significantly in birds when compared to zebrafish; birds have individual red and green cones and unique paired double cones that express a specific opsin not found in fish [199-202], while zebrafish have paired double cones that have red and green sensitive counterparts [156,161,203]. *cry4* may also be lowly expressed in the red/green double cones of zebrafish, but this requires further investigation. In support of UV cones being important for fish navigation, they have previously been suggested to mediate the detection of polarized light [204,205]. Also, when migratory salmon reach sexual maturity and return to their natal streams, a population of UV cones regenerate after most degenerate during metamorphosis [206-208]. It is tempting to suggest a magnetoreceptive link with *cry4*'s expression in UV cones, but more work is needed to formally test this idea.

These among other recent findings provide exciting evidence that fish may contain a light-dependent magnetoreceptor. New, robust behavioral experiments [26,40] utilization of genome editing (CRISPR-Cas9; [209]) next gen RNA-Sequencing after magnetic field manipulations [210,211] and advances in visualizing neuronal activity (Ca<sup>2+</sup> imaging; [212,213]) will be key in determining the requirement of Cry and cone photoreceptors in fish magnetoreception.

**Table 1. Transgenic zebrafish lines used in experiments.**

Genotype	Description	ZFin ID	Reference
<i>Tg(sws1:nfsb-mCherry)</i>	This line expresses nitroreductase ( <i>nfsb</i> gene)-mCherry fusion protein in UV cones ( <i>sws1</i> ). Nitroreductase converts prodrugs such as MTZ into DNA cross-linking agents, inducing targeted ablation via apoptosis. The mCherry tag allows fluorescent visualization of these cells.	ZDB-ALT-080227-1	[174]
<i>Tg(sws2:nfsb-mCherry)</i>	This line expresses nitroreductase ( <i>nfsb</i> gene)-mCherry fusion protein in blue cones ( <i>sws2</i> ), which can allow for targeted ablation as described above.	ZDB-ALT-160425-3	[174]

**Table 2. Primers used for Cryptochrome riboprobe synthesis.**

Gene	ZFin ID	Primer sequences (forward, reverse; <b>T7 promoter sequence in red</b> )
<i>cry2</i>	ZDB-GENE-010426-6	F: 5' CCCTTGTCGCTCTTTGGTCA '3 R: 5' <b>TAATACGACTCACTATAG</b> GGACTGCCGTTTCCTGTTTTCT '3
<i>cry4</i>	ZDB-GENE-010426-7	F:5' GACAGTGGCGCAGGAAAATG '3 R: 5' <b>TAATACGACTCACTATAG</b> GGCGCACCTGACGCATCAATTC '3

**Table 3. RT-qPCR primers used for Cryptochrome mRNA quantification.**

Gene	ZFin ID	Primer sequences (forward, reverse)	Amplicon length (bp)	Slope of $\Delta$ CT vs. log (input)	Amplicon location (exon #/ total exons)
<i>cry2</i>	ZDB- GENE- 010426 -6	F: 5'- GCAGTGACCGCAGGT TGAA-3'  R: 5'- GGATGGTTCGGAGAG GTGAA-3'	78	0.02	3'UTR (11 exons)
<i>cry4</i>	ZDB- GENE- 010426 -7	F: 5'- GGCTGCATCATCGGT AAAGAC-3'  R: 5'- CGCATCAATTCAGGT TCCT-3'	80	0.09	9/11
<i>sws1</i>	ZDB- GENE- 991109 -25	F: 5'- TCCTCCCGCAGCACAT TTAC-3'  R: 5'- AAAGTTACGGGATTT GAACAATCAG-3'	80	0.07	5/5
<i>sws2</i>	ZDB- GENE- 990604 -40	F: 5'- CTATCTTTGCAATCTG GGTGGTT-3'  R: 5'- AAAGGCAGGAGGGAA TGTT-3'	78	0.09	4/5
$\beta$ - <i>actin</i>	ZDB- GENE- 000329 -1	F: 5'- CGGACAGGTCATCACC ATTG-3'  R: 5'- GATGTCGACGTCACAC TTCA-3'	136	Validated in [183] †	4-5/5

†  $\beta$ -actin transcript abundance was found to be stable across treatments herein; Ct values not significantly different when UV or blue cones were ablated (Also see Figure 11).

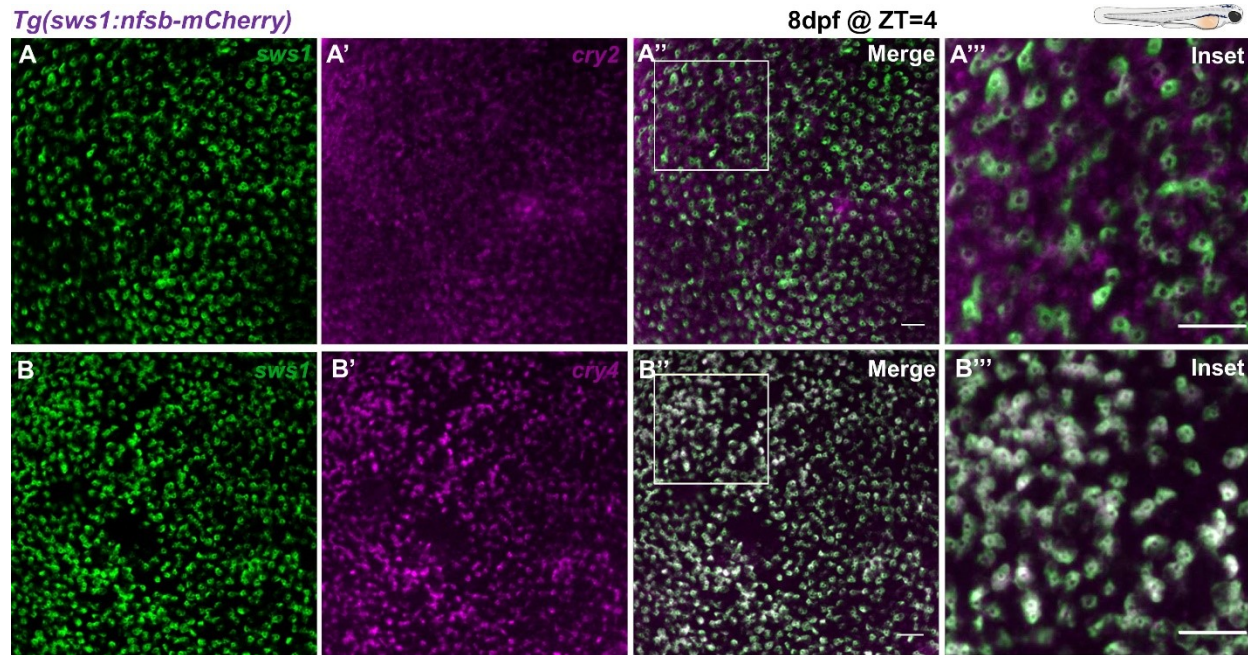


**Figure 5. Larval zebrafish UV cones express *cry4* during the day. A-A''')** Double fluorescent *in situ* hybridization on flat-mounted larval zebrafish retinae reveals *cry2* mRNA (magenta) is not co-expressed with *sws1* opsin (green), a marker for UV cones. **B-B''')** Riboprobe against *cry4* mRNA reveals overlapping expression with *sws1*, suggesting they are co-expressed. Tissue was collected at 8 days post fertilization (dpf) 4 hours after lights were turned on (Zeitgeber Time, ZT=4). *Tg(sws1:nfsb-mCherry)*= UV cone ablation line, where UV cones can be ablated upon the addition of a prodrug MTZ. Larvae were not treated in this experiment. Scale bars = 20  $\mu$ M for both magnifications. White square denotes Inset location. Inset = 10x magnification.

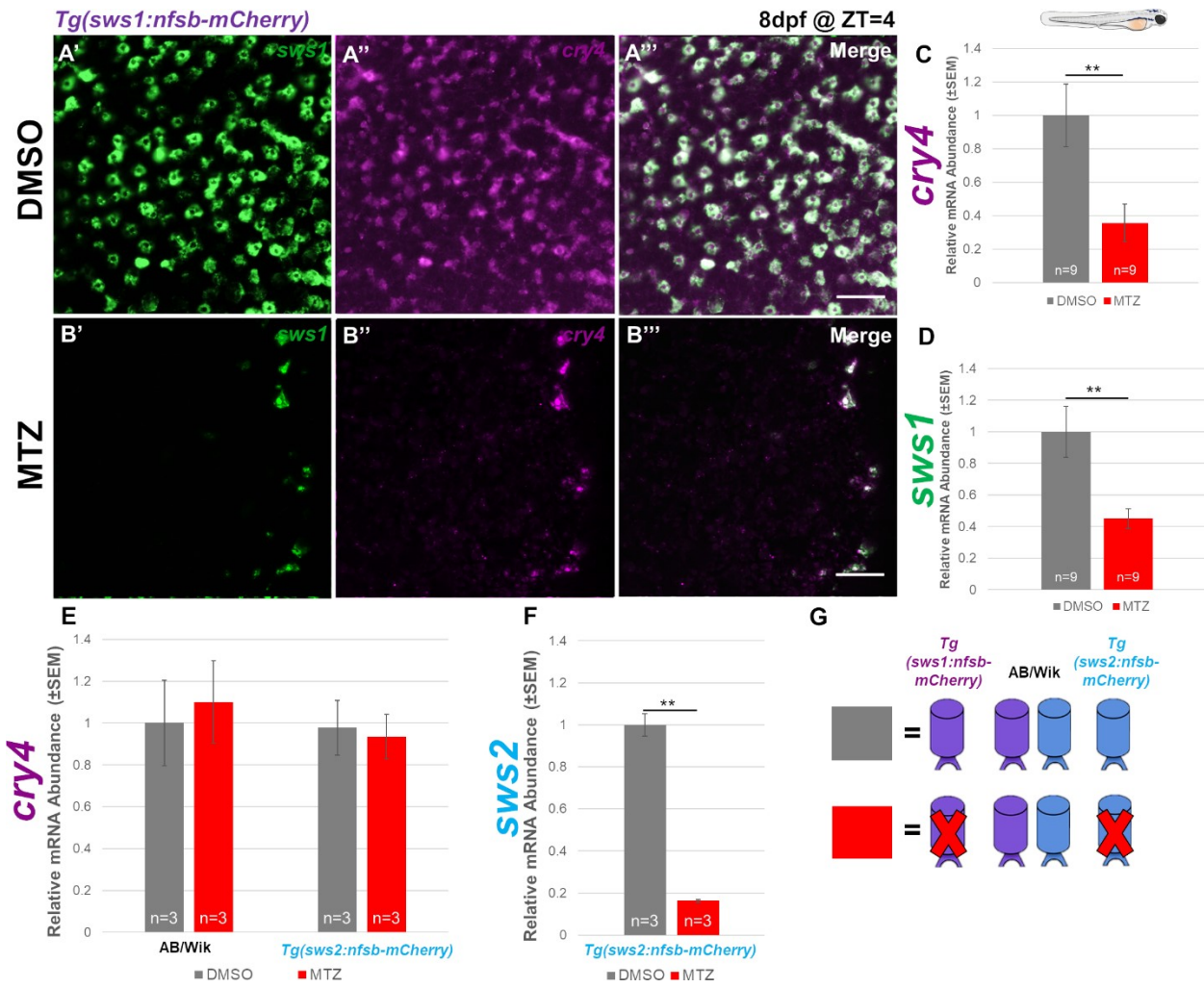


**Figure 6. Ablation of UV cones, but not blue cones, drastically decreases *cry4* in larval zebrafish. A-A''')** DMSO vehicle control treated larval retina shows *cry4* (magenta) is co-expressed with UV cones (*sws1*; green). **B-B''')** *Tg(sws1:nfsb-mCherry)* retinae treated with prodrug metronidazole (MTZ) to induce ablation of UV cones shows decreased *sws1* and *cry4* expression. The remaining UV cones continue to express *cry4*. **C-D)** mRNA levels of *cry4* and *sws1* (respectively) were reduced after treatment and MTZ (red) when compared to DMSO (grey) as measured using reverse transcription quantitative-PCR (RT-qPCR). mRNA abundance was normalized to levels of the endogenous control  $\beta$ -actin and standardized to vehicle control (DMSO) fish. Abundances are plotted as mean with SEM. **E)** *cry4* is not decreased after blue cone ablation in larval zebrafish *Tg(sws2:nfsb-mCherry)*, as quantified by RT-qPCR. AB/Wik serves as a non-transgenic control, showing addition of the prodrug and vehicle control does not alter endogenous *cry4* mRNA levels. **F)** *sws2* opsin (blue cone opsin) is decreased after addition of MTZ, ensuring ablation and RT-qPCR are sufficient experimental methods. **G)** Summary of treatments on zebrafish lines. Tissue was collected at 8 days post fertilization (dpf) 4 hours after lights ON (ZT=4); n= number of biological replicates (one biological replicate = pool of 5 individual 8dpf fish); Scale bars = 20  $\mu$ M; *Tg(sws1:nfsb-mCherry)* = UV cone ablation line, *Tg(sws2:nfsb-mCherry)* =blue cone ablation line; DMSO=Dimethyl sulfoxide. Statistical tests: C-D) Mann-Whitney U Test, E-F) Unpaired t-test with Welch's correction; \*=p<0.05, \*\*=p<0.01; SEM= Standard Error of the Mean.

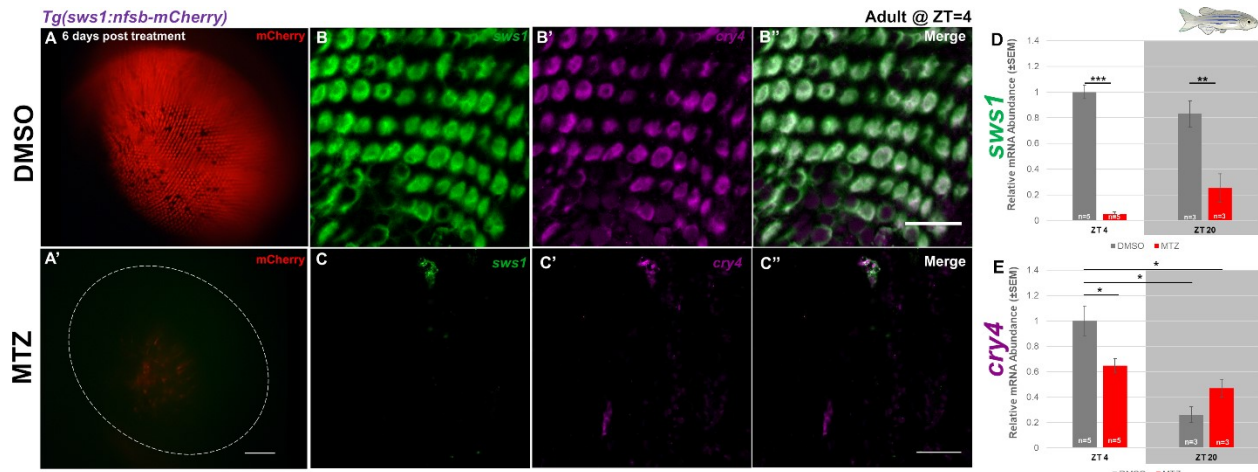


**Figure 7. UV cone ablation decreases *cry4* expression in adult zebrafish retina. A-A')** Live fundus imaging reveals MTZ is sufficient to ablate UV cones in adult *Tg(sws1:nfsb-mCherry)* retina. mCherry is fused to nitroreductase (*nfsb*) and expressed in UV cones. Zebrafish were treated with MTZ or DMSO for 24 hours and allowed to recover for 5 additional days. After 6 days post treatment, eyes were collected at either 4-hours after lights were turned on (ZT=4) or 6 hours after lights were turned off (ZT=20) in the dark under red light. RT-qPCR was performed as described in STAR Methods. **B-C''** *cry4* (magenta) is expressed in UV cones (green) and decreased after UV cone ablation as seen in larvae at ZT=4. **D**) *sws1* opsin is significantly decreased after UV cone ablation at both ZT=4 and ZT=20 which causes **E**) a significant decrease in *cry4* after UV cone ablation at ZT=4, but not ZT=20. *cry4* is significantly decreased from ZT=4 to ZT=20. Scale bars: A-A) = 50  $\mu$ M, B-C'') = 20  $\mu$ M, n= single whole fish eye from different individuals. Statistical test: Mann-Whitney U Test, \*=p<0.05, \*\*=p<0.01, \*\*\*=p<0.001; SEM= Standard Error of the Mean.

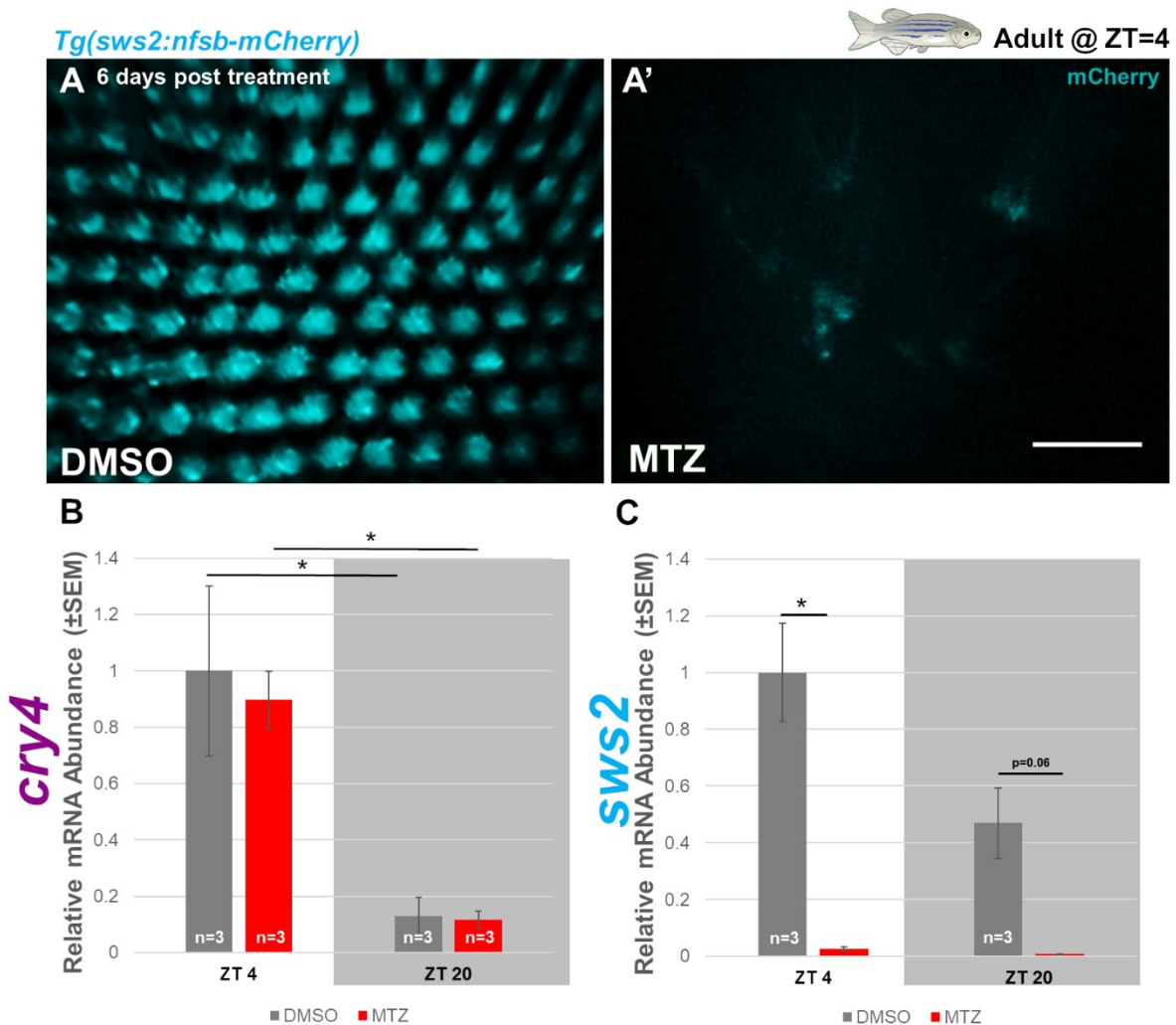


**Figure 8. Effective blue cone ablation does not disrupt *cry4* expression in adult zebrafish retina.** A-A') Live fundus imaging shows blue cone ablation was effective after MTZ treatment on *Tg(sws2:nfsb-mCherry)* adult zebrafish for 24 hours. mCherry marks nitroreductase (*nfsb*) in blue cones. B) *cry4* expression was unchanged after blue cone ablation at ZT=4 and ZT=20 but was significantly decreased from ZT=4 to ZT=20. C) *sws2* (blue opsin) is decreased after MTZ treatment at both ZT=4 and ZT=20. Scale bars: A-A) = 20  $\mu$ M, B-C') = 20  $\mu$ M, n= single whole fish eye from different individuals. Statistical test: Mann-Whitney U Test, \*= $p < 0.05$ , \*\*= $p < 0.01$ ; SEM= Standard Error of the Mean.

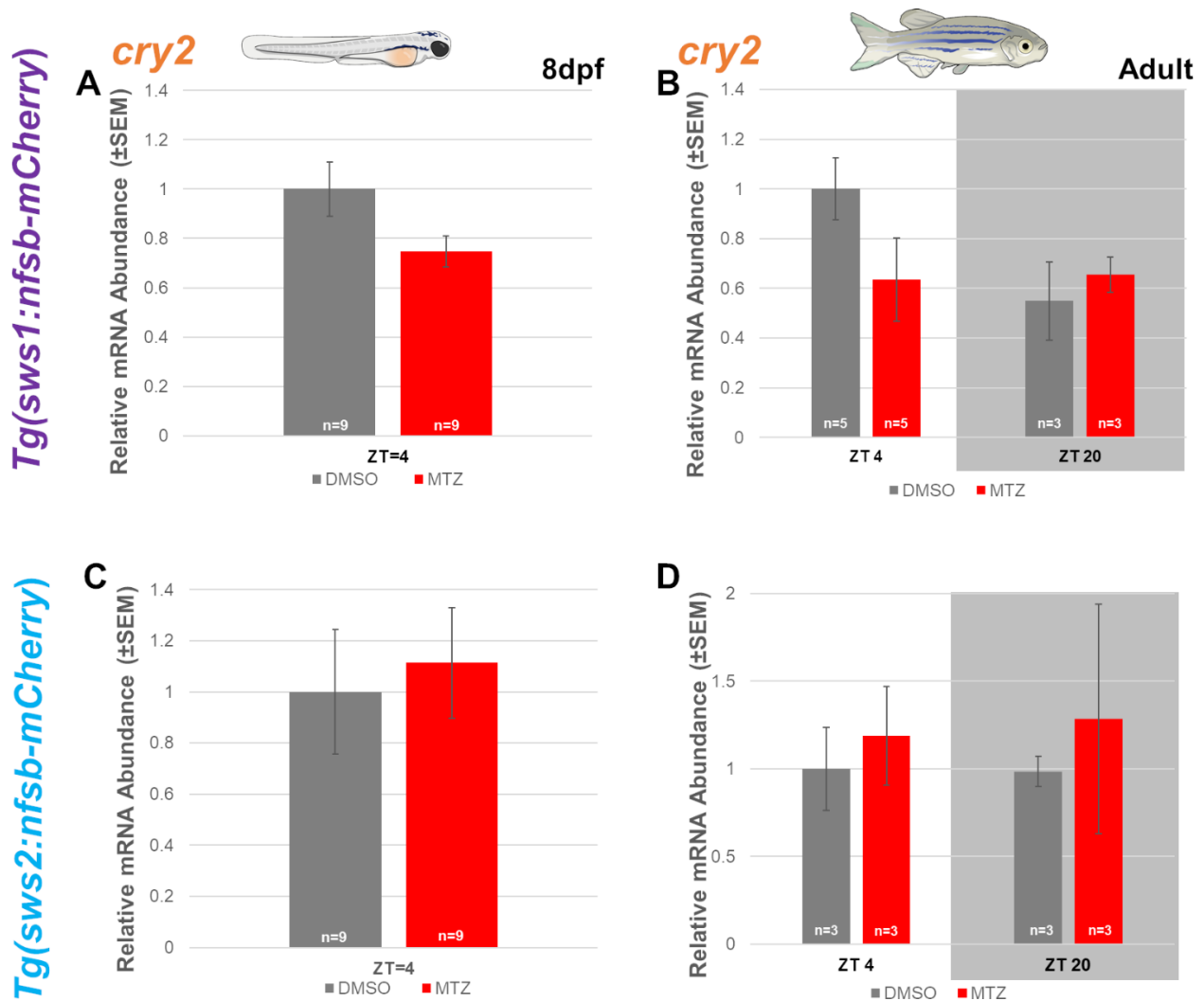


**Figure 9. *cry2* expression is not changed significantly after both UV cone and blue cone ablation in larval and adult zebrafish.** After UV cone ablation **A-B)** *cry2* mRNA is unchanged in 8dpf larval zebrafish at ZT=4 and in adult eye at ZT=4 and ZT=20. **C-D)** Blue cone ablation does not change *cry2* in 8dpf larval zebrafish at ZT=4 and in adult eye at ZT=4 and ZT=20. For adult RT=qPCR: n= single whole fish eye from different individuals. For larval RT-qPCR: n= number of biological replicates (one biological replicate = 5 individual 8dpf fish). Statistical tests: A-C) Mann-Whitney U Test, B-D) Unpaired t-test with Welch's Correction, SEM= Standard Error of the Mean.

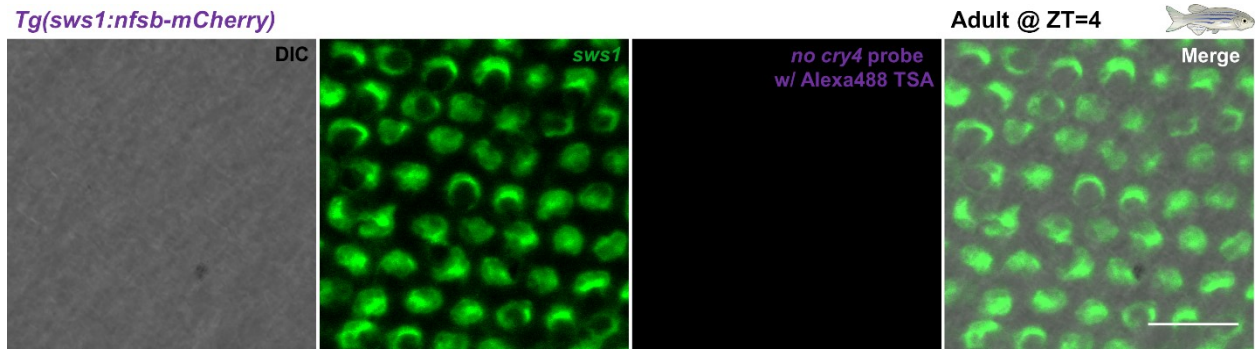


**Figure 10.** No *cry4* probe control for double fluorescent *in situ* hybridization on adult retina. *In situ* hybridization was performed as described (See STAR Methods). In the magenta channel, no signal is seen when no *cry4* probe is added. Alexa488 tyramide (pseudocolored magenta) was added, and colour reactions were developed as described. DIC= Differential interference contrast; Scale bar= 20  $\mu$ M.

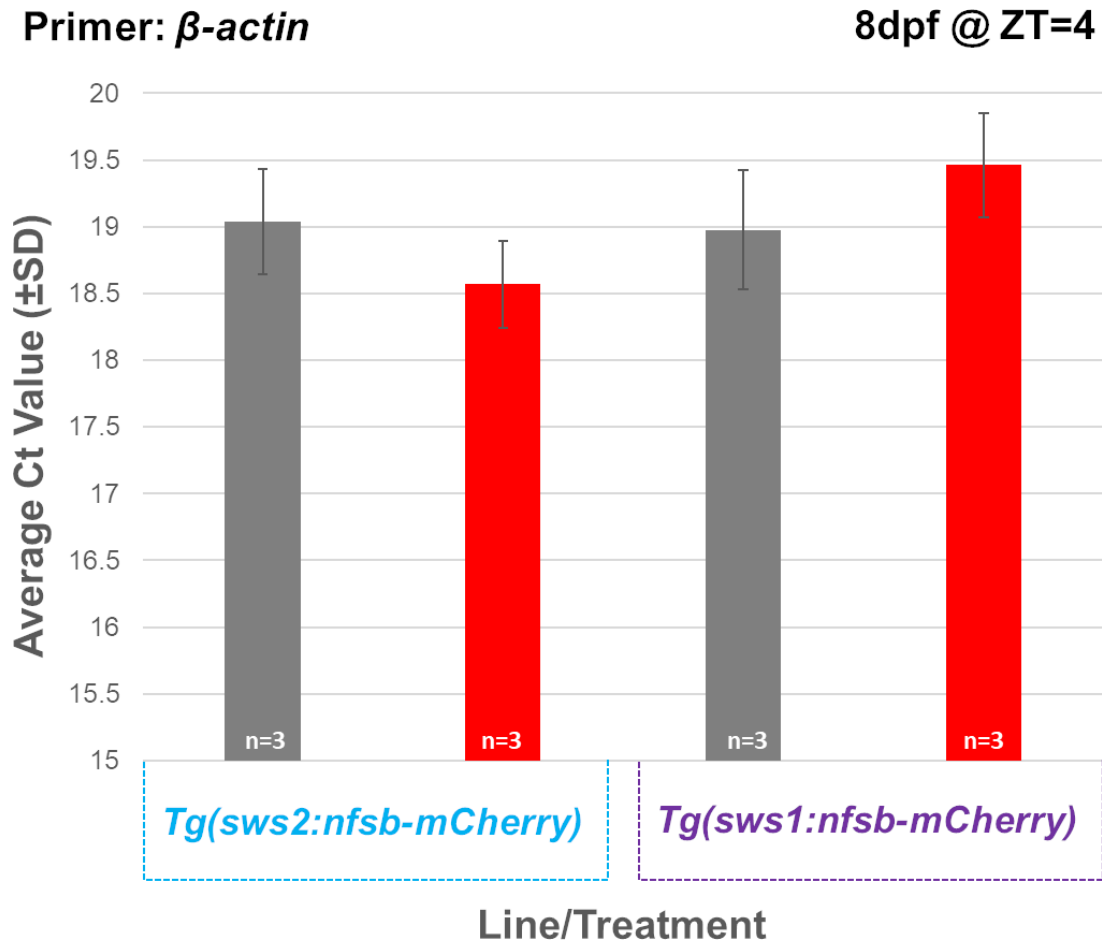


**Figure 11.  $\beta$ -actin is a suitable endogenous control for RT-qPCR experiments.** Squares denote biological replicates (n=5 whole larvae) treated with either DMSO or MTZ. Tissue was collected at 8dpf at ZT=4. Ct= Cycle threshold; SD= Standard deviation. Primer sequences are found in Table S3.

### 3 GENERAL DISCUSSION AND FUTURE DIRECTIONS

This work provides evidence that larval and adult zebrafish UV cones express a putative light-dependent magnetoreceptor, *cry4*. How (and if) *cry4* and cone photoreceptors process magnetic information remains unknown, but in a wide variety of taxa, *cry* appears to be associated with these cells. Short-wavelength photoreceptors such as UV cones appear to be particularly suited for magnetoreception due to the localization of *cry* in their outer segments and their spectral sensitivity, which overlaps with magnetoreceptive behavioral outputs [73,124,138]. The retina seems poised to receive magnetic signals based its hemispherical shape and the orientation of cone photoreceptors. One notable feature of the adult zebrafish retina is its mosaic nature, where rows of alternating UV and blue cones are separated by rows of green and red double cones [160,161,193]. Other teleosts such as flounders, trout, goldfish, guppies and medaka also have highly-ordered photoreceptor mosaics [157,158,214-218] that vary from the zebrafish arrangement. The function of these highly ordered cellular networks remains mysterious and a potential role in magnetoreception is discussed in section 3.1 below.

#### 3.1 The role of UV cones and cone mosaics in magnetoreception

To separate visual information from magnetic information it has been suggested that a system with two side-by-side photoreceptors, that receive the same light input, would be beneficial [33,124]. In this system, magnetic signals can be filtered from light signals by comparison between both photoreceptors. Horizontal cells (HCs) are well-characterized retinal neurons that receive input from cone subtypes. HCs also send feedback signals to specific photoreceptors, which helps improve contrast and color constancy [190,191,219].

In zebrafish, H3 cells are specifically innervated by UV and blue cones, suggesting information is being compared between these two photoreceptors [191,192]. The abundance of *cry4* in UV cones and apparent absence in neighboring blue cones (Figure 5-9) could suggest a cellular connection with magnetoreceptive purpose. The spectral sensitivities of UV and blue cones overlaps significantly at about 375 nm-400 nm in zebrafish [156,193,194], allowing for a similar light stimulus to be processed between these two photoreceptors. The separation of magnetic signals could be accomplished by *cry4*-containing UV cones comparing their output to neighboring, similarly short-wavelength sensitive, non-*cry4* containing blue cones via H3 cells. This could theoretically allow the retina to compare light + magnetic information (via UV cones) to light only information (via Blue cones), allowing the magnetic signal to be filtered out. Additionally, zebrafish UV cones and blue cones are connected at the cone synaptic level via fine processes called telodendria [186] suggesting they are communicating prior to sending signals to HCs. Telodendria have been proposed to add visual acuity and decrease signal to noise ratio, which could be useful if magnetic signals alter visual perception [186,220,221]. This type of immediate signal integration could point to the retina's early efforts to disentangle magnetic and visual information. This system has been proposed to function in European robins which harbor Cry1a in their UV cones [138,139]. In this case, robins exhibit magnetoreceptive behaviors when exposed to short-wavelength light that encompasses UV cone and blue cone activation [69], which coincides with activated Cry1a detection in the retina [189].

Could UV cones and *cry4* be interacting similarly in the zebrafish retina? The maximum wavelength sensitivity ( $\lambda_{max}$ ) of zebrafish UV cones (~360 nm; [156]) is remarkably similar to the absorption spectra of the fully oxidized version of FAD (~370 nm

for  ${}^S\text{FAD}^*$  or  $\text{FAD}_{\text{ox}}$  in Figure 12) and the magnetically sensitive radical  ${}^S\text{FAD}^{\bullet-}$  or  ${}^T\text{FAD}^{\bullet-}$  (~370 nm) of Cry [14,222-225]. The matched spectra of UV opsin and FAD in redox states that are required for Cry activation, and creation of magnetically sensitive radicals, points to UV cones potentially being co-opted for magnetoreception. Interestingly, blue cones  $\lambda_{\text{max}}$  (~410 nm) is still encompassed within the absorption spectra of both  ${}^S\text{FAD}^*$  and  $\text{FAD}^{\bullet-}$  but falls on a sharp decrease and plateau of  $\text{FAD}^{\bullet-}$ 's absorption spectra (Figure 12). Co-activation of blue cones and Cry from the same wavelength is less likely when compared to UV cones: this further supports that blue cones are not as useful for direct magnetic detection and may be functioning to help UV cones filter light and magnetic information. Although the cellular architecture of UV cones appears to make them ideal for LDRPM, are the visual outputs from these photoreceptors useful for magnetoreception?

### 3.1.1 UV vision may be suited for visually perceiving magnetic fields

Evidence for UV vision is well-established in a variety of animals, including fish (for recent review see [226]). Prey capture, mate selection and polarized light detection are some of the proposed functions of UV vision [227]. Although UV light has been suggested to be processed as a colour in fish [228,229], how these wavelengths are perceived remains unknown. Recently, an in-depth study outlined potential ecological implications for zebrafish UV monochromatic vision [197]. Neural circuits for UV vision appear to be most suited to detect stimuli in the upper and frontal visual field (i.e. directly above the animal). At the photoreceptor level this coincides with a dense population of UV cones in the larval zebrafish ventral-temporal retina [197]. In this area of the visual field, it is thought that little

colour information is processed, and instead visual input is predominated by silhouettes/shadows created by UV reflection and penetrance. Indeed, UV vision as a basis for prey detection has been suggested in zebrafish [197,230,231], as common food items such as unicellular paramecia scatter light that is biased to UV [167,232]. A visual circuit designed to detect short-wavelength shadows and silhouettes could be useful if it was also processing magnetic signals. It has been argued that a cone-mediated magnetoreceptor would be non-functional during the day because opsins would saturate photoreceptor signals upon photon absorption [33]. However, in shallow water (where zebrafish are found), short-wavelengths from sky illumination are mostly lost, shifting the spectrum of available light towards longer wavelengths [196,197,233]. The absorption peak of zebrafish UV opsin is at the extreme far end of the short-wavelength light available in the water [196], making these cones unlikely to function effectively in scenarios that require high signal-to-noise ratio, such as high acuity colour vision. In support of this, chromatic aberration of short-wavelength light makes the receptors especially likely to blur a formed image on the retina [226]. As such, UV cones may be acting to provide a “fuzzy” contrast for zebrafish. This would theoretically be apt for visually altered magnetosensing, as the receptor thought to mediate this should be contrast-sensitive, rather than involved in colour input (Personal communication, Dr. John Phillips). Long-wavelengths that dominate in the water column would be largely used to mediate high acuity functions while short-wavelengths would be used for contrast detection. The idea that short-wavelength photoreceptors mediate contrast has been suggested elsewhere [227,234]; blue photoreceptors have been proposed to constantly adjust a fish’s sensitivity to the environmental background [216]. For these reasons, it appears UV cones and UV vision are well-suited to participate in magnetoreception within aquatic environments.

### 3.1.2 Fine tuning of visually mediated magnetoreception may be accomplished by long-wavelength photoreceptors

Despite a large body of evidence suggesting short-wavelength photoreceptors are equipped to be magnetoreceptors, the complete story is most likely more complicated. Cry4 was recently found to be localized in photoreceptors sensitive to longer wavelengths [124]. These include chicken and European robin double cones ( $\lambda_{\max} = \sim 580$  nm) and single long-wavelength cones ( $\lambda_{\max} = \sim 610$  nm) [235-237]. Most importantly, Cry4 is clearly not localized in bird UV cones [124]. This finding is especially interesting when compared to *cry4*'s localization to UV cones in zebrafish (Figure 5-7). There are many reasons why this difference may exist between fish and birds (described in Chapter 2); regardless, it provides an important discussion point for the potential involvement of long-wavelength cones in magnetoreception. Why would Cry4, a short-wavelength sensitive photoreceptive molecule, be found in long-wavelength sensitive cones? This could be beneficial when trying to separate cone-mediated visual output and Cry-mediated magnetic output. Since the spectral sensitivity of red cones and the magnetically sensitive radical of Cry are on the opposite side of the wavelength spectrum, activation of each would require different portions of the available light. This would prevent competition for similar wavelengths between opsin and Cry and ensure each output (magnetic versus visual) was using a distinct portion of light. Double cones also fulfill the requirement of a similar light stimulus being presented between photoreceptors, as was discussed with UV and blue cones.

It is possible that *cry4* is also expressed in a subset of double cones within the zebrafish retina, but this requires further investigation. It is worth noting that the many opsins that define green and red cones have extremely unique expression patterns

throughout different developmental time points, and areas within the zebrafish retina [203]. Specifically, expression of *lws1* and *rh2-4* is restricted to a subset of cones in the ventral adult retina [203,238,239]. Double cones here would be most sensitive to light directly above and in front of the animal, similar to where UV cone circuits are proposed to be most active. It would be interesting to see if *cry4*'s expression differed spatially throughout the retina and localized to double cones in ventral areas. Characterizing this type of spatial patterning has yet to be done for *crys* in adult zebrafish but in the larval eye, *cry4* appears to be expressed broadly throughout most areas of the retina (Figure 5). The expression of *cry4* may tighten to a spatially restricted subset of photoreceptors as the mosaic is established throughout development, but this requires further investigation.

Additionally,  ${}^{\text{S}}\text{FAD}^*/\text{FAD}_{\text{ox}}$  has a second absorption peak around 440 nm to 480 nm and  $\text{FAD}^{\bullet-}$  has one around 480-500 nm, which matches the  $\lambda_{\text{max}}$  of the green opsins (*rh2-1* to *rh2-4*; ~480 nm to 505 nm) [156,222,223,225,240]. Since this is within the active spectrum of Cry, the potentially pro-magneto green cones could add acuity to the general signal created by UV cones. Indeed, a small number of bipolar cell connections in the zebrafish retina are UV-green cone specific [241], suggesting they are also sharing information in the early stages of retinal processing. The green cone signal could add sharp bright lines to the relatively fuzzy image created by UV cones alone (Figure 4). *cry4* in the longer-wavelength red cones may also add to the acuity of magnetoreception; the absorption spectra for  $\text{FADH}^{\bullet}$ , the non-magnetically sensitive radical, is broad, but extends into wavelengths far above 500 nm [225]. Red cone opsin's (*lws1*)  $\lambda_{\text{max}}$  is ~565 nm, and only  $\text{FADH}^{\bullet}$  of Cry can absorb in this spectral range [156,240]. If *cry4* was located in zebrafish red cones as seen in birds, it could represent the long-wavelength extreme end of *cry*-cone

mediated magnetoreception. Ultimately the signals created by absorption of FADH• would serve as an “end-point” to a certain magnetic stimulus, where the magnetically sensitive radical is abolished, and Cry returns to its ground-state (Figure 3). This could theoretically be visualized as sharp black lines, which complement the overall bright pattern generated from UV cones and activated Cry, and sharp bright lines generated by green cones and Cry (Figure 4). The interplay between different photoreceptors is likely if LDRPM results in altering a fish’s visual perception but needs further exploration before it can be tested.

### **3.2 *cry2* and *cry4*'s function in zebrafish retina: magnetoreception, circadian photoreception or neither**

The unknown function of zebrafish *cry2* and *cry4*, and the supported role of Cry in magnetoreception in other models makes them most likely to have a magnetoreceptive role in zebrafish. However, *cry* also has known roles in tuning circadian rhythms. *crys* normally regulate the circadian clock by entering the nucleus and inhibiting CLOCK:BMAL1 mediated transcription in an autoregulatory negative feedback loop (for review see [242,243]. Zebrafish *cry4* does not contain a NLS and cannot repress activation of the CLOCK:BMAL1 complex [118,125], making it unlikely to participate in core circadian regulation. Another unique characteristic of zebrafish Cry4 is that it has been isolated with bound FAD [126] and can undergo light-dependent conformational changes [244,245], which are two requirements for magnetically sensitive radical-pairs to be created. For these reasons, and its association with UV cones, *cry4* is a promising candidate for light-dependent magnetoreception in zebrafish. Through similar reasoning, it is possible that *cry4* could have

a yet to be discovered role in circadian rhythms, as it may be acting as an upstream light-sensor used to drive gene expression necessary to entrain the circadian clock [243,246,247]. Indeed, *cry4* appears to be more evolutionarily related to Type I Crys found in invertebrates, which provide light-input to the circadian clock [112,119]. It is possible that *cry4*'s localization in UV cones at ZT=4 (Figure 5-7) is a consequence of a cell-dependent circadian rhythm of *cry*. Expression of *cry4* appears to move throughout the retina during the circadian day: spatial expression starts in the ONL and INL in early hours after lights have been turned on, and progressively moves forward through the retina into the GCL later in the day [119]. At night, *cry4* is almost non-existent in the retina, suggesting the presence of light influences this cycle [119,125]. It has been suggested that *cry4* cycles in a similar pattern in constant light or dark conditions, but these experiments need to be validated [125]. For now, it is unknown if zebrafish *cry4*'s expression is regulated exogenously (light-dependent) or it cycles endogenously. Regardless, an alternative role for *cry4* in circadian input is possible. Further experiments will be required to elucidate *cry4*'s role in UV cones, and in zebrafish in general.

*cry2*'s role in zebrafish biology is even more mysterious. *cry2* is found in both the nucleus and cytoplasm but has lost its NLS. Additionally, it can only weakly bind CLOCK: BMAL1, and is predicted to be insufficient in regulation of circadian transcription [118]. In larval retina expression of *cry2* did not overlap with UV opsin, suggesting *cry2* is not localized to UV cones in larval stages (Figure 5). Despite this, although not statistically significant, *cry2* expression did decrease close to the magnitude of *cry4* after UV cone ablation at ZT=4 in adult zebrafish (Figure 9). *cry2* may be very lowly expressed in adult UV cones, or its expression may somehow be regulated by the presence of UV cones, but this requires further

exploration. It was previously suggested that *cry2* is expressed in zebrafish short-wavelength photoreceptors at ZT=23 [119], but effective ablation of either UV or blue cones did not decrease *cry2* in the adult retina at ZT=20 (Figure 9). Recently, transcriptional profiles of zebrafish rods suggest that *cry2* is highly expressed in these photoreceptors compared to other retinal cells [248]. Cry-rhodopsin interactions have been speculated in the magnetoreception literature [249,250], but rods extreme sensitivity to low levels of light makes them unlikely to function as a daytime magnetoreceptor [139]. It is currently unknown if *cry2* has the appropriate biochemical underpinnings to create magnetically sensitive radical-pairs, but theoretically if it does, *cry*-rod interactions may mediate magnetoreception in scotopic scenarios.

The role of *cry* and cone photoreceptors in fish magnetoreception can only be inferred from molecular association. To test functional significance: behavioral assays, genetic manipulation and neuronal recordings must also be performed.

### 3.3 Future Experiments to test LDRPM in Zebrafish

#### 3.3.1 Behavioral experiments to test for LDRPM

Evidence for magnetoreception has been built off behavioral observations in a staggering number of animals. To properly test the role of UV cones and *cry* in magnetoreception, behavioral experiments after manipulation of these variables must be performed. Without an innate compass preference or a migratory heading, testing magnetoreception mechanisms is less intuitive in zebrafish when compared to migratory birds or fish. The first step in doing so, is to define a robust, repeatable magnetic behavior. Bimodal orientation (the preference to align along an axis) has been demonstrated a number of times in zebrafish, and is observed when fish have access to light and would theoretically be using LDRPM [40,58,164]. However, this behavior appears to be innate, and is not constant across zebrafish (i.e. individual fish don't all have the same bimodal orientation) making it a potentially difficult behavior to evaluate after manipulation of UV cones or *cry*.

An alternative experiment may include motivating the animal to respond to a magnetic stimulus. This could be done by giving zebrafish a reward (food) that is paired to a magnetic vector (such as North). One could use a 4-arm plus maze and manipulate the magnetic field, so each arm would represent a magnetic direction. Through conditioning experiments, removal of food should cause zebrafish to spend more time in the arm of the maze that is associated with the trained magnetic vector (North). A problem with these experiments is that the motivation of the zebrafish can result in poor response rates. Limiting food intake before experiments would ensure that zebrafish were primed to search

for food, but if zebrafish were tested in a relatively inconsequential environment, they may search for food randomly in each arm and ignore magnetic cues. To add extra motivation, the arms of the maze could be inclined, causing lower water levels further into the arm of the maze (a risky environment for zebrafish; Personal communication, Dr. John Phillips). If food was only given in these shallow sections, and was paired with the magnetic stimulus, zebrafish may expend more energy on choosing the right arm via magnetic cues, in attempt to spend less time in a risky environment. Additionally, increasing the potency of the reward may effectively reveal magnetic behaviors. Recently, zebrafish were rapidly trained to self-administer opioids by swimming over a sensor [251]. This assay also worked with food rewards, but fish took much longer to show learned responses. Using drugs as a reward has many downfalls but this work could at least be used to promote research into characterizing non-harmful substances that are effective in zebrafish training assays. Regardless of assay, LDRPM has rarely, if ever, been tested in zebrafish, leaving many critical experiments open to complete.

An intuitive next step would be to test if magnetically induced training to a reward was wavelength specific. If LDRPM via *cry* was responsible for this behavior it would be predicted that training would be possible in monochromatic short-wavelength light (that encompassed UV cone and FAD activation) but would be inhibited in monochromatic long-wavelength light (outside activation spectra of UV cones and FAD). Additionally, this behavior should be limited if zebrafish were tested in complete darkness. Despite this logic, zebrafish have been shown to exhibit magnetic behaviors in the dark [40,56], making it very likely that an alternative magnetoreception mechanism exists. To tease apart these mechanisms, targeted cone ablation could be used to test if *cry4* expressing UV cones were

required for magnetic behaviors. If zebrafish were using LDRPM, trials in short-wavelengths should be influenced by UV cones/ *cry*. After ablation of UV cones, it would be predicted that the behavioral response would be diminished. If another LDRPM-independent mechanism was compensating, a complete abolishment of the trained response may not be observed, and instead, only a moderate decrease may be seen after UV cone ablation in short-wavelengths. Additionally, if a trained response was observed in darkness or long-wavelengths (in favour of another mechanism) it would be predicted that UV cone ablation would not substantially affect the behavior in these trials.

Use of monochromatic wavelengths and ablation of UV cones could also be used to test innate bimodal orientation. Here, it would be also predicted that the behavior would be observed in short-wavelengths sufficient for UV cone and *cry* activation and decreased/ unobserved after UV cone ablation, or during exposure to monochromatic long-wavelength light. Bimodal orientation has only been demonstrated during trials when zebrafish are exposed to light, making it a promising behavior mediated by LDRPM. In the dark, zebrafish exhibit a unimodal response (align towards one vector only, such as North), which may be mediated by magnetite or some other yet to be found receptor.

As discussed in Chapter 1, other diagnostic tests for LDRPM also exist: use of various types of radio frequencies can alter singlet-to-triplet interconversion of radical-pairs and disrupt orientation in birds and turtles [67,98,101,107]. To my knowledge, radio-frequency field experiments have yet to be completed when testing fish magnetoreception. If application of radio frequency fields disrupted bimodal orientation or a trained magnetic response, it would provide substantial evidence that zebrafish use radical-pair

magnetoreception. These experiments, combined with UV cone ablation, would be a powerful way to test if *cry4* expressing UV cones mediated LDRPM. However, ablation of a whole photoreceptor subtype is bound to have other effects on visual processing and could potentially make it difficult to define changes in behavior as a specific loss of magnetoreception. Targeted mutagenesis is another powerful alternative that can be used to directly test the requirement of *cry* in zebrafish magnetoreception.

### 3.3.2 Genome editing of *cry* in zebrafish

Zebrafish are amenable to next generation genome editing techniques such as targeted mutagenesis via the Clustered Regularly Interspaced Short Palindromic Repeat (CRISPR) and CRISPR associated protein (Cas) system. Cas is a nuclease that digests DNA and is used in the prokaryotic immune system to protect against foreign genetic material [252]. This function has been exploited to edit genomes of model organisms [253] and is done by generating a synthetic guide RNA (sgRNA) specific to the gene of interest. Co-injecting the sgRNA with Cas protein (such as Cas9) into a single-cell staged zebrafish will cause Cas and the sgRNA to make a complex and bind the target sequence [209]. Once it binds to the specific area it is designed to, Cas will cut the DNA. Normally the DNA will attempt to repair itself via non-homologous end joining, which ultimately introduces deletions or insertions into the target sequence.

Disrupting *cry4* and showing a concerted decline in magnetoreceptive abilities would be a powerful way to show *cry4* is necessary for magnetoreception. A caveat with whole

organism gene silencing is disrupting the genes endogenous function can have unattended effects in other tissues it is expressed in. Additionally, although knockout of *cry* would create evidence that it is required for magnetoreception, it does not directly point to what sensory system is being exploited for this behavior. For example, besides retinal expression and specific localization to UV cones, *cry4* is expressed largely in the developing zebrafish brain and intestine [118,119]. Knockout of *cry4* in these tissues may alter normal zebrafish development, and cause disruption in other cellular processes that may result in a general behavioral decline, that could be misinterpreted as a loss of magnetoreception. Ideally, *cry4* would be manipulated specifically in the cells thought necessary for magnetoreception (such as UV cones). Tissue specific gene knockout using CRISPR has been developed in zebrafish [253,254] and will be extremely important when testing the potential role of *cry4* and cones in magnetoreception. To utilize this, one creates a sgRNA targeted to bind somewhere in the *cry4* gene. Slightly upstream of the FAD-binding domain would be ideal, to increase the chance that the introduced mutation would inhibit the translation of a functional protein. Then, using a cone specific promoter such as *crx* (for early development), *gnat2* (for post-mitotic cones) [255] or *sws1* (for UV cones) and Tol2 transposase technology (where transgenes can be inserted into the genome of an animal; [256]), a sgRNA seeding clone can be made that will drive expression of the sgRNA in the tissue specified by the promoter of interest (cones). After injection of the sgRNA construct, Tol2 mRNA, and Cas, one can confirm integration into the genome, and cutting with tissue specific sequencing/ genotyping assays [209].

*cry* zebrafish mutants will be important to test if behavioral outputs are changed but will be particularly useful to ask if *cry* is required for neuronal processing of magnetic

information. Measuring neural activity in response to magnetic stimuli is especially important in systems that may have multiple modes of magnetoreception. For example, if *cry* knockout doesn't change behavioral outputs, another light-independent mechanism may be compensating. Neuronal recordings could potentially detect minute changes in the way magnetic fields are being processed in the presence or absence of *cry*, and ultimately provide clues to the neuronal area required for fish magnetoreception.

### 3.3.3 Imaging magnetically dependent neuronal activity via $\text{Ca}^{2+}$

Standard recording techniques such as electrophysiology are not applicable for magnetoreception experiments since altering static magnetic fields usually requires running current through copper wires in a coil system [257]. Due to this, there is potential for electrical noise to confound recording outputs [175]. New, non-invasive live-imaging techniques appear to be more suited to test magnetoreception in fish. Genetically encoded calcium indicators (GECIs) consist of fluorescent molecules fused to proteins that bind  $\text{Ca}^{2+}$  such as calmodulin [258]. Activation of neurons normally cause cellular changes of  $\text{Ca}^{2+}$  which can be visualized by changes in fluorescence intensity of GECIs. Using this, one could manipulate experimental magnetic fields and observe neuronal changes in free swimming zebrafish. This technique could be combined with either: *a)* targeted cone ablation to test the role of UV cones in magnetic processing and/or *b)* UV cone specific knockout of *cry4* to test its role in magnetic detection. Here, it would be predicted that under natural conditions (unaltered retina), retinal recipients involved in visual processing such as the optic tectum would show increased activity when magnetic fields are manipulated. Other, non-visual

areas that receive input from the retina such as the anterior thalamus [259], may also show increased activation during magnetic experiments. Retinal-thalamic pathways in zebrafish may be particularly interesting because the thalamofugal pathway in birds is thought to mediate magnetoreception ([84,260]. Alteration of magnetic fields after UV cone ablation may show specific neuronal areas dedicated for processing LDRPM mediated information. For now, neuronal areas dedicated for magnetoreception remain unknown in zebrafish, and could potentially be part of a yet to be described circuit.

Our lab has already begun to engineer a GECI in zebrafish by using Calcium-Modulated Photoactivatable Ratiometric Integrators (CaMPARI) [212]. When CaMPARI is expressed in all neurons (via the *elavl3* promoter), the presence of high intercellular  $Ca^{2+}$  and a photoconversion light causes an irreversible change in the emitted wavelength of a fluorescent protein from green to red [212]. A caveat here is the use of the photoconversion laser; its wavelength (405 nm) theoretically could activate UV cones, blue cones and various intermediates of Cry. By turning the laser on to photoconvert, it is likely that neuronal areas that receive information from short-wavelength cones and/or Cry will show  $Ca^{2+}$  changes, regardless of magnetic information. It would be interesting to see if the presence of magnetic fields showed more activation, or slightly altered activation patterns across the zebrafish retina and brain after manipulation of the magnetic field. It is likely that if magnetic information is processed in the same area as visual information is integrated, such as the optic tectum, CaMPARI will be unable to separate these two signals. For this reason, traditional GECIs may be more useful for magnetoreception experiments.

Another potential issue with using this imaging method and other GECIs in the retina is the presence of the retinal pigmented epithelium (RPE). Under natural conditions, melanin deposits in the RPE block visualization of fluorescent molecules in photoreceptors. Using the CRISPR-Cas9 system, I generated a zebrafish mutant that has a non-pigmented RPE by knocking out a melanin synthesizing gene *slc45a2* (Appendix A; [261]). I crossed *slc45a2* mutants to fish with no melanophores in the body (*nacre*) [262] and no iridophores (*roy*) [263] to create a pigmentless zebrafish line (*crystal*) to improve fluorescent imaging potential [261]. Another benefit of using *crystal* is that they do not require treatment with a common melanin synthesis inhibitor, PTU, which is used to prevent pigment formation. This drug has been shown to alter various aspects of development including eye formation, making it non-ideal for experiments testing visually mediated behaviors [264,265]. Furthermore, Ca<sup>2+</sup> imaging in the retina of *crystal* fish has been demonstrated during exposure to visual stimuli [261], but recordings after magnetic changes have yet to be described. Currently, CaMPARI in *crystal* mutants is being established in our lab. GECIs provide a promising way to visualize magnetically dependent retinal activity in zebrafish.

### **3.4 Final Conclusions**

Magnetoreception has been demonstrated in an overwhelming number of organisms across a variety of taxa but continues to be one of the remaining senses without an identified receptor. LDRPM via Cry is the leading hypothesis for magnetoreception in migratory birds but cannot easily be tested at the molecular level due to the genetic inaccessibility of the

avian model. The retina, specifically cone photoreceptors, harbors magnetoreceptive Cry and may allow the alteration of visual perception by magnetic fields. This thesis work provides the first evidence that zebrafish have *cry* in retinal cone photoreceptors. Specifically, *cry4* mRNA is localized in UV cones in both larval and adult zebrafish. Using targeted cone ablation, I thoroughly validated this association: ablation of UV cones but not neighboring blue cones, decreased *cry4* in zebrafish retina. Paralogous *cry2* was undisturbed after UV and blue cone ablation, supporting that *cry4* is specifically associated with UV cones. Moving forward, a multi-faceted approach will be key in elucidating the mysteries of magnetoreception. Optically transparent imaging with retinal GECs, molecular manipulations via cone ablation or *cry* knockout and environmental control through magnetic and radio frequency fields can all be achieved with zebrafish. These highly versatile vertebrates will be crucial in advancing our understanding of this complex phenomenon.

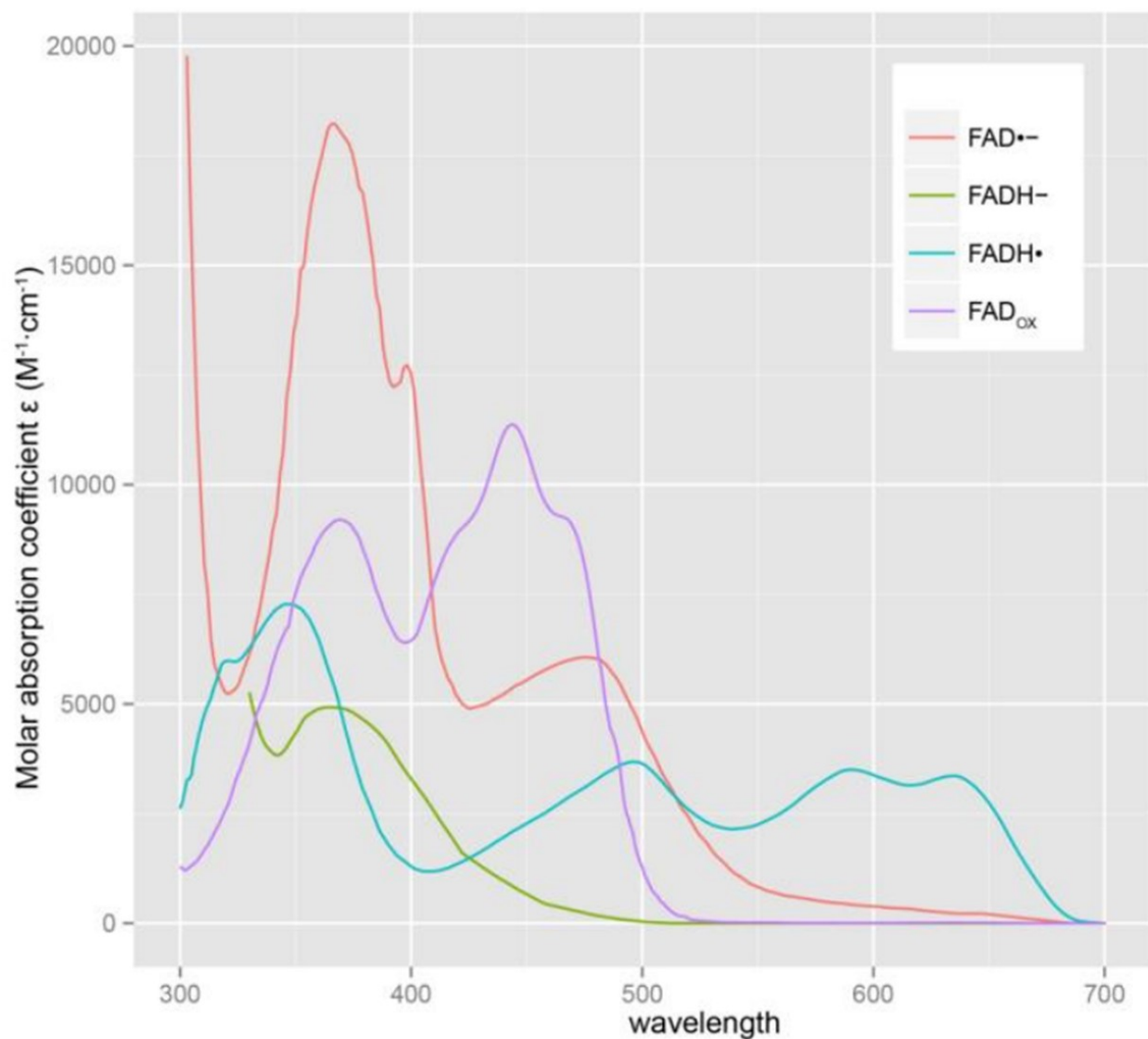


**Figure 12. Molar absorption spectra of FAD in different Cry redox states.** Spectra reused with permission from Bazalova et al., [14].  $FAD_{ox}$  originally from Islam et al., [223];  $FAD^{\bullet-}$  and  $FADH^{\bullet}$  from Palfey and Massey [222];  $FADH^-$  from Muller [225].

## Literature Cited

1. Tarduno, J.A., Cottrell, R.D., Davis, W.J., Nimmo, F., and Bono, R.K. (2015). A Hadean to Paleoproterozoic geodynamo recorded by single zircon crystals. *Science* 352, 521-524.
2. Mouritsen, H. (2015). Magnetoreception in birds and its use for long-distance migration. *Sturkie's Avian Physiology* 113-133.
3. Wiltschko, R. (2012). *Magnetic orientation in animals* Springer Science & Business Media).
4. Phillips, J.B. (1986). Magnetic compass orientation in the Eastern red-spotted newt (*Notophthalmus viridescens*). *Journal of Comparative Physiology A* 1, 103-109.
5. Quinn, T.P. (1980). Evidence for celestial and magnetic compass orientation in lake migrating sockeye salmon fry. *Journal of Comparative Physiology* 3, 243-248.
6. Kimchi, T., Etienne, A.S., and Terkel, J. (2004). A subterranean mammal uses the magnetic compass for path integration. *Proc. Natl. Acad. Sci. U. S. A.* 4, 1105-1109.
7. Putman, N.F., Scanlan, M.M., Billman, E.J., O'Neil, J.P., Couture, R.B., Quinn, T.P., Lohmann, K.J., and Noakes, D.L. (2014). An inherited magnetic map guides ocean navigation in juvenile Pacific salmon. *Current Biology* 4, 446-450.
8. Lohmann, K.J., Cain, S.D., Dodge, S.A., and Lohmann, C.M. (2001). Regional magnetic fields as navigational markers for sea turtles. *Science* 291, 364-366.
9. Durif, C.M., Browman, H.I., Phillips, J.B., Skiftesvik, A.B., Vøllestad, L.A., and Stockhausen, H.H. (2013). Magnetic compass orientation in the European eel. *PLoS One* 3, e59212.
10. Lohmann, K., Pentcheff, N., Nevitt, G., Stetten, G., Zimmer-Faust, R., Jarrard, H., and Boles, L.C. (1995). Magnetic orientation of spiny lobsters in the ocean: experiments with undersea coil systems. *J. Exp. Biol.* 10, 2041-2048.
11. Phillips, J.B., and Sayeed, O. (1993). Wavelength-dependent effects of light on magnetic compass orientation in *Drosophila melanogaster*. *Journal of Comparative Physiology A* 3, 303-308.
12. Gegear, R.J., Casselman, A., Waddell, S., and Reppert, S.M. (2008). Cryptochrome mediates light-dependent magnetosensitivity in *Drosophila*. *Nature* 455, 1014.
13. Gegear, R.J., Foley, L.E., Casselman, A., and Reppert, S.M. (2010). Animal cryptochromes mediate magnetoreception by an unconventional photochemical mechanism. *Nature* 465, 804.
14. Bazalova, O., Kvicálová, M., Valková, T., Slaby, P., Bartoš, P., Netušil, R., Tomanová, K., Braeunig, P., Lee, H., and Sauman, I. (2016). Cryptochrome 2 mediates directional magnetoreception in cockroaches. *Proceedings of the National Academy of Sciences* 6, 1660-1665.
15. Wiltschko, W., and Wiltschko, R. (1972). Magnetic compass of European robins. *Science* 176, 62-64.

16. Phillips, J.B., and Borland, S.C. (1992). Behavioural evidence for use of a light-dependent magnetoreception mechanism by a vertebrate. *Nature* 6391, 142.
17. Boles, L.C., and Lohmann, K.J. (2003). True navigation and magnetic maps in spiny lobsters. *Nature* 6918, 60.
18. Lohmann, K.J., Lohmann, C.M., and Putman, N.F. (2007). Magnetic maps in animals: nature's GPS. *J. Exp. Biol.* 21, 3697-3705.
19. Hein, C.M., Engels, S., Kishkinev, D., and Mouritsen, H. (2011). Robins have a magnetic compass in both eyes. *Nature* 7340, E1.
20. Eerven, J., Begall, S., Koubek, P., Novikov, P., and Burda, H. (2011). Directional preference may enhance hunting accuracy in foraging foxes. *Biology letters* rsbl20101145.
21. Putman, N.F., Lohmann, K.J., Putman, E.M., Quinn, T.P., Klimley, A.P., and Noakes, D.L. (2013). Evidence for geomagnetic imprinting as a homing mechanism in Pacific salmon. *Current Biology* 4, 312-316.
22. Malkemper, E.P., Eder, S.H., Begall, S., Phillips, J.B., Winklhofer, M., Hart, V., and Burda, H. (2015). Magnetoreception in the wood mouse (*Apodemus sylvaticus*): influence of weak frequency-modulated radio frequency fields. *Scientific reports* 9917.
23. Putman, N.F. (2015). Inherited magnetic maps in salmon and the role of geomagnetic change. *Integrative and comparative biology* 3, 396-405.
24. Bottesch, M., Gerlach, G., Halbach, M., Bally, A., Kingsford, M.J., and Mouritsen, H. (2016). A magnetic compass that might help coral reef fish larvae return to their natal reef. *Current Biology* 24, R1267.
25. Cresci, A., Paris, C.B., Durif, C.M., Shema, S., Bjelland, R.M., Skiftesvik, A.B., and Browman, H.I. (2017). Glass eels (*Anguilla anguilla*) have a magnetic compass linked to the tidal cycle. *Science advances* 6, e1602007.
26. Putman, N.F., Scanlan, M.M., Pollock, A.M., O'Neil, J.P., Couture, R.B., Stoner, J.S., Quinn, T.P., Lohmann, K.J., and Noakes, D.L. (2018). Geomagnetic field influences upward movement of young Chinook salmon emerging from nests. *Biology letters* 2, 20170752.
27. Wiltschko, R., and Wiltschko, W. (2013). The magnetite-based receptors in the beak of birds and their role in avian navigation. *Journal of Comparative Physiology A* 2, 89-98.
28. Diebel, C.E., Proksch, R., Green, C.R., Neilson, P., and Walker, M.M. (2000). Magnetite defines a vertebrate magnetoreceptor. *Nature* 6793, 299-302.
29. Kirschvink, J.L., Jones, D.S., and MacFadden, B.J. (2013). Magnetite biomineralization and magnetoreception in organisms: a new biomagnetism Springer Science & Business Media).
30. Schulten, K., Swenberg, C.E., and Weller, A. (1978). A biomagnetic sensory mechanism based on magnetic field modulated coherent electron spin motion. *Zeitschrift für Physikalische Chemie* 1, 1-5.

31. Liedvogel, M., and Mouritsen, H. (2010). Cryptochromes—a potential magnetoreceptor: what do we know and what do we want to know? *Journal of the Royal Society Interface Suppl 2*, S162.
32. Solov'yov, I., Hore, P.J., Ritz, T., and Schulten, K. (2014). *Chemical compass for bird navigation*. In *Quantum effects in biology*, Cambridge University Press)
33. Hore, P.J., and Mouritsen, H. (2016). The radical-pair mechanism of magnetoreception. *Annual review of biophysics* 299-344.
34. Werner, H., Schulten, K., and Weller, A. (1978). Electron transfer and spin exchange contributing to the magnetic field dependence of the primary photochemical reaction of bacterial photosynthesis. *Biochimica et Biophysica Acta (BBA)-Bioenergetics* 2, 255-268.
35. Schulten, K., and Wolynes, P.G. (1978). Semiclassical description of electron spin motion in radicals including the effect of electron hopping. *J. Chem. Phys.* 7, 3292-3297.
36. Ritz, T., Adem, S., and Schulten, K. (2000). A model for photoreceptor-based magnetoreception in birds. *Biophys. J.* 2, 707-718.
37. Phillips, J.B. (1986). Two magnetoreception pathways in a migratory salamander. *Science* 4765, 765-767.
38. Thalau, P., Ritz, T., Burda, H., Wegner, R.E., and Wiltschko, R. (2006). The magnetic compass mechanisms of birds and rodents are based on different physical principles. *Journal of the royal Society Interface* 9, 583-587.
39. Wiltschko, R., Stapput, K., Ritz, T., Thalau, P., and Wiltschko, W. (2007). Magnetoreception in birds: different physical processes for two types of directional responses. *HFSP journal* 1, 41.
40. Myklatun, A., Lauri, A., Eder, S.H., Cappetta, M., Shcherbakov, D., Wurst, W., Winklhofer, M., and Westmeyer, G.G. (2018). Zebrafish and medaka offer insights into the neurobehavioral correlates of vertebrate magnetoreception. *Nature communications* 1, 802.
41. Walker, M.M. (2008). A model for encoding of magnetic field intensity by magnetite-based magnetoreceptor cells. *J. Theor. Biol.* 1, 85-91.
42. Davila, A.F., Fleissner, G., Winklhofer, M., and Petersen, N. (2003). A new model for a magnetoreceptor in homing pigeons based on interacting clusters of superparamagnetic magnetite. *Physics and Chemistry of the Earth, Parts A/B/C* 16-19, 647-652.
43. Johnsen, S., and Lohmann, K.J. (2005). The physics and neurobiology of magnetoreception. *Nature Reviews Neuroscience* 9, 703.
44. Winklhofer, M. (2015). Magnetoreception. *Journal of the Royal Society Interface* 102,
45. Blakemore, R. (1975). Magnetotactic bacteria. *Science* 4212, 377-379.

46. Lambinet, V., Hayden, M.E., Reigl, K., Gomis, S., and Gries, G. (2017). Linking magnetite in the abdomen of honey bees to a magnetoreceptive function. *Proc.R.Soc.B* 1851, 20162873.
47. Eder, S.H., Cadiou, H., Muhamad, A., McNaughton, P.A., Kirschvink, J.L., and Winklhofer, M. (2012). Magnetic characterization of isolated candidate vertebrate magnetoreceptor cells. *Proceedings of the National Academy of Sciences* 30, 12022-12027.
48. Dixon, A. (2012). Zebrafish magnetite and long-lived Rohon-Beard neurons: expanding our view of two zebrafish sensory systems in development and adulthood California Institute of Technology).
49. Walker, M.M., Diebel, C.E., Haugh, C.V., Pankhurst, P.M., Montgomery, J.C., and Green, C.R. (1997). Structure and function of the vertebrate magnetic sense. *Nature* 6658, 371.
50. Diebel, C.E., Proksch, R., Green, C.R., Neilson, P., and Walker, M.M. (2000). Magnetite defines a vertebrate magnetoreceptor. *Nature* 6793, 299.
51. Edelman, N.B., Fritz, T., Nimpf, S., Pichler, P., Lauwers, M., Hickman, R.W., Papadaki-Anastasopoulou, A., Ushakova, L., Heuser, T., and Resch, G.P. (2015). No evidence for intracellular magnetite in putative vertebrate magnetoreceptors identified by magnetic screening. *Proceedings of the National Academy of Sciences* 1, 262-267.
52. Treiber, C.D., Salzer, M.C., Riegler, J., Edelman, N., Sugar, C., Breuss, M., Pichler, P., Cadiou, H., Saunders, M., and Lythgoe, M. (2012). Clusters of iron-rich cells in the upper beak of pigeons are macrophages not magnetosensitive neurons. *Nature* 7394, 367.
53. Krylov, V.V., Izyumov, Y.G., Izvekov, E.I., and Nepomnyashchikh, V.A. (2014). Magnetic fields and fish behavior. *Biology Bulletin Reviews* 3, 222-231.
54. Beason, R.C., and Semm, P. (1987). Magnetic responses of the trigeminal nerve system of the bobolink (*Dolichonyx oryzivorus*). *Neurosci. Lett.* 2, 229-234.
55. Hellinger, J., and Hoffmann, K. (2012). Magnetic field perception in the rainbow trout *Oncorhynchus mykiss*: magnetite mediated, light dependent or both? *Journal of Comparative Physiology A* 8, 593-605.
56. Pais-Roldán, P., Singh, A.P., Schulz, H., and Yu, X. (2016). High magnetic field induced otolith fusion in the zebrafish larvae. *Scientific reports* 24151.
57. Ward, B.K., Tan, G.X., Roberts, D.C., Della Santina, C.C., Zee, D.S., and Carey, J.P. (2014). Strong static magnetic fields elicit swimming behaviors consistent with direct vestibular stimulation in adult zebrafish. *PloS one* 3, e92109.
58. Takebe, A., Furutani, T., Wada, T., Koinuma, M., Kubo, Y., Okano, K., and Okano, T. (2012). Zebrafish respond to the geomagnetic field by bimodal and group-dependent orientation. *Scientific reports* 727.
59. Quinn, T.P., and Brannon, E.L. (1982). The use of celestial and magnetic cues by orienting sockeye salmon smolts. *Journal of Comparative Physiology A: Neuroethology, Sensory, Neural, and Behavioral Physiology* 4, 547-552.

60. Hellinger, J., and Hoffmann, K. (2009). Magnetic field perception in the rainbow trout, *Oncorhynchus mykiss*. *Journal of Comparative Physiology A* 9, 873-879.
61. Holland, R.A., Kirschvink, J.L., Doak, T.G., and Wikelski, M. (2008). Bats use magnetite to detect the earth's magnetic field. *PLoS One* 2, e1676.
62. Marhold, S., Wiltschko, W., and Burda, H. (1997). A magnetic polarity compass for direction finding in a subterranean mammal. *Naturwissenschaften* 9, 421-423.
63. Lohmann, K.J., and Lohmann, C.M.F. (1993). A light-independent magnetic compass in the leatherback sea turtle. *Biol. Bull.* 1, 149-151.
64. Lohmann, K.J., and Lohmann, C.M. (1996). Detection of magnetic field intensity by sea turtles. *Nature* 6569, 59.
65. Lohmann, K., and Lohmann, C. (1994). Detection of magnetic inclination angle by sea turtles: a possible mechanism for determining latitude. *J. Exp. Biol.* 1, 23-32.
66. Courtillot, V., Hulot, G., Alexandrescu, M., Mouel, J.I., and Kirschvink, J.L. (1997). Sensitivity and evolution of sea-turtle magnetoreception: observations, modelling and constraints from geomagnetic secular variation. *Terra Nova-Oxford*- 203-207.
67. Landler, L., Painter, M.S., Youmans, P.W., Hopkins, W.A., and Phillips, J.B. (2015). Spontaneous magnetic alignment by yearling snapping turtles: rapid association of radio frequency dependent pattern of magnetic input with novel surroundings. *PLoS One* 5, e0124728.
68. Wiltschko, R., Stapput, K., Thalau, P., and Wiltschko, W. (2009). Directional orientation of birds by the magnetic field under different light conditions. *Journal of the Royal Society Interface* rsif20090367.
69. Wiltschko, W., Wiltschko, R., and Ritz, T. (2011). The mechanism of the avian magnetic compass. *Procedia Chemistry* 1, 276-284.
70. Muheim, R., Edgar, N.M., Sloan, K.A., and Phillips, J.B. (2006). Magnetic compass orientation in C57BL/6J mice. *Learning & Behavior* 4, 366-373.
71. Foley, L.E., Gegeer, R.J., and Reppert, S.M. (2011). Human cryptochrome exhibits light-dependent magnetosensitivity. *Nature communications* 356.
72. Muheim, R., Bäckman, J., and Akesson, S. (2002). Magnetic compass orientation in European robins is dependent on both wavelength and intensity of light. *J. Exp. Biol.* 24, 3845-3856.
73. Wiltschko, W., and Wiltschko, R. (2001). Light-dependent magnetoreception in birds: the behaviour of European robins, *Erithacus rubecula*, under monochromatic light of various wavelengths and intensities. *J. Exp. Biol.* 19, 3295-3302.
74. Wiltschko, R., Stapput, K., Bischof, H., and Wiltschko, W. (2007). Light-dependent magnetoreception in birds: increasing intensity of monochromatic light changes the nature of the response. *Frontiers in Zoology* 1, 5.

75. Muheim, R., Sjöberg, S., and Pinzon-Rodriguez, A. (2016). Polarized light modulates light-dependent magnetic compass orientation in birds. *Proceedings of the National Academy of Sciences* 6, 1654-1659.
76. Worster, S., Mouritsen, H., and Hore, P.J. (2017). A light-dependent magnetoreception mechanism insensitive to light intensity and polarization. *Journal of The Royal Society Interface* 134, 20170405.
77. Deutschlander, M.E., Borland, S.C., and Phillips, J.B. (1999). Extraocular magnetic compass in newts. *Nature* 6742, 324.
78. Phillips, J.B., Deutschlander, M.E., Freake, M.J., and Borland, S.C. (2001). The role of extraocular photoreceptors in newt magnetic compass orientation: parallels between light-dependent magnetoreception and polarized light detection in vertebrates. *J. Exp. Biol.* 14, 2543-2552.
79. Demaine, C., and Semm, P. (1985). The avian pineal gland as an independent magnetic sensor. *Neurosci. Lett.* 1, 119-122.
80. Maffei, L., Meschini, E., and Papi, F. (1983). Pineal body and magnetic sensitivity: homing in pinealectomized pigeons under overcast skies. *Ethology* 2, 151-156.
81. Schneider, T., Thalau, H., Semm, P., and Wiltschko, W. (1994). Melatonin is crucial for the migratory orientation of pied flycatchers (*Ficedula hypoleuca* Pallas). *J. Exp. Biol.* 1, 255-262.
82. Semm, P., and Demaine, C. (1986). Neurophysiological properties of magnetic cells in the pigeon's visual system. *Journal of Comparative Physiology A* 5, 619-625.
83. Ramírez, E., Marín, G., Mpodozis, J., and Letelier, J. (2014). Extracellular recordings reveal absence of magneto sensitive units in the avian optic tectum. *Journal of Comparative Physiology A* 12, 983-996.
84. Zapka, M., Heyers, D., Hein, C.M., Engels, S., Schneider, N., Hans, J., Weiler, S., Dreyer, D., Kishkinev, D., Wild, J.M. *et al.* (2009). Visual but not trigeminal mediation of magnetic compass information in a migratory bird. *Nature* 7268, 1274-1277.
85. Mouritsen, H., Janssen-Bienhold, U., Liedvogel, M., Feenders, G., Stalleicken, J., Dirks, P., and Weiler, R. (2004). Cryptochromes and neuronal-activity markers colocalize in the retina of migratory birds during magnetic orientation. *Proc. Natl. Acad. Sci. U. S. A.* 39, 14294-14299.
86. Mouritsen, H., Feenders, G., Liedvogel, M., Wada, K., and Jarvis, E.D. (2005). Night-vision brain area in migratory songbirds. *PNAS* 23, 8339-8344.
87. Zapka, M., Heyers, D., Liedvogel, M., Jarvis, E.D., and Mouritsen, H. (2010). Night-time neuronal activation of Cluster N in a day- and night-migrating songbird. *Eur J Neurosci* 4, 619-624.
88. Ritz, T., Dommer, D.H., and Phillips, J.B. (2002). Shedding light on vertebrate magnetoreception. *Neuron* 4, 503-506.

89. Ritz, T., Ahmad, M., Mouritsen, H., Wiltschko, R., and Wiltschko, W. (2010). Photoreceptor-based magnetoreception: optimal design of receptor molecules, cells, and neuronal processing. *Journal of the Royal Society Interface Suppl 2*, S146.
90. Solov'yov, I.A., Mouritsen, H., and Schulten, K. (2010). Acuity of a cryptochrome and vision-based magnetoreception system in birds. *Biophys. J.* 1, 40-49.
91. Mouritsen, H., and Hore, P.J. (2012). The magnetic retina: light-dependent and trigeminal magnetoreception in migratory birds. *Curr. Opin. Neurobiol.* 2, 343-352.
92. Cintolesi, F., Ritz, T., Kay, C., Timmel, C.R., and Hore, P.J. (2003). Anisotropic recombination of an immobilized photoinduced radical pair in a 50- $\mu$ T magnetic field: a model avian photomagnetoreceptor. *Chem. Phys.* 3, 385-399.
93. Timmel, C.R., Till, U., Brocklehurst, B., McLauchlan, K.A., and Hore, P.J. (1998). Effects of weak magnetic fields on free radical recombination reactions. *Mol. Phys.* 1, 71-89.
94. Brocklehurst, B. (2002). Magnetic fields and radical reactions: recent developments and their role in nature. *Chem. Soc. Rev.* 5, 301-311.
95. Maeda, K., Robinson, A.J., Henbest, K.B., Hogben, H.J., Biskup, T., Ahmad, M., Schleicher, E., Weber, S., Timmel, C.R., and Hore, P.J. (2012). Magnetically sensitive light-induced reactions in cryptochrome are consistent with its proposed role as a magnetoreceptor. *Proceedings of the National Academy of Sciences* 13, 4774-4779.
96. Hiscock, H.G., Worster, S., Kattinig, D.R., Steers, C., Jin, Y., Manolopoulos, D.E., Mouritsen, H., and Hore, P.J. (2016). The quantum needle of the avian magnetic compass. *Proceedings of the National Academy of Sciences* 17, 4634-4639.
97. Maeda, K., Henbest, K.B., Cintolesi, F., Kuprov, I., Rodgers, C.T., Liddell, P.A., Gust, D., Timmel, C.R., and Hore, P.J. (2008). Chemical compass model of avian magnetoreception. *Nature* 7193, 387.
98. Ritz, T., Thalau, P., Phillips, J.B., Wiltschko, R., and Wiltschko, W. (2004). Resonance effects indicate a radical-pair mechanism for avian magnetic compass. *Nature* 6988, 177.
99. Henbest, K.B., Kukura, P., Rodgers, C.T., Hore, P.J., and Timmel, C.R. (2004). Radio frequency magnetic field effects on a radical recombination reaction: a diagnostic test for the radical pair mechanism. *J. Am. Chem. Soc.* 26, 8102-8103.
100. Rodgers, C.T., Henbest, K.B., Kukura, P., Timmel, C.R., and Hore, P.J. (2005). Low-field optically detected EPR spectroscopy of transient photoinduced radical pairs. *The Journal of Physical Chemistry A* 23, 5035-5041.
101. Thalau, P., Ritz, T., Stapput, K., Wiltschko, R., and Wiltschko, W. (2005). Magnetic compass orientation of migratory birds in the presence of a 1.315 MHz oscillating field. *Naturwissenschaften* 2, 86-90.

102. Engels, S., Schneider, N., Lefeldt, N., Hein, C.M., Zapka, M., Michalik, A., Elbers, D., Kittel, A., Hore, P.J., and Mouritsen, H. (2014). Anthropogenic electromagnetic noise disrupts magnetic compass orientation in a migratory bird. *Nature* 7500, 353.
103. Schwarze, S., Schneider, N., Reichl, T., Dreyer, D., Lefeldt, N., Engels, S., Baker, N., Hore, P.J., and Mouritsen, H. (2016). Weak broadband electromagnetic fields are more disruptive to magnetic compass orientation in a night-migratory songbird (*Erithacus rubecula*) than strong narrow-band fields. *Frontiers in behavioral neuroscience* 55.
104. Kavokin, K., Chernetsov, N., Pakhomov, A., Bojarinova, J., Kobylkov, D., and Namozov, B. (2014). Magnetic orientation of garden warblers (*Sylvia borin*) under 1.4 MHz radiofrequency magnetic field. *Journal of the Royal Society Interface* 97, 20140451.
105. Keary, N., Ruploh, T., Voss, J., Thalau, P., Wiltschko, R., Wiltschko, W., and Bischof, H. (2009). Oscillating magnetic field disrupts magnetic orientation in Zebra finches, *Taeniopygia guttata*. *Frontiers in zoology* 1, 25.
106. Vácha, M., Půžová, T., and Kvíčalová, M. (2009). Radio frequency magnetic fields disrupt magnetoreception in American cockroach. *J. Exp. Biol.* 21, 3473-3477.
107. Nießner, C., and Winklhofer, M. (2017). Radical-pair-based magnetoreception in birds: radio-frequency experiments and the role of cryptochrome. *Journal of Comparative Physiology A* 6-7, 499-507.
108. Ahmad, M., and Cashmore, A.R. (1993). HY4 gene of *A. thaliana* encodes a protein with characteristics of a blue-light photoreceptor. *Nature* 6451, 162.
109. Thompson, C.L., and Sancar, A. (2002). Photolyase/cryptochrome blue-light photoreceptors use photon energy to repair DNA and reset the circadian clock. *Oncogene* 58, 9043.
110. Chaves, I., Pokorny, R., Byrdin, M., Hoang, N., Ritz, T., Brettel, K., Essen, L., van der Horst, Gijssbertus TJ, Batschauer, A., and Ahmad, M. (2011). The cryptochromes: blue light photoreceptors in plants and animals. *Annual review of plant biology* 335-364.
111. Lin, C., and Shalitin, D. (2003). Cryptochrome structure and signal transduction. *Annual Review of Plant Biology* 1, 469-496.
112. Mei, Q., and Dvornyk, V. (2015). Evolutionary History of the Photolyase/Cryptochrome Superfamily in Eukaryotes. *PloS one* 9, e0135940.
113. Aubert, C., Vos, M.H., Mathis, P., Eker, A.P., and Brettel, K. (2000). Intraprotein radical transfer during photoactivation of DNA photolyase. *Nature* 6786, 586.
114. Solov'yov, I.A., Chandler, D.E., and Schulten, K. (2007). Magnetic field effects in *Arabidopsis thaliana* cryptochrome-1. *Biophys. J.* 8, 2711-2726.
115. Giachello, C.N., Scrutton, N.S., Jones, A.R., and Baines, R.A. (2016). Magnetic fields modulate blue-light-dependent regulation of neuronal firing by cryptochrome. *Journal of Neuroscience* 42, 10742-10749.

116. Sancar, A. (2000). Cryptochrome: the second photoactive pigment in the eye and its role in circadian photoreception. *Annu. Rev. Biochem.* *1*, 31-67.
117. Mei, Q., Sadovy, Y., and Dvornyk, V. (2015). Molecular evolution of cryptochromes in fishes. *Gene* *1*, 112-120.
118. Liu, C., Hu, J., Qu, C., Wang, L., Huang, G., Niu, P., Zhong, Z., Hong, F., Wang, G., Postlethwait, J.H. *et al.* (2015). Molecular evolution and functional divergence of zebrafish (*Danio rerio*) cryptochrome genes. *Scientific Reports* 8113.
119. Haug, M.F., Gesemann, M., Lazović, V., and Neuhauss, S.C.F. (2015). Eumetazoan cryptochrome phylogeny and evolution. *Genome biology and evolution* *2*, 601-619.
120. Henbest, K.B., Maeda, K., Hore, P.J., Joshi, M., Bacher, A., Bittl, R., Weber, S., Timmel, C.R., and Schleicher, E. (2008). Magnetic-field effect on the photoactivation reaction of *Escherichia coli* DNA photolyase. *Proceedings of the National Academy of Sciences* *38*, 14395-14399.
121. Wiltschko, R., Ahmad, M., Nießner, C., Gehring, D., and Wiltschko, W. (2016). Light-dependent magnetoreception in birds: the crucial step occurs in the dark. *J R Soc Interface* *118*,
122. Solov'yov, I.A., and Schulten, K. (2009). Magnetoreception through cryptochrome may involve superoxide. *Biophys. J.* *12*, 4804-4813.
123. Kutta, R.J., Archipowa, N., Johannissen, L.O., Jones, A.R., and Scrutton, N.S. (2017). Vertebrate cryptochromes are vestigial flavoproteins. *Scientific reports* 44906.
124. Günther, A., Einwich, A., Sjulstok, E., Feederle, R., Bolte, P., Koch, K., Solov'yov, I.A., and Mouritsen, H. (2018). Double-Cone Localization and Seasonal Expression Pattern Suggest a Role in Magnetoreception for European Robin Cryptochrome 4. *Current Biology*
125. Kobayashi, Y., Ishikawa, T., Hirayama, J., Daiyasu, H., Kanai, S., Toh, H., Fukuda, I., Tsujimura, T., Terada, N., and Kamei, Y. (2000). Molecular analysis of zebrafish photolyase/cryptochrome family: two types of cryptochromes present in zebrafish. *Genes to Cells* *9*, 725-738.
126. Ozturk, N., Selby, C.P., Song, S., Ye, R., Tan, C., Kao, Y., Zhong, D., and Sancar, A. (2009). Comparative photochemistry of animal type 1 and type 4 cryptochromes. *Biochemistry (N. Y.)* *36*, 8585-8593.
127. Marley, R., Giachello, C.N., Scrutton, N.S., Baines, R.A., and Jones, A.R. (2014). Cryptochrome-dependent magnetic field effect on seizure response in *Drosophila* larvae. *Scientific reports* 5799.
128. Yoshii, T., Ahmad, M., and Helfrich-Förster, C. (2009). Cryptochrome mediates light-dependent magnetosensitivity of *Drosophila*'s circadian clock. *PLoS biology* *4*, e1000086.
129. Fedele, G., Edwards, M.D., Bhutani, S., Hares, J.M., Murbach, M., Green, E.W., Dissel, S., Hastings, M.H., Rosato, E., and Kyriacou, C.P. (2014). Genetic analysis of circadian responses to low frequency electromagnetic fields in *Drosophila melanogaster*. *PLoS genetics* *12*, e1004804.

130. Fedele, G., Green, E.W., Rosato, E., and Kyriacou, C.P. (2014). An electromagnetic field disrupts negative geotaxis in *Drosophila* via a CRY-dependent pathway. *Nature communications* 4391.
131. Bae, J., Bang, S., Min, S., Lee, S., Kwon, S., Lee, Y., Lee, Y., Chung, J., and Chae, K. (2016). Positive geotactic behaviors induced by geomagnetic field in *Drosophila*. *Molecular brain* 1, 55.
132. Rivera, A.S., Ozturk, N., Fahey, B., Plachetzki, D.C., Degnan, B.M., Sancar, A., and Oakley, T.H. (2012). Blue-light-receptive cryptochrome is expressed in a sponge eye lacking neurons and opsin. *J. Exp. Biol.* 8, 1278-1286.
133. Müller, W.E., Schröder, H.C., Markl, J.S., Grebenjuk, V.A., Korzhev, M., Steffen, R., and Wang, X. (2013). Cryptochrome in sponges: a key molecule linking photoreception with phototransduction. *Journal of Histochemistry & Cytochemistry* 11, 814-832.
134. Mazzotta, G., Rossi, A., Leonardi, E., Mason, M., Bertolucci, C., Caccin, L., Spolaore, B., Martin, A.J., Schlichting, M., and Grebler, R. (2013). Fly cryptochrome and the visual system. *Proceedings of the National Academy of Sciences* 15, 6163-6168.
135. Guerra, P.A., Gegear, R.J., and Reppert, S.M. (2014). A magnetic compass aids monarch butterfly migration. *Nature communications* 4164.
136. Bolte, P., Bleibaum, F., Einwich, A., Günther, A., Liedvogel, M., Heyers, D., Depping, A., Wöhlbrand, L., Rabus, R., Janssen-Bienhold, U. *et al.* (2016). Localisation of the Putative Magnetoreceptive Protein Cryptochrome 1b in the Retinae of Migratory Birds and Homing Pigeons. *PLOS ONE* 3, e0147819.
137. Nießner, C., Gross, J.C., Denzau, S., Peichl, L., Fleissner, G., Wiltschko, W., and Wiltschko, R. (2016). Seasonally Changing Cryptochrome 1b Expression in the Retinal Ganglion Cells of a Migrating Passerine Bird. *PLOS ONE* 3, e0150377.
138. Niener, C., Denzau, S., Gross, J.C., Peichl, L., Bischof, H., Fleissner, G., Wiltschko, W., and Wiltschko, R. (2011). Avian ultraviolet/violet cones identified as probable magnetoreceptors. *PLoS One* 5, e20091.
139. Bischof, H., Nießner, C., Peichl, L., Wiltschko, R., and Wiltschko, W. (2011). Avian ultraviolet/violet cones as magnetoreceptors: The problem of separating visual and magnetic information. *Communicative & integrative biology* 6, 713-716.
140. Nießner, C., Denzau, S., Malkemper, E.P., Gross, J.C., Burda, H., Winklhofer, M., and Peichl, L. (2016). Cryptochrome 1 in retinal cone photoreceptors suggests a novel functional role in mammals. *Scientific reports* 21848.
141. Thompson, C.L., Rickman, C.B., Shaw, S.J., Ebright, J.N., Kelly, U., Sancar, A., and Rickman, D.W. (2003). Expression of the blue-light receptor cryptochrome in the human retina. *Invest. Ophthalmol. Vis. Sci.* 10, 4515-4521.
142. Phillips, J.B., Muheim, R., and Jorge, P.E. (2010). A behavioral perspective on the biophysics of the light-dependent magnetic compass: a link between directional and spatial perception? *J. Exp. Biol.* 19, 3247-3255.

143. Wiltschko, W., and Wiltschko, R. (2005). Magnetic orientation and magnetoreception in birds and other animals. *Journal of Comparative Physiology A* 8, 675-693.
144. Light, P., Salmon, M., and Lohmann, K.J. (1993). Geomagnetic orientation of loggerhead sea turtles: evidence for an inclination compass. *J. Exp. Biol.* 1, 1-10.
145. Neuhauss, S.C. (2003). Behavioral genetic approaches to visual system development and function in zebrafish. *Developmental Neurobiology* 1, 148-160.
146. Robinson, J., Schmitt, E.A., and Dowling, J.E. (1995). Temporal and spatial patterns of opsin gene expression in zebrafish (*Danio rerio*). *Vis. Neurosci.* 5, 895-906.
147. Fimbel, S.M., Montgomery, J.E., Burket, C.T., and Hyde, D.R. (2007). Regeneration of inner retinal neurons after intravitreal injection of ouabain in zebrafish. *Journal of Neuroscience* 7, 1712-1724.
148. Curado, S., Stainier, D.Y., and Anderson, R.M. (2008). Nitroreductase-mediated cell/tissue ablation in zebrafish: a spatially and temporally controlled ablation method with applications in developmental and regeneration studies. *Nature protocols* 6, 948.
149. Cameron D.A. (2000). Cellular proliferation and neurogenesis in the injured retina of adult zebrafish. *Vis. Neurosci.* 5, 789-797.
150. Duval, M.G., Chung, H., Lehmann, O.J., and Allison, W.T. (2013). Longitudinal fluorescent observation of retinal degeneration and regeneration in zebrafish using fundus lens imaging. *Molecular vision* 1082.
151. Fleisch, V.C., Fraser, B., and Allison, W.T. (2011). Investigating regeneration and functional integration of CNS neurons: lessons from zebrafish genetics and other fish species. *Biochimica et Biophysica Acta (BBA)-Molecular Basis of Disease* 3, 364-380.
152. Raymond, P.A. (1991). Retinal regeneration in teleost fish. *Regeneration of vertebrate sensory receptor cells* 171-191.
153. Wilken, M.S., and Reh, T.A. (2016). Retinal regeneration in birds and mice. *Curr. Opin. Genet. Dev.* 57-64.
154. Chinen, A., Hamaoka, T., Yamada, Y., and Kawamura, S. (2003). Gene duplication and spectral diversification of cone visual pigments of zebrafish. *Genetics* 2, 663-675.
155. Raymond, P.A., Barthel, L.K., Rounsifer, M.E., Sullivan, S.A., and Knight, J.K. (1993). Expression of rod and cone visual pigments in goldfish and zebrafish: a rhodopsin-like gene is expressed in cones. *Neuron* 6, 1161-1174.
156. Allison, W., Haimberger, T.J., Hawryshyn, C.W., and Temple, S.E. (2005). Visual pigment composition in zebrafish: Evidence for a rhodopsin–porphyropsin interchange system. *Vis. Neurosci.* 2, 249.
157. Engström, K. (1960). Cone types and cone arrangement in the retina of some cyprinids. *Acta Zoologica* 3, 277-295.

158. Ahlbert, I. (1976). Organization of the cone cells in the retinae of salmon (*Salmo salar*) and trout (*Salmo trutta trutta*) in relation to their feeding habits. *Acta zoologica* *1*, 13-35.
159. Raymond, P.A., Colvin, S.M., Jabeen, Z., Nagashima, M., Barthel, L.K., Hadidjojo, J., Popova, L., Pejaver, V.R., and Lubensky, D.K. (2014). Patterning the cone mosaic array in zebrafish retina requires specification of ultraviolet-sensitive cones. *PLoS One* *1*, e85325.
160. Raymond, P.A., and Barthel, L.K. (2004). A moving wave patterns the cone photoreceptor mosaic array in the zebrafish retina. *Int. J. Dev. Biol.* *8-9*, 935-945.
161. Allison, W.T., Barthel, L.K., Skebo, K.M., Takechi, M., Kawamura, S., and Raymond, P.A. (2010). Ontogeny of cone photoreceptor mosaics in zebrafish. *J. Comp. Neurol.* *20*, 4182-4195.
162. Glasauer, S.M., and Neuhauss, S.C. (2014). Whole-genome duplication in teleost fishes and its evolutionary consequences. *Molecular genetics and genomics* *6*, 1045-1060.
163. Shcherbakov, D., Winklhofer, M., Petersen, N., Steidle, J., Hilbig, R., and Blum, M. (2005). Magnetosensation in zebrafish. *Current Biology* *5*, R162.
164. Krylov, V.V., Osipova, E.A., Pavlova, V.V., and Batrakova, A.A. (2016). Influence of magnetic field on the spatial orientation in zebrafish (*Danio rerio*). *J. Ichthyol.* *3*, 456-461.
165. Cresci, A., De Rosa, R., Putman, N.F., and Agnisola, C. (2017). Earth-strength magnetic field affects the rheotactic threshold of zebrafish swimming in shoals. *Comparative Biochemistry and Physiology Part A: Molecular & Integrative Physiology* *169-176*.
166. Engeszer, R.E., Patterson, L.B., Rao, A.A., and Parichy, D.M. (2007). Zebrafish in the wild: a review of natural history and new notes from the field. *Zebrafish* *1*, 21-40.
167. Spence, R., Gerlach, G., Lawrence, C., and Smith, C. (2008). The behaviour and ecology of the zebrafish, *Danio rerio*. *Biological Reviews* *1*, 13-34.
168. Bridgewater, J.A., Springer, C.J., Knox, R.J., Minton, N.P., Michael, N.P., and Collins, M.K. (1995). Expression of the bacterial nitroreductase enzyme in mammalian cells renders them selectively sensitive to killing by the prodrug CB1954. *Eur. J. Cancer* *13-14*, 2362-2370.
169. Curado, S., Stainier, D.Y., and Anderson, R.M. (2008). Nitroreductase-mediated cell/tissue ablation in zebrafish: a spatially and temporally controlled ablation method with applications in developmental and regeneration studies. *Nature protocols* *6*, 948.
170. Fraser, B., DuVal, M.G., Wang, H., and Allison, W.T. (2013). Regeneration of cone photoreceptors when cell ablation is primarily restricted to a particular cone subtype. *PLoS One* *1*, e55410.
171. Montgomery, J.E., Parsons, M.J., and Hyde, D.R. (2010). A novel model of retinal ablation demonstrates that the extent of rod cell death regulates the origin of the regenerated zebrafish rod photoreceptors. *J. Comp. Neurol.* *6*, 800-814.
172. White, D.T., and Mumm, J.S. (2013). The nitroreductase system of inducible targeted ablation facilitates cell-specific regenerative studies in zebrafish. *Methods* *3*, 232-240.

173. Hagerman, G.F., Noel, N.C., Cao, S.Y., DuVal, M.G., Oel, A.P., and Allison, W.T. (2016). Rapid recovery of visual function associated with blue cone ablation in zebrafish. *PloS one* *11*, e0166932.
174. Yoshimatsu, T., D'Orazi, F.D., Gamlin, C.R., Suzuki, S.C., Suli, A., Kimelman, D., Raible, D.W., and Wong, R.O. (2016). Presynaptic partner selection during retinal circuit reassembly varies with timing of neuronal regeneration in vivo. *Nature communications* 10590.
175. Nordmann, G.C., Hochstoeger, T., and Keays, D.A. (2017). Magnetoreception—A sense without a receptor. *PLoS biology* *10*, e2003234.
176. Liedvogel, M., Maeda, K., Henbest, K., Schleicher, E., Simon, T., Timmel, C.R., Hore, P.J., and Mouritsen, H. (2007). Chemical magnetoreception: bird cryptochrome 1a is excited by blue light and forms long-lived radical-pairs. *PloS one* *10*, e1106.
177. O'Connor, J., and Muheim, R. (2017). Pre-settlement coral-reef fish larvae respond to magnetic field changes during the day. *J. Exp. Biol.* *16*, 2874-2877.
178. Westerfield, M. (2000). The zebrafish book: a guide for the laboratory use of zebrafish. [http://zfin.org/zf\\_info/zfbook/zfbk.html](http://zfin.org/zf_info/zfbook/zfbk.html)
179. Karlsson, J., von Hofsten, J., and Olsson, P. (2001). Generating transparent zebrafish: a refined method to improve detection of gene expression during embryonic development. *Marine Biotechnology* *6*, 522-527.
180. Barthel, L.K., and Raymond, P.A. (2000). [39] In situ hybridization studies of retinal neurons. In *Methods in enzymology*, Elsevier) pp. 579-590.
181. Bustin, S.A., Benes, V., Garson, J.A., Hellems, J., Huggett, J., Kubista, M., Mueller, R., Nolan, T., Pfaffl, M.W., and Shipley, G.L. (2009). The MIQE guidelines: minimum information for publication of quantitative real-time PCR experiments. *Clin. Chem.* *4*, 611-622.
182. Tang, R., Dodd, A., Lai, D., McNabb, W.C., and Love, D.R. (2007). Validation of zebrafish (*Danio rerio*) reference genes for quantitative real-time RT-PCR normalization. *Acta biochimica et biophysica Sinica* *5*, 384-390.
183. Fleisch, V.C., Leighton, P.L., Wang, H., Pillay, L.M., Ritzel, R.G., Bhinder, G., Roy, B., Tierney, K.B., Ali, D.W., and Waskiewicz, A.J. (2013). Targeted mutation of the gene encoding prion protein in zebrafish reveals a conserved role in neuron excitability. *Neurobiol. Dis.* 11-25.
184. Ginzinger, D.G. (2002). Gene quantification using real-time quantitative PCR: an emerging technology hits the mainstream. *Exp. Hematol.* *6*, 503-512.
185. Walker, M.M. (1984). Learned magnetic field discrimination in yellowfin tuna, *Thunnus albacares*. *Journal of Comparative Physiology A: Neuroethology, Sensory, Neural, and Behavioral Physiology* *5*, 673-679.
186. Noel, N.C., and Allison, W.T. (2018). Connectivity of cone photoreceptor telodendria in the zebrafish retina. *J. Comp. Neurol.* *4*, 609-625.

187. Mouritsen, H., Atema, J., Kingsford, M.J., and Gerlach, G. (2013). Sun compass orientation helps coral reef fish larvae return to their natal reef. *PLoS One* 6, e66039.
188. Pinzon-Rodriguez, A., Bensch, S., and Muheim, R. (2018). Expression patterns of cryptochrome genes in avian retina suggest involvement of Cry4 in light-dependent magnetoreception. *Journal of The Royal Society Interface* 140, 20180058.
189. Nießner, C., Denzau, S., Stapput, K., Ahmad, M., Peichl, L., Wiltschko, W., and Wiltschko, R. (2013). Magnetoreception: activated cryptochrome 1a concurs with magnetic orientation in birds. *J R Soc Interface* 88,
190. Klaassen, L.J., Sun, Z., Steijaert, M.N., Bolte, P., Fahrenfort, I., Sjoerdsma, T., Klooster, J., Claassen, Y., Shields, C.R., and Ten Eikelder, H.M. (2011). Synaptic transmission from horizontal cells to cones is impaired by loss of connexin hemichannels. *PLoS biology* 7, e1001107.
191. Klaassen, L.J., de Graaff, W., Van Asselt, J.B., Klooster, J., and Kamermans, M. (2016). Specific connectivity between photoreceptors and horizontal cells in the zebrafish retina. *J. Neurophysiol.* 6, 2799-2814.
192. Stell, W.K., and Lightfoot, D.O. (1975). Color-specific interconnections of cones and horizontal cells in the retina of the goldfish. *J. Comp. Neurol.* 4, 473-501.
193. Robinson, J., Schmitt, E.A., Harosi, F.I., Reece, R.J., and Dowling, J.E. (1993). Zebrafish ultraviolet visual pigment: absorption spectrum, sequence, and localization. *Proceedings of the National Academy of Sciences* 13, 6009-6012.
194. Hughes, A., Saszik, S., Bilotta, J., DEMARCO, P.J., and PATTERSON, W.F. (1998). Cone contributions to the photopic spectral sensitivity of the zebrafish ERG. *Vis. Neurosci.* 6, 1029-1037.
195. Nießner, C., Denzau, S., Peichl, L., Wiltschko, W., and Wiltschko, R. (2014). Magnetoreception in birds: I. Immunohistochemical studies concerning the cryptochrome cycle. *J. Exp. Biol.* 23, 4221-4224.
196. Chiao, C., Cronin, T.W., and Osorio, D. (2000). Color signals in natural scenes: characteristics of reflectance spectra and effects of natural illuminants. *JOSA A* 2, 218-224.
197. Zimmermann, M.J., Nevala, N.E., Yoshimatsu, T., Osorio, D., Nilsson, D., Berens, P., and Baden, T. (2017). Zebrafish differentially process colour across visual space to match natural scenes. *bioRxiv* 230144.
198. Tilley, R.J. (2010). *Colour and the optical properties of materials: an exploration of the relationship between light, the optical properties of materials and colour* John Wiley & Sons).
199. Crescitelli, F., Wilson, B.W., and Lilyblade, A.L. (1964). The visual pigments of birds: I. The turkey. *Vision Res.* 5-6, 275-280.
200. Hart, N.S. (2001). Variations in cone photoreceptor abundance and the visual ecology of birds. *Journal of Comparative Physiology A* 9, 685-697.

201. Yoshizawa, T., and Kuwata, O. (1991). Iodopsin, a red-sensitive cone visual pigment in the chicken retina. *Photochem. Photobiol.* 6, 1061-1070.
202. Kram, Y.A., Mantey, S., and Corbo, J.C. (2010). Avian cone photoreceptors tile the retina as five independent, self-organizing mosaics. *PloS one* 2, e8992.
203. Takechi, M., and Kawamura, S. (2005). Temporal and spatial changes in the expression pattern of multiple red and green subtype opsin genes during zebrafish development. *J. Exp. Biol.* 7, 1337-1345.
204. Hawryshyn, C.W., and McFarland, W.N. (1987). Cone photoreceptor mechanisms and the detection of polarized light in fish. *Journal of Comparative Physiology A* 4, 459-465.
205. Hawryshyn, C.W. (2010). Ultraviolet polarization vision and visually guided behavior in fishes. *Brain Behav. Evol.* 3, 186-194.
206. Hawryshyn, C.W., Martens, G., Allison, W.T., and Anholt, B.R. (2003). Regeneration of ultraviolet-sensitive cones in the retinal cone mosaic of thyroxin-challenged post-juvenile rainbow trout (*Oncorhynchus mykiss*). *J. Exp. Biol.* 15, 2665-2673.
207. Flamarique, I.N. (2000). The ontogeny of ultraviolet sensitivity, cone disappearance and regeneration in the sockeye salmon *Oncorhynchus nerka*. *J. Exp. Biol.* 7, 1161-1172.
208. Allison, W.T., Dann, S.G., Veldhoen, K.M., and Hawryshyn, C.W. (2006). Degeneration and regeneration of ultraviolet cone photoreceptors during development in rainbow trout. *J. Comp. Neurol.* 5, 702-715.
209. Gagnon, J.A., Valen, E., Thyme, S.B., Huang, P., Ahkmetova, L., Pauli, A., Montague, T.G., Zimmerman, S., Richter, C., and Schier, A.F. (2014). Efficient mutagenesis by Cas9 protein-mediated oligonucleotide insertion and large-scale assessment of single-guide RNAs. *PloS one* 5, e98186.
210. Fitak, R.R., Wheeler, B.R., Ernst, D.A., Lohmann, K.J., and Johnsen, S. (2017). Candidate genes mediating magnetoreception in rainbow trout (*Oncorhynchus mykiss*). *Biology letters* 4, 20170142.
211. Arniella, M.B., Fitak, R.R., and Johnsen, S. (2018). Unmapped sequencing reads identify additional candidate genes linked to magnetoreception in rainbow trout. *Environ. Biol. Fishes* 1-11.
212. Fosque, B.F., Sun, Y., Dana, H., Yang, C., Ohyama, T., Tadross, M.R., Patel, R., Zlatic, M., Kim, D.S., and Ahrens, M.B. (2015). Labeling of active neural circuits in vivo with designed calcium integrators. *Science* 6223, 755-760.
213. Kim, D.H., Kim, J., Marques, J.C., Grama, A., Hildebrand, D.G., Gu, W., Li, J.M., and Robson, D.N. (2017). Pan-neuronal calcium imaging with cellular resolution in freely swimming zebrafish. *nature methods* 11, 1107.
214. Müller, H. (1951). Über das Zapfenmosaik in der Netzhaut des „Guppy“ (*Lebistes reticulatus*). *Naturwissenschaften* 19, 459-460.
215. Lyall, A.H. (1957). Cone arrangements in teleost retinae. *J. Cell. Sci.* 42, 189-201.

216. Marc, R.E., and Sperling, H.G. (1976). The chromatic organization of the goldfish cone mosaic. *Vision Res.* *11*, IN6.
217. Ohki, H., and Aoki, K. (1985). Development of Visual Acuity in the Larval Medaka, *Oryzias latipes* (COMMUNICATION)(Physiology). *Zool. Sci.* *1*, 123-126.
218. Mader, M.M., and Cameron, D.A. (2004). Photoreceptor differentiation during retinal development, growth, and regeneration in a metamorphic vertebrate. *Journal of Neuroscience* *50*, 11463-11472.
219. Kamermans, M., Kraaij, D.A., and Spekreijse, H. (1998). The cone/horizontal cell network: a possible site for color constancy. *Vis. Neurosci.* *5*, 787-797.
220. Lamb, T.D., and Simon, E.J. (1976). The relation between intercellular coupling and electrical noise in turtle photoreceptors. *J. Physiol. (Lond.)* *2*, 257-286.
221. DeVries, S.H., Qi, X., Smith, R., Makous, W., and Sterling, P. (2002). Electrical coupling between mammalian cones. *Current Biology* *22*, 1900-1907.
222. Palfey, B.A., and Massey, V. (1998). *Flavin-dependent enzymes*.
223. Islam, S.D., Susdorf, T., Penzkofer, A., and Hegemann, P. (2003). Fluorescence quenching of flavin adenine dinucleotide in aqueous solution by pH dependent isomerisation and photo-induced electron transfer. *Chem. Phys.* *2*, 137-149.
224. Song, S., Dick, B., Penzkofer, A., Pokorny, R., Batschauer, A., and Essen, L. (2006). Absorption and fluorescence spectroscopic characterization of cryptochrome 3 from *Arabidopsis thaliana*. *Journal of Photochemistry and Photobiology B: Biology* *1*, 1-16.
225. Muller, F. (2018). *Chemistry and biochemistry of flavoenzymes* CRC Press).
226. Cronin, T.W., and Bok, M.J. (2016). Photoreception and vision in the ultraviolet. *J. Exp. Biol.* *18*, 2790-2801.
227. Losey, G.S., Cronin, T.W., Goldsmith, T.H., Hyde, D., Marshall, N.J., and McFarland, W.N. (1999). The UV visual world of fishes: a review. *J. Fish Biol.* *5*, 921-943.
228. Neumeyer, C. (1986). Wavelength discrimination in the goldfish. *Journal of Comparative Physiology A* *2*, 203-213.
229. Neumeyer, C. (1992). Tetrachromatic color vision in goldfish: evidence from color mixture experiments. *Journal of Comparative Physiology A: Neuroethology, Sensory, Neural, and Behavioral Physiology* *5*, 639-649.
230. Flamarique, I.N. (2013). Opsin switch reveals function of the ultraviolet cone in fish foraging. *Proceedings of the Royal Society of London B: Biological Sciences* *1752*, 20122490.

231. Flamarique, I.N. (2016). Diminished foraging performance of a mutant zebrafish with reduced population of ultraviolet cones. *Proc.R.Soc.B* 1826, 20160058.
232. Leech, D.M., and Johnsen, S. (2006). Ultraviolet vision and foraging in juvenile bluegill (*Lepomis macrochirus*). *Can. J. Fish. Aquat. Sci.* 10, 2183-2190.
233. Morris, D.P., Zagarese, H., Williamson, C.E., Balseiro, E.G., Hargreaves, B.R., Modenutti, B., Moeller, R., and Queimalinos, C. (1995). The attenuation of solar UV radiation in lakes and the role of dissolved organic carbon. *Limnol. Oceanogr.* 8, 1381-1391.
234. Morris, V.B. (1970). Symmetry in a receptor mosaic demonstrated in the chick from the frequencies, spacing and arrangement of the types of retinal receptor. *J. Comp. Neurol.* 3, 359-397.
235. Maier, E.J., and Bowmaker, J.K. (1993). Colour vision in the passeriform bird, *Leiothrix lutea*: correlation of visual pigment absorbance and oil droplet transmission with spectral sensitivity. *Journal of Comparative Physiology A* 3, 295-301.
236. Jones, C.D., Osorio, D., and Baddeley, R.J. (2001). Colour categorization by domestic chicks. *Proceedings of the Royal Society of London B: Biological Sciences* 1481, 2077-2084.
237. Lind, O., Chavez, J., and Kelber, A. (2014). The contribution of single and double cones to spectral sensitivity in budgerigars during changing light conditions. *Journal of Comparative Physiology A* 3, 197-207.
238. Tsujimura, T., Chinen, A., and Kawamura, S. (2007). Identification of a locus control region for quadruplicated green-sensitive opsin genes in zebrafish. *Proceedings of the National Academy of Sciences* 31, 12813-12818.
239. Tsujimura, T., Masuda, R., Ashino, R., and Kawamura, S. (2015). Spatially differentiated expression of quadruplicated green-sensitive RH2 opsin genes in zebrafish is determined by proximal regulatory regions and gene order to the locus control region. *BMC genetics* 1, 130.
240. Endeman, D., Klaassen, L.J., and Kamermans, M. (2013). Action spectra of zebrafish cone photoreceptors. *PloS one* 7, e68540.
241. Li, Y.N., Tsujimura, T., Kawamura, S., and Dowling, J.E. (2012). Bipolar cell-photoreceptor connectivity in the zebrafish (*Danio rerio*) retina. *J. Comp. Neurol.* 16, 3786-3802.
242. Cahill, G.M. (2002). Clock mechanisms in zebrafish. *Cell Tissue Res.* 1, 27-34.
243. Vatine, G., Vallone, D., Gothilf, Y., and Foulkes, N.S. (2011). It's time to swim! Zebrafish and the circadian clock. *FEBS Lett.* 10, 1485-1494.
244. Mitsui, H., Maeda, T., Yamaguchi, C., Tsuji, Y., Watari, R., Kubo, Y., Okano, K., and Okano, T. (2015). Overexpression in yeast, photocycle, and in vitro structural change of an avian putative magnetoreceptor cryptochrome4. *Biochemistry (N. Y.)* 10, 1908-1917.
245. Watari, R., Yamaguchi, C., Zemba, W., Kubo, Y., Okano, K., and Okano, T. (2012). Light-dependent structural change of chicken retinal cryptochrome4. *J. Biol. Chem.* 51, 42634-42641.

246. Cermakian, N., Pando, M.P., Thompson, C.L., Pinchak, A.B., Selby, C.P., Gutierrez, L., Wells, D.E., Cahill, G.M., Sancar, A., and Sassone-Corsi, P. (2002). Light induction of a vertebrate clock gene involves signaling through blue-light receptors and MAP kinases. *Current Biology* 10, 844-848.
247. Hirayama, J., Miyamura, N., Uchida, Y., Asaoka, Y., Honda, R., Sawanobori, K., Todo, T., Yamamoto, T., Sassone-Corsi, P., and Nishina, H. (2009). Common light signaling pathways controlling DNA repair and circadian clock entrainment in zebrafish. *Cell Cycle* 17, 2794-2801.
248. Sun, C., Galicia, C., and Stenkamp, D.L. (2018). Transcripts within rod photoreceptors of the Zebrafish retina. *BMC Genomics* 1, 127.
249. Gunkel, M., Schöneberg, J., Alkhaldi, W., Irsen, S., Noé, F., Kaupp, U.B., and Al-Amoudi, A. (2015). Higher-order architecture of rhodopsin in intact photoreceptors and its implication for phototransduction kinetics. *Structure* 4, 628-638.
250. Stoneham, A.M., Gauger, E.M., Porfyrakis, K., Benjamin, S.C., and Lovett, B.W. (2012). A new type of radical-pair-based model for magnetoreception. *Biophys. J.* 5, 961-968.
251. Bossé, G.D., and Peterson, R.T. (2017). Development of an opioid self-administration assay to study drug seeking in zebrafish. *Behav. Brain Res.* 158-166.
252. Horvath, P., and Barrangou, R. (2010). CRISPR/Cas, the immune system of bacteria and archaea. *Science* 5962, 167-170.
253. Ablain, J., Durand, E.M., Yang, S., Zhou, Y., and Zon, L.I. (2015). A CRISPR/Cas9 vector system for tissue-specific gene disruption in zebrafish. *Developmental cell* 6, 756-764.
254. Ablain, J., and Zon, L.I. (2016). Tissue-specific gene targeting using CRISPR/Cas9. In *Methods in cell biology*, Elsevier) pp. 189-202.
255. Kennedy, B.N., Alvarez, Y., Brockerhoff, S.E., Stearns, G.W., Sapetto-Rebow, B., Taylor, M.R., and Hurley, J.B. (2007). Identification of a zebrafish cone photoreceptor-specific promoter and genetic rescue of achromatopsia in the *nof* mutant. *Invest. Ophthalmol. Vis. Sci.* 2, 522-529.
256. Suster, M.L., Kikuta, H., Urasaki, A., Asakawa, K., and Kawakami, K. (2009). Transgenesis in zebrafish with the *tol2* transposon system. In *Transgenesis techniques*, Springer) pp. 41-63.
257. Kirschvink, J.L. (1992). Uniform magnetic fields and double-wrapped coil systems: improved techniques for the design of bioelectromagnetic experiments. *Bioelectromagnetics* 5, 401-411.
258. Palmer, A.E., and Tsien, R.Y. (2006). Measuring calcium signaling using genetically targetable fluorescent indicators. *Nature protocols* 3, 1057.
259. Cheng, R., Krishnan, S., Lin, Q., Kibat, C., and Jesuthasan, S. (2017). Characterization of a thalamic nucleus mediating habenula responses to changes in ambient illumination. *BMC biology* 1, 104.
260. Liedvogel, M., Feenders, G., Wada, K., Troje, N.F., Jarvis, E.D., and Mouritsen, H. (2007). Lateralized activation of Cluster N in the brains of migratory songbirds. *Eur J Neurosci* 4, 1166-1173.

261. Antinucci, P., and Hindges, R. (2016). A crystal-clear zebrafish for in vivo imaging. *Scientific reports* 29490.
262. Lister, J.A., Robertson, C.P., Lepage, T., Johnson, S.L., and Raible, D.W. (1999). Nacre encodes a zebrafish microphthalmia-related protein that regulates neural-crest-derived pigment cell fate. *Development* 17, 3757-3767.
263. White, R.M., Sessa, A., Burke, C., Bowman, T., LeBlanc, J., Ceol, C., Bourque, C., Dovey, M., Goessling, W., and Burns, C.E. (2008). Transparent adult zebrafish as a tool for in vivo transplantation analysis. *Cell stem cell* 2, 183-189.
264. Li, Z., Ptak, D., Zhang, L., Walls, E.K., Zhong, W., and Leung, Y.F. (2012). Phenylthiourea specifically reduces zebrafish eye size. *PLoS One* 6, e40132.
265. Orger, M.B., Gahtan, E., Muto, A., Page-McCaw, P., Smear, M.C., and Baier, H. (2004). Behavioral screening assays in zebrafish. In *Methods in cell biology*, Elsevier) pp. 53-68.
266. Irion, U., Krauss, J., and Nüsslein-Volhard, C. (2014). Precise and efficient genome editing in zebrafish using the CRISPR/Cas9 system. *Development* 24, 4827-4830.
267. Meeker, N.D., Hutchinson, S.A., Ho, L., and Trede, N.S. (2007). Method for isolation of PCR-ready genomic DNA from zebrafish tissues. *BioTechniques* 5, 610.

## APPENDIX A

### A.1 Generation of *slc45a2* mutant zebrafish

I aimed to create a zebrafish mutant that lacked melanin in the RPE to allow for better visualization of fluorescent reporters in zebrafish photoreceptors. To do this, I utilized CRISPR-Cas9 genome editing based on [209].

#### A.1.1 sgRNA creation

sgRNA synthesis was completed as previously described [209]. Briefly, gene-specific oligonucleotides designed after [266] containing the SP6 promoter sequence, the 20-base pair target site without the Protospacer adjacent motif (PAM) sequence, and a complementary region were annealed to a constant oligo (Table A1). ssDNA was filled with T4 DNA polymerase (NEB, M0203S). sgRNA template was purified using QIAquick PCR Purification Kit (Qiagen, 28104) and transcribed using mMACHINE™ SP6 Transcription Kit (Invitrogen, AM1340). sgRNA was treated with DNase I (Qiagen, 79254) and quantified using Nanodrop spectrophotometer (GE Healthcare 28 9244-02). sgRNA was also run out on a 3% agarose gel to confirm transcription.

#### A.1.2 Injection process

Zebrafish nacre strain (*mitfa*<sup>-/-</sup>) were injected with 2-3 nl of injection solution (5 µl: 2 µl ~200 ng/µl sgRNA, 2 µl of 20 µM Cas9, 0.5 µl 1x Cas9 Nuclease Buffer (NEB, M0646M), 0.5 µl phenol

red into the cell of one-cell staged embryos. Embryos were grown and screened for pigment defects in the RPE at 3-4 days post fertilization (dpf) (Figure A1). Fish with pigment alterations were grown to adulthood.

### A.1.3 Genotyping via sequencing and RFLP

Adult zebrafish pigment mutants were fin clipped and genomic DNA (gDNA) was extracted as previously described [267]. PCR primers (Table A2) were used to amplify the CRISPR site target region. Template was cloned into pCR 2.1 plasmids via TA TOPO cloning (Invitrogen, 450641) and transformed. Colonies were picked and cultured in LB media, and plasmid DNA was isolated via QIAprep Spin Miniprep Kit (Qiagen, 27104). Plasmids were sequenced at the Molecular Biology Services Unit at the University of Alberta with amplicon specific primers (Table A2) to identify mutations.

A 22 base-pair (bp) deletion mutation was identified in fish with pigment defects, which causes a frameshift and early STOP codon at amino acid position 447 in SLC45A2 (Figure A1E). These mutants (*ua5015; slc45a2<sup>-/-</sup>; mitfa<sup>-/-</sup>*) were subsequently outcrossed to *nacre* background (*slc45a2<sup>+/+</sup>; mitfa<sup>-/-</sup>*) to determine germline transmission. Heterozygotes for *ua5015* were identified by restriction fragment length polymorphism analysis (RFLP).

Primers were designed to amplify a 235 bp region including the *ua5015 slc45a2* locus (Table A2). PCR product was digested with MspI restriction enzyme (NEB, R0106S) and run on a gel to identify wild-type, heterozygous or homozygous *ua5015* alleles.

#### A.1.4 Generation of *crystal* and *crystal*-based transgenics

To generate *crystal* mutants [261], ua5015 were crossed to *casper* mutants (*slc45a2*<sup>+/+</sup>; *nacre*<sup>-/-</sup>; *roy*<sup>-/-</sup>) [263], genotyped as described above and in-crossed to create our *crystal* line (ua5020; *slc45a2*<sup>-/-</sup>; *nacre*<sup>-/-</sup>; *roy*<sup>-/-</sup>) (Figure A4).

u5020 was outcrossed to *Tg(sws1:nfsb-mCherry; sws2:GFP)* in a *roy*<sup>-/-</sup> background [174,179], genotyped and in-crossed as described to create *Tg<sub>ua5020</sub>(sws1:nfsb-mCherry; sws2:GFP)* (Figure A5) which allow fluorescent visualization of UV and blue cones. Additionally, UV cones can be ablated in this line. Overall, *Tg<sub>ua5020</sub>(sws1:nfsb-mCherry; sws2:GFP)* combined with GECI technology can be used to determine the role of UV cones in neuronal processing of magnetic information.

**Table A1. Oligonucleotides used for sgRNA synthesis.**

<b>Oligo</b>	<b>Oligo sequences (SP6 promoter, <i>slc45a2</i> CRISPR site, overlap region for annealing)</b>
<i>slc45a2</i> <i>sgRNA</i>	ATTTAGGTGACACTATAAGGTTTGGGAACCGGTCTGATGTTTTAGAGCTAGAAATAGCAAG
<b>Constant oligo</b>	AAAAGCACCGACTCGGTGCCACTTTTTCAAGTTGATAACGGACTAGCCTTATTTAACTTGCTATTTCTAGCTCTAAAAC

**Table A2. Primers used for ua5015 and ua5020 genotyping.**

<b>Gene and Primer Use</b>	<b>Amplicon Size (bp)</b>	<b>Primer sequences (forward, reverse)</b>
<i>slc45a2</i> ; ua5015 TOPO cloning and sequencing	733	F: 5' ATTGTATATAAGGGGAATCCGTATGCT '3 R: 5' CTCTTCTGCCTTGTGGTACTC '3
<i>slc45a2</i> ; ua5015 RFLP	235	F: 5' TTCATCCATTTGTTCTGCATTAAGGC '3 R: 5' GAGTCATGTCCAGCACTCTCTACAC '3

nacre (*mitfa*<sup>-/-</sup>)

3dpf

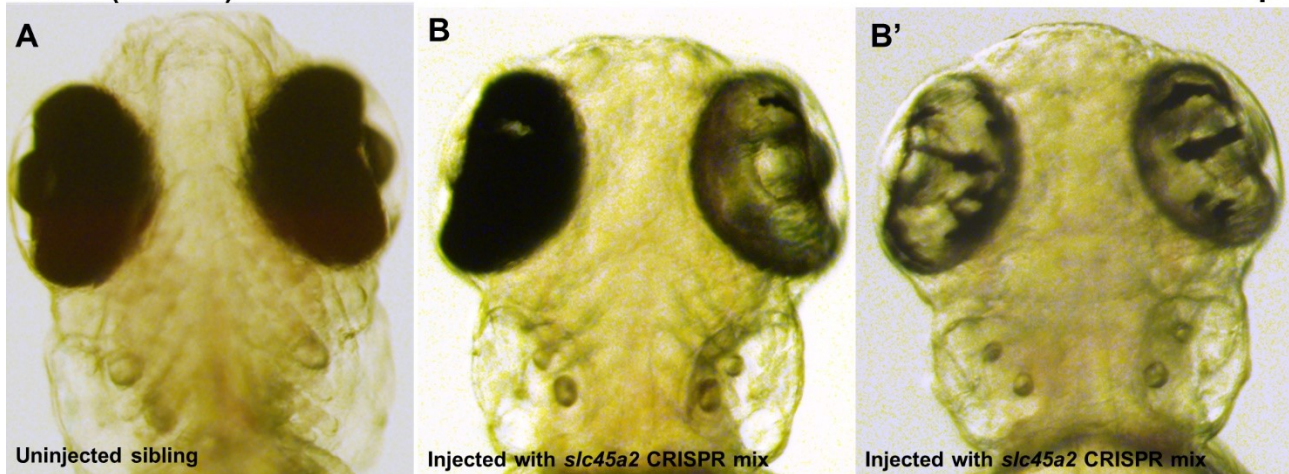


**Figure A1. Larval nacre zebrafish injected with *slc45a2* CRISPR mix show mosaic pigment defects. A) Uninjected sibling with large deposits of melanin in the RPE B-B')** Various mosaic pigment phenotypes are observed when nacre zebrafish are injected with *slc45a2* CRISPR mix. Larvae observed at 3 days post fertilization (dpf). RPE= retinal pigmented epithelium.

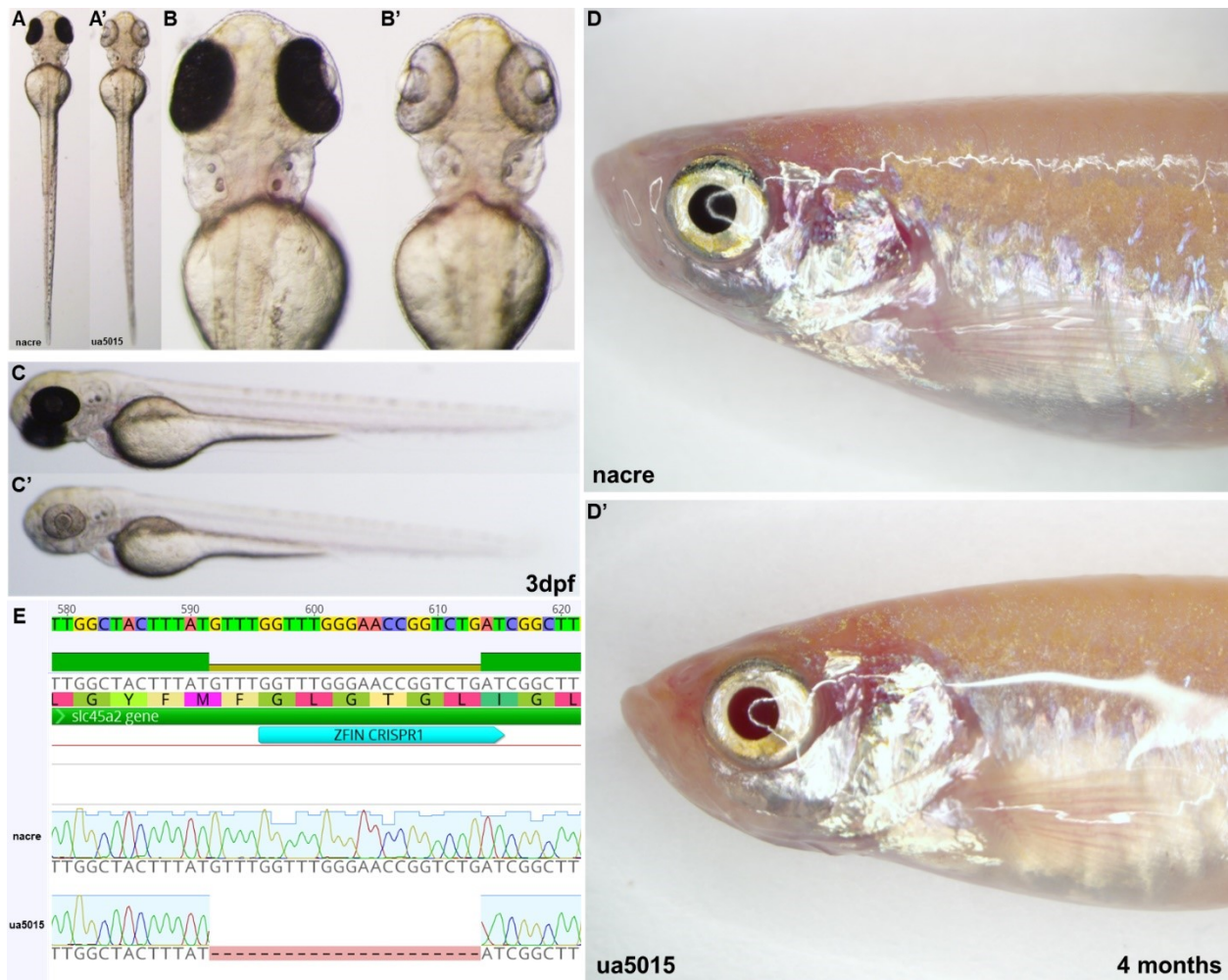
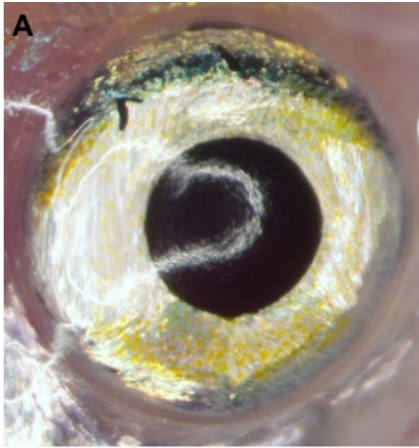
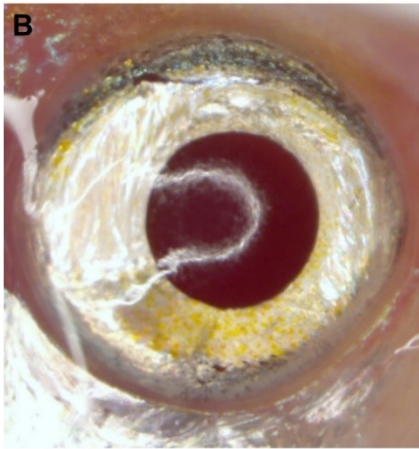


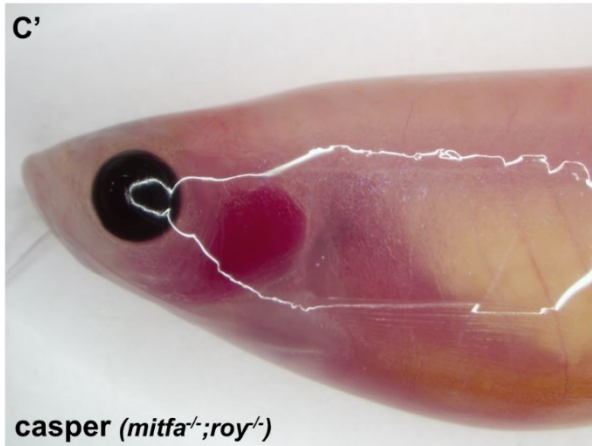
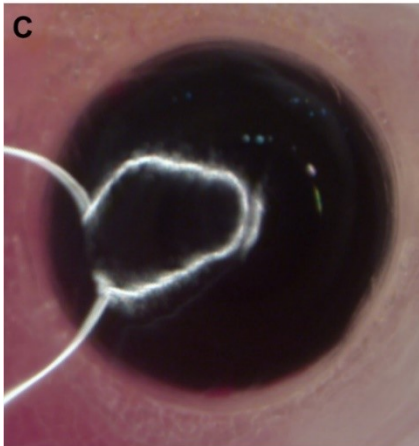
**Figure A2. ua5015 (*slc45a2*<sup>-/-</sup>; *mitfa*<sup>-/-</sup>) have no pigment in the RPE and can be observed through development. nacre fish have a pigmented RPE at A-C) 3dpf and D) 4 months while ua5015 fish have transparent RPE's at A'-C') 3dpf and D') 4 months. E) ua5015 is defined by a 22 base pair deletion in *slc45a2*. ZFIN CRISPR1 from [266].**



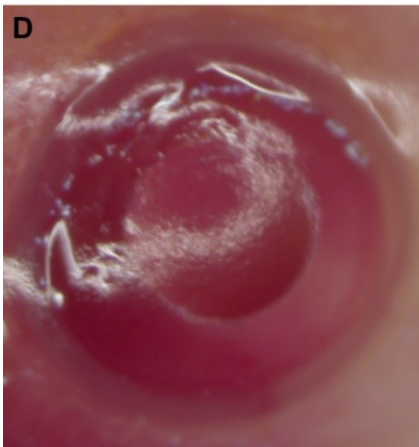
**nacre (*mitfa*<sup>-/-</sup>)**



**ua5015 (*mitfa*<sup>-/-</sup>;*slc45a2*<sup>-/-</sup>)**



**casper (*mitfa*<sup>-/-</sup>;*roy*<sup>-/-</sup>)**



**ua5020 (*mitfa*<sup>-/-</sup>;*roy*<sup>-/-</sup>;*slc45a2*<sup>-/-</sup>)**

**Figure A3. Pigmentless ua5020 mutants are generated from crossing ua5015 to casper. A)** Close up of nacre eye, showing iridophores around the eye and melanin in the RPE. **A')** Iridophores in body of nacre can be seen. **B)** Close up of ua5015 eye, showing iridophores but no melanin in the RPE due to mutation in *slc45a2*. **B')** Iridophores in body of ua5015 can still be observed. **C)** Close up of casper eye, showing no iridophores due to a mutation in *roy*. Melanin can still be seen in the RPE. **C')** Iridophores and melanophores are absent in body of casper. **D)** Close up of ua5020 eye, showing no iridophores and no melanin in RPE. **D')** Iridophores and melanophores are absent in body of ua5020.

*Tg<sub>ua5020</sub>(sws1:nfsb-mCherry; sws2:GFP)*

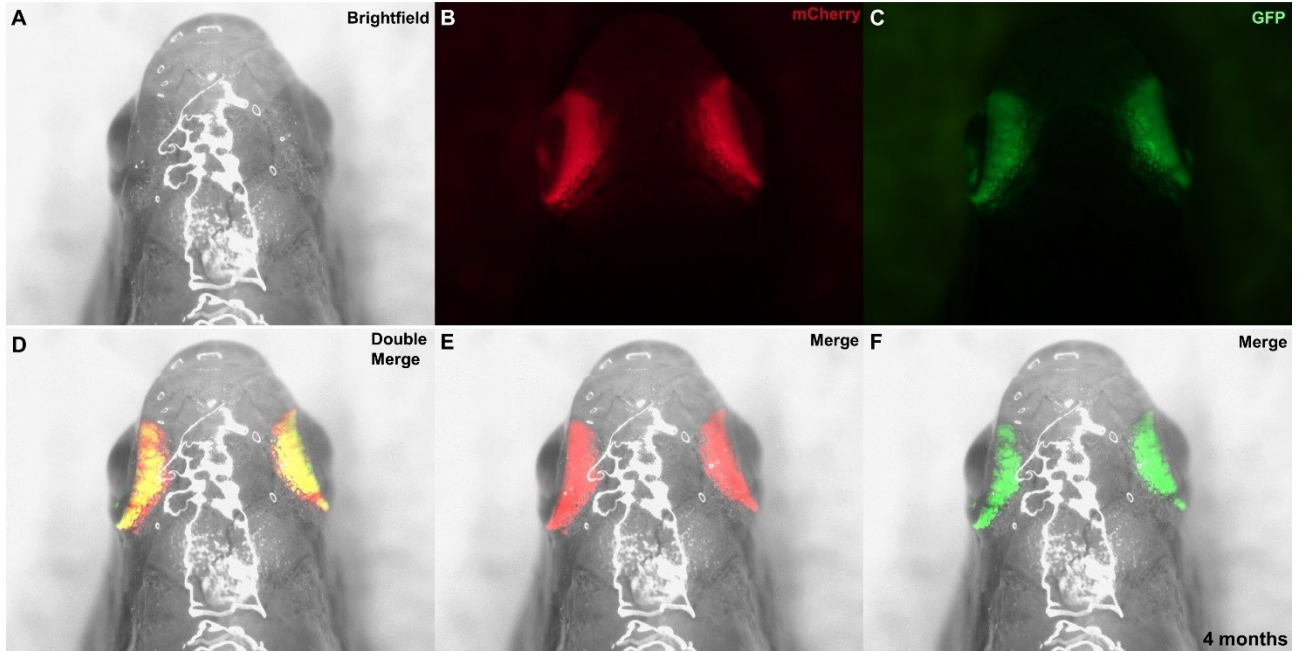


**Figure A4.** *Tg<sub>ua5020</sub>(sws1:nfsb-mCherry; sws2:GFP)* transgenics allow easy visualization of fluorescent reporters in zebrafish retina. **A)** Dorsal view of adult (4 months old) ua5020 head in brightfield. Transparent eyes can be seen on either side. **B)** mCherry marks nitroreductase in UV cones and **C)** GFP marks blue cones. **D)** Overlay of both channels, **E)** the mCherry channel and **F)** the GFP channel on a dorsal brightfield image.